

INAUGURAL-DISSERTATION

zur
Erlangung der Doktorwürde
der
Naturwissenschaftlich-Mathematischen Gesamtfakultät
der
Ruprecht-Karls-Universität
Heidelberg

vorgelegt von
Mag. rer. nat. Martina Rembold
aus Kitzbühel (Österreich)

Tag der mündlichen Prüfung:

Thema

**Cell behaviour
during
optic vesicle morphogenesis
in medaka**

Gutachter: Prof. Dr. G. Elisabeth Pollerberg
Dr. Jan Ellenberg

DISSERTATION

submitted to the
Combined Faculties for the Natural Sciences and for Mathematics
of the
Ruperto-Carola University of Heidelberg, Germany
for the degree of
Doctor of Natural Sciences

presented by
Mag. rer. nat. Martina Rembold
born in Kitzbühel (Austria)

Oral examination:

SUMMARY	3
ZUSAMMENFASSUNG	5
1 INTRODUCTION	7
1.1 MORPHOGENETIC CELL MOVEMENTS	8
1.2 THE EMBRYONIC ORIGIN OF THE EYE	15
1.2.1 SPECIFICATION OF THE ANTERIOR NEURAL PLATE AND INDUCTION OF THE EYE FIELD	16
1.2.1.1 Neural induction	17
1.2.1.2 Establishment of anterior identity	18
1.2.1.2.1 Movement away from posteriorizing signals	18
1.2.1.2.2 A Wnt signaling gradient defines anterior and posterior	20
1.2.1.3 Induction of the eye field	22
1.2.1.3.1 Homeobox transcription factors pattern the eye field	23
1.2.1.3.1.1 Six3	23
1.2.1.3.1.2 Pax6	24
1.2.1.3.1.3 Otx2	25
1.3 MORPHOGENETIC MOVEMENTS SHAPE THE EMBRYO	26
1.3.1 GENERAL EARLY MORPHOGENESIS	26
1.3.1.1 Gastrulation and convergent extension in zebrafish	26
1.3.1.2 Wnt/PCP and Wnt/Ca ²⁺ signaling in CE	27
1.3.2 MORPHOGENESIS OF THE EYE FIELD AND OPTIC VESICLE	29
1.3.2.1 The eye field	29
1.3.2.2 The optic vesicle	31
1.3.2.2.1 Rx is indispensable for optic vesicle formation	32
1.3.2.2.1.1 Rx genes and proliferation	35
1.3.2.2.2 Other factors involved	35
1.4 GENERATING TWO EYES	36
1.5 DORSO-VENTRAL PATTERNING OF THE OPTIC VESICLE	38
1.6 CREATING THE DIVERSE CELL TYPES OF THE NEURORETINA	39
1.7 AIM OF THE THESIS	41
2 RESULTS	42
2.1 <i>IN VIVO</i> TIME-LAPSE IMAGING IN MEDAKA	43
2.2 <i>IN VIVO</i> ANALYSIS OF OPTIC VESICLE MORPHOGENESIS	49
2.2.1 <i>Rx3</i> MODULATES THE MOVEMENT OF EYE FIELD CELLS	49
2.2.2 NEURULATION-LIKE BEHAVIOUR IN <i>Rx3</i> MUTANT CELLS	54
2.2.3 ANALYSIS OF CELL SHAPE CHANGES DURING OPTIC VESICLE FORMATION	60
2.2.4 OPTIC VESICLE FORMATION INVOLVES SINGLE CELL MIGRATION	63
2.2.5 A MODEL FOR OPTIC VESICLE FORMATION	66
2.3 APPENDIX	68
3 DISCUSSION	71
3.1 IMAGING IN MEDAKA	72
3.2 <i>EYELESS</i> EXHIBITS A UNIQUE PHENOTYPE	73
3.3 MODULATION OF CONVERGENCE BY <i>Rx3</i>	74
3.4 <i>Rx3</i> MODULATES CELL SHAPE CHANGES	78

3.5	SINGLE CELL MIGRATION	79
3.6	RX3 AND PROLIFERATION	82
3.7	CELL FATE AND CELL BEHAVIOUR – FUTURE ASPECTS	84
4	MATERIALS AND METHODS	86
4.1	MATERIALS	87
4.1.1	FISH STRAINS	87
4.1.2	BUFFERS AND MEDIA	87
4.1.3	ENZYMES, KITS AND STANDARDS	89
4.1.4	ANTIBODIES	90
4.1.5	BACTERIA	90
4.1.6	VECTORS AND OLIGOS	90
4.1.7	CHEMICALS	91
4.1.8	ADDITIONAL MATERIALS	91
4.1.9	EQUIPMENT	92
4.2	METHODS	92
4.2.1	TRANSGENIC FISH	92
4.2.2	TRANSCRIPTION OF MRNA <i>IN VITRO</i>	93
4.2.3	MICROINJECTION	94
4.2.4	HATCHING ENZYME	94
4.2.5	DECHORIONISATION	94
4.2.6	HEPTANOL TREATMENT AND MOUNTING	95
4.2.7	MICROSCOPY	95
4.2.8	IMAGE ANALYSIS	96
4.2.9	CELL TRACKING	96
4.2.10	IMMUNOSTAINING AND <i>IN SITU</i> HYBRIDIZATION	97
4.2.11	TRANSPLANTATION	98
	ABBREVIATIONS	99
5	REFERENCES	101
	PUBLICATIONS	121
	ACKNOWLEDGEMENTS	122

Summary

Vertebrate eye morphogenesis starts with the bilateral evagination of optic vesicles from the forebrain. A failure of evagination leads to the complete absence of eyes. Despite a good knowledge about patterning and retina differentiation, the mechanism underlying evagination remained largely unknown. Studies on optic vesicle morphogenesis and its underlying cellular basis were missing. I therefore used an *in vivo* imaging approach in medaka fish to investigate the cellular movements and dynamics of early eye formation.

Early medaka embryos were not amenable to *in vivo* imaging due to contractile movements that cause them to rotate in the chorion or in the embedding medium. I first established an *in vivo* imaging set up for medaka that was the basis for the further 4D analysis of eye morphogenesis. This analysis shows that optic vesicle morphogenesis requires the modulation of the morphogenetic behaviour of anterior neuroectodermal cells within the eye field during late gastrulation, before evagination is evident. While prospective telencephalic cells lateral to the eye field converge towards the midline, retinal precursor cells are retained in their medial movement. Together with the ventrally and laterally directed movement of medial eye field cells, a widened domain in the forebrain is formed that primes evagination. The importance of these movements is demonstrated in *eyeless* embryos that harbour a mutation in the homeobox transcription factor *Rx3* that is specifically expressed in the eye field. *Eyeless* embryos fail to form optic vesicles. Mutant retinal precursor cells converge towards the midline to the same extent as anteriorly and laterally located telencephalic progenitors and eventually form a neural keel-like structure. The wide domain in the forebrain is absent. Moreover, *Rx3* function is required for the modulation of cell shape changes and correct polarization of cells. In wild-type, retinal precursor cells elongate mediolaterally as they move laterally into the growing optic vesicles. In *eyeless* the cells at the lateral border of the neurula stage eye field adopt a columnar

epithelium-like shape reminiscent of the neural tube. They surround medial cells of the neurula stage eye field that remain rounded, indicating a defective polarization of mutant cells. Mosaic analysis showed that optic vesicle evagination can be rescued cell-autonomously by wild-type cells. Detailed 4D time-lapse analysis revealed that the rescue is due to the modulation of medial directed movement and individual cells migrating actively from medial positions laterally in the optic vesicles. This demonstrates that optic vesicle evagination depends on the locally coordinated migration of single cells rather than the movement of a tissue as whole.

Zusammenfassung

Die Morphogenese des Wirbeltierauges beginnt mit der Ausstülpung (Evagination) von zwei bilateralen Augenvesikeln aus dem Vorderhirn. Störungen im Prozeß der Evagination haben das komplette Fehlen des Auges zur Folge. Die frühe Musterbildung in der Augenanlage sowie die Differenzierung der Retina wurden detailliert untersucht und sind Paradigmen der Organogenese. Der Mechanismus der Evagination blieb jedoch relativ unerforscht. Studien über die Dynamik der Morphogenese des Augenvesikels sowie der ihr zugrundeliegenden zellulären Basis fehlten. Aus diesen Gründen untersuchte ich den Prozeß der frühen Augenbildung mittels 4D Mikroskopie am lebenden Embryo mit subzellulärer Auflösung. Da kontraktile Bewegungen innerhalb des Periderms dazu führen, daß sich Medaka Embryos auch in stringentem Einbettmedium bewegen, etablierte ich Bedingungen für die *in vivo* Mikroskopie in Medaka. Diese bildeten die Voraussetzung für die nachfolgende Analyse.

Die Morphogenese des Augenvesikels kann bis zur Augenanlage (Augenfeld) am Beginn der Neurulation zurückverfolgt werden, schon bevor erste Anzeichen der Evagination sichtbar sind. Die morphogenetischen Bewegungen der Zellen des anterioren Neuroektoderms in Richtung der Mittellinie des Embryos werden innerhalb des Augenfeldes moduliert. Während Vorläuferzellen des Telencephalons, die ursprünglich lateral zum Augenfeld liegen, sich zur Mittellinie des Embryos bewegen, ist diese Bewegung innerhalb der Augenfeldpopulation verlangsamt. Zusammen mit der ventral und lateral gerichteten Bewegung der Zellen des mittleren Augenfeldes führt dies zu einer Erweiterung im Vorderhirn. Diese Erweiterung ist das erste Anzeichen der nachfolgenden Evagination. Das Homeobox Gen *Rx3* ist spezifisch im Augenfeld exprimiert. Ist dieses Gen mutiert, wie in der *Eyeless* Mutante, bilden sich aufgrund einer fehlenden Evagination der Augenvesikel keine Augen aus. Eine Analyse der mutanten Zellen des Augenfeldes zeigt, daß sich diese wie die Vorläuferzellen des Tel- und Diencephalon in Richtung Mittellinie bewegen. Die Folge ist die Ausbildung einer Neuralrohr-ähnlichen Struktur an Stelle des Augenvesikels. Überdies finden dynamische Änderungen der Zellform nicht statt. Im Wildtyp nehmen die Zellen eine elongierte Form an, während sie in die Augenvesikel wandern. In der *Eyeless* Mutante bildet sich stattdessen eine epitheliale Struktur, die

runde Zellen im Neuralrohr umschließt. Dies deutet auf eine defekte Polarisierung der Zellen hin. Eine Mosaikanalyse, bei der Wildtyp-Zellen in ein mutantes Augenfeld transplantiert wurden, zeigte daß die Ausstülpung des Augenvesikels auf der koordinierten Migration einzelner Zellen beruht.

1 INTRODUCTION

1.1 Morphogenetic cell movements

“Cell migration in the vertebrate embryo more closely resembles the tangled network of highways around Los Angeles than the tranquil lanes of a rural area” (Driever, 2000).

And there is heavy traffic indeed as the embryo develops from the fertilized egg, whole sheets of cells move during gastrulation, mesendodermal cells involute and move towards the animal pole while the ectoderm continues its pace towards the vegetal pole. Later in development myocardial precursors move towards the midline, neural crest cells migrate from the dorsal side of the neural tube ventralwards, while germ cells pass by on their way to the gonads, to name just a few. All these movements along with tissue rearrangements are necessary to ultimately shape the form of the embryo and to give rise to its various organs. The formation of an organ (or the embryo as a whole) comprises three key steps corresponding to the three major concepts of developmental biology: cellular differentiation, growth and morphogenesis. Morphogenesis comes from the greek words *morphê* (shape) and *genesis* (creation) and refers to the control of the spatial distribution of cells to give an organ or embryo its definitive form (and function). Organs are often formed in successive stages and are refined during their development. This also comprises the modulation of the gene expression patterns within the cells of an organ during development. Patterning and morphogenesis are tightly connected and a certain gene can elicit a downstream change in cell behaviour and/or cell shape in the course of organ formation and refinement. How the determination of cell fate by one or several transcription factors alters the shape or controls the movement of a cell is a major question in biology that is now starting to be unraveled.

Several different mechanisms contribute to morphogenesis. These include cell movement, cell shape changes and proliferation. Although proliferation is strictly speaking part of growth, oriented cell divisions can contribute to the shape of an organ, as it seems the case in the formation of the heart chambers from a simple linear heart tube (Auman and Yelon, 2004) or in axis elongation during zebrafish convergent extension (CE) movements (Gong et al., 2004). Moreover, morphogenetic

processes and proliferation have to be properly coordinated, as some processes are mutually exclusive to proliferation such as migration. For example, proliferation has to be blocked in the paraxial mesoderm in *Xenopus* to ensure its proper convergent extension movements (Leise and Mueller, 2004). Similarly, a mitotic block in the ventral furrow at the onset of gastrulation in *Drosophila* ensures proper and rapid mesoderm internalization (Grosshans and Wieschaus, 2000; Mata et al., 2000; Seher and Leptin, 2000).

The following chapter will outline basic principles of morphogenesis. Cell movement during morphogenesis can be accomplished in different ways ranging from cell shape changes without movement, over cell rearrangement to cell migration. Migration can be a single cell event but may also be a coordinated mass migration (Figure 1) (Leptin, 2005; Locascio and Nieto, 2001; Montero and Heisenberg, 2004; Wallingford et al., 2002). This categorization is of course not mutually exclusive and different movements occur in a combination during morphogenesis. For example, gastrulation in *Drosophila* and the formation of mesoderm requires first the formation of the ventral furrow, driven by cell shape changes and later a spreading of these cells that involves a transition from an epithelium to mesenchyme and migration away from the site of invagination (Wilson et al., 2005).

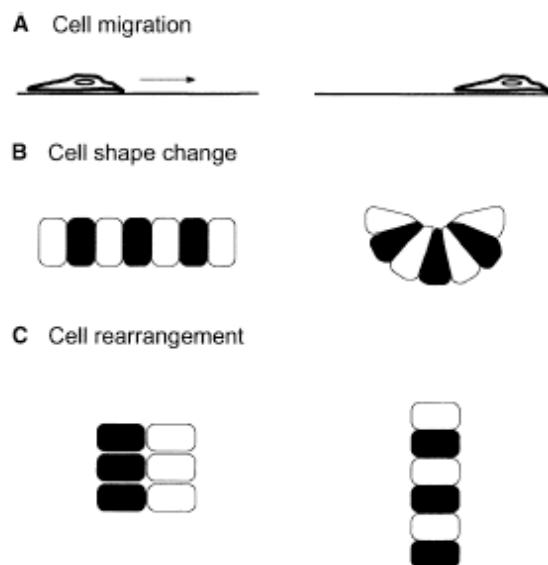


Figure 1. Categories of Morphogenetic Movement

(A) Directed cell migration of single cells or a small group of cells. (B) Coordinated cell shape change in a population effects the movement of a tissue as a whole. Individual cells do not change position relative to their neighboring cells. (C) Cell rearrangement, in which cells exert traction on neighboring cells in order to change their positions relative to one another, thus reshaping the population. Adapted from (Wallingford et al., 2002).

A coordinated change of shape without movement is for example responsible for hinge point formation of the neural tube (e.g. (Schoenwolf and Smith, 1990)). A well studied example are the shape changes occurring in the involuting mesoderm during furrow formation in *Drosophila* gastrulation. The ventral mesoderm is the first to enter the inside of the blastoderm stage embryo. A deep invagination (ventral furrow) is formed by an apical constriction and baso-apical shortening of the cells. The same type of shape changes occur within the posterior endoderm as it invaginates. These shape changes depend on the transcription factors *Snail* and *Twist* (Leptin, 1994; Leptin, 2005).

Another type of movement is individual cell migration. In this case cells migrate freely over long distances to new locations in the embryo. Directional migration is elicited in response to a variety of extracellular cues such as gradients of chemokines, growth factors or extracellular matrix molecules mediated by G-protein coupled receptors or tyrosine kinases (reviewed by (Ridley et al., 2003)). Single cell migration is a cyclic process that is driven by cytoskeletal dynamics that are transferred to the extracellular scaffold or another cell via adhesion receptors. The leading edge of the cell generates protrusive force. It usually extends a lamellipodium in the direction of migration coupled with the development of new cell adhesions to the substrate, in most cases mediated via integrin receptors. These adherence sites serve as traction sites over which the cell migrates. Retraction of the cells rear end and translocation of the cell body requires the disassembly of adhesions and actomyosin contractility. Cell polarization relies on positive interlinked feedback loops involving Rho family GTPases, phospho-inositide 3-kinases (PI3K) and integrins. Rho GTPases play an essential role in cell polarization. Cdc42 and Rac are activated at the leading edge and mediate the organization of actin filaments and integrin adhesion complex assembly. Actin polymerization to a branching dendritic network in lamellipodia is mediated by the Arp2/3 complex, that is activated by WASP/WAVE family members. Arp2/3 binds to the tip of an existing filament and induces branching of a new filament. Filopodial protrusions contain long parallel actin bundles that are probably created by a filament tread-milling process. Ena/VASP proteins are among others enriched at filopodial tips. They bind to the barbed end of actin filaments, prevent capping and

allow continuous elongation. (Pollard and Borisy, 2003; Welch and Mullins, 2002).

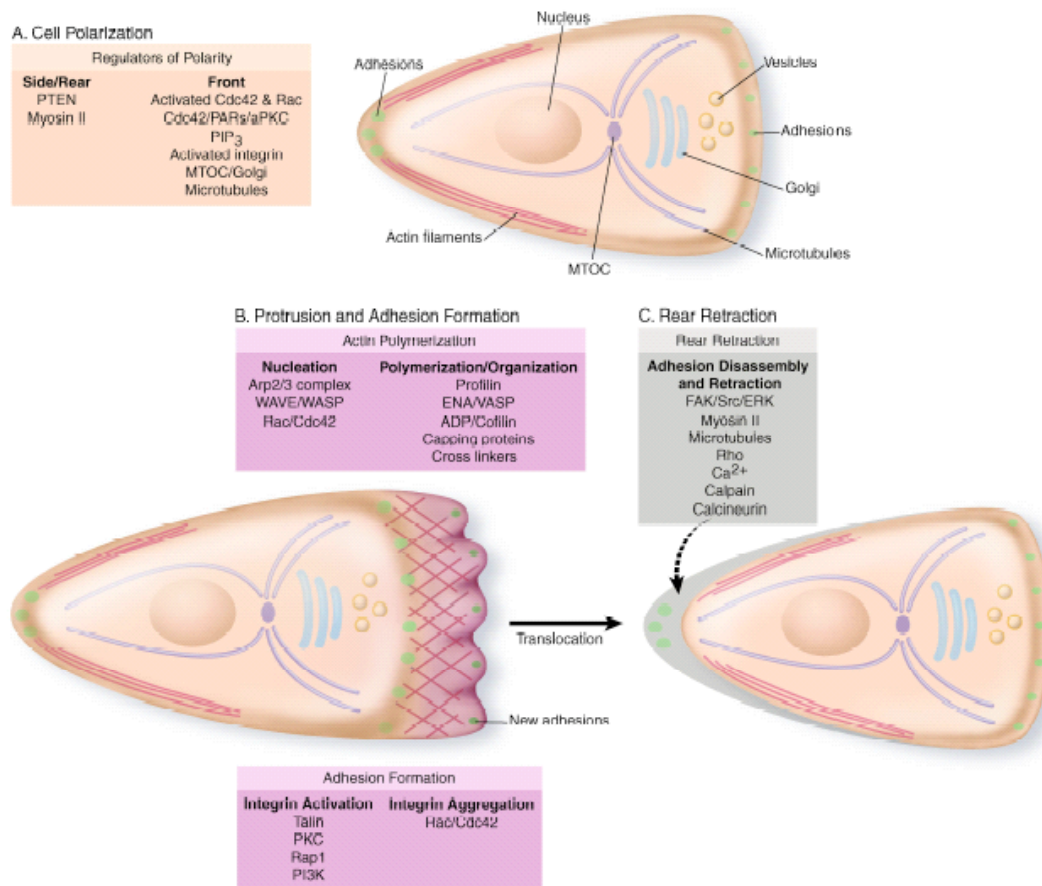


Figure 2. Steps and molecules involved in cell migration.

Initial cell polarization (**A**) leads to actin polymerization and the protrusion of a lamellipodium at the leading end, integrin activation and clustering (**B**). Shortening of membrane-tethered actin filaments results in local cell contraction, rear retraction and forward gliding of the cell (**C**). Adapted from (Ridley et al., 2003).

Localized activation of Rac and Cdc42 at the leading edge restricts Rho activity to the rear end where it is required for inhibition of protrusions and myosin contractility. PI3K activity is enhanced at the leading edge, which leads to accumulation of the signaling molecules PtdIns(3,4,5)P₃ (PIP₃) and PtdIns(3,4)P₂ [PI(3,4)P₂]. These translate and amplify a shallow gradient of a chemokine into a steep intracellular signaling gradient. It also feeds back on Rac activation. The phosphatase PTEN which removes these second messengers becomes localized to the rear end. Adhesions formed by integrin clustering, linked to the actin cytoskeleton and the extracellular matrix (ECM) transmit propulsive forces and serve as traction points over which the cell moves. The migration cycle is completed as adhesions disassemble and the rear end retracts (see (Ridley et al., 2003) and references therein).

The small GTPases Cdc42, Rac and Rho are not only involved in cell migration. They also play a role in adhesion and epithelial organization. They are required for the formation of adherens junctions and tight junctions (together with atypical protein kinase C) and in determining apical basolateral polarity. Integrins are involved in polarity as well by mediating the cell's interaction with the ECM at the basal surface (Etienne-Manneville and Hall, 2002). During embryogenesis Rho family GTPases are involved in numerous processes, e.g., cell polarization and movement during convergent extension (see later chapter), *Drosophila* dorsal closure or wound healing. Similarly, the small GTPases play a role in the polarization of differentiating neurons (see (Etienne-Manneville and Hall, 2002)).

A prominent example for individual cell migration in development is the migration of primordial germ cells (PGCs) to the developing gonads (Molyneaux and Wylie, 2004; Raz, 2003; Raz, 2004). Primordial germ cells are formed at positions far from their destination organ and thus have to migrate there during development. Migration is guided in mouse and fish by the chemokine Sdf-1 (stromal derived factor 1) that acts as an attractant to PGCs and is sensed by the 7-transmembrane G-protein coupled receptor Cxcr4 that is expressed in PGCs during their migration. Interfering with the function of receptor or ligand leaves cells motile but they lack a defined direction. In fish, this pathway controls all steps of the migration while in mouse it is only required for later steps and also mediates survival of PGC cells (Ara et al., 2003; Doitsidou et al., 2002; Knaut et al., 2003; Molyneaux et al., 2003). Another example is the migration of neural crest cells in vertebrates (Bronner-Fraser, 1994; Christiansen et al., 2000).

Cells may not necessarily migrate individually but can also engage in mass migration whereby a tissue moves in a co-ordinated manner. The cells interact locally with each other to induce global changes in the arrangement and shape of the tissue. Collective cell migration shares in general many features with individual cell migration. Also collectively moving cells develop cytoskeletal dynamics at the leading edge and generate contact to the substrate. The difference to single cell migration is the rear end and the maintenance of stable cell contacts. If the cells are connected to other cells by cell-cell junctions and these are not released upon rear retraction then the neighbour cells are dragged along. The leading edge exerts thus force towards both, the ECM and the cell-cell junction. Leading edge extension as well as rear retraction seem to be

a collective process involving several cells that are coupled, while other cells can be dragged along passively (Friedl et al., 2004). A prominent example of a mass migration event is the spreading of the mesoderm on the blastocoel roof in *Xenopus*. The cohesion of the cells is essential for polarity as well as directional and efficient migration (Winklbauer et al., 1992). PI3K, for example, that mediates polarity via accumulation of the second messenger PIP₃ in individual cell migration (Raftopoulou and Hall, 2004; Stephens et al., 2002) has been shown to control the directional migration of these mesodermal cells and the correct orientation of protrusions downstream of Platelet Derived Growth Factor (PDGF) in *Xenopus* (Nagel et al., 2004). Also in fish, PI3K controls the formation of oriented cellular protrusions downstream of PDGF signaling (Montero et al., 2003). PIP₃ accumulates at the leading edge and mediates the polarization of the actin cytoskeleton via Protein kinase B (PKB). The conversion of a mass migration event to single cell migration involves an epithelial-to-mesenchymal transition (EMT) but might also occur via delamination of single cells.

Cells can also coordinately rearrange within a sheet. A good example for the coordinated cell rearrangement is the mediolateral intercalation of mesodermal and ectodermal cells that underlies convergent extension in *Xenopus* gastrulation (Keller et al., 2000). A short and wide domain of mesoderm and ectoderm is narrowed to form the elongated body. Mediolateral intercalation is driven by polarized protrusive activity (Shih and Keller, 1992a; Shih and Keller, 1992b). The cells seem to use one another as substrate on which they move. Via their medial and lateral lamellipodia they exert traction on the elongate anterior and posterior surface of adjacent cells and thereby pull them between one another mediolaterally. Adhesions along the elongate anterior and posterior sides hold the cells together and provide stiffness, they can however also slide in the plane of the membrane and turnover rapidly and so allow cell intercalation to occur (reviewed in (Keller, 2002)). It is not precisely known what determines the direction of intercalation and cells send protrusions in both, medial and lateral directions. One mechanism seems to be “boundary capture” that occurs at the interface of notochord and somite. Cells that reached this boundary attach to it and send out protrusions only on their free side thus pulling neighbouring cells towards this boundary (Shih and Keller, 1992a; Shih and Keller, 1992b). Recently it has been shown that anterior-posterior tissue polarity is required for convergent extension to

occur indicating that AP polarity gives a guidance cue (Ninomiya et al., 2004). A later chapter will give more details on movements during convergent extension and the molecules involved in polarization of the cells. Cell rearrangement also occurs in *Drosophila* germ band extension, the lengthening of the segmented part of the embryo (Irvine and Wieschaus, 1994). Also here the cells are polarized. Myosin II is asymmetrically distributed within the plane of the epithelium and is enriched at those junctions that shorten and reduce contact between neighbouring cells. If myosin function is impaired junction remodeling and shortening of the contact fails, implicating myosin contractility in this process (Bertet et al., 2004).

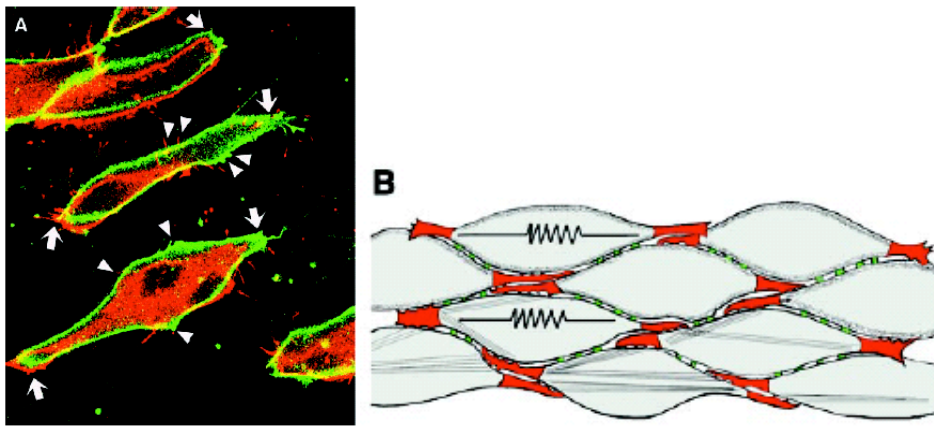


Figure 3. (A) Intercalating frog mesodermal cells. The arrows point to polarized lamellipodia at the medial and lateral end of the cells. Arrowheads indicate short filiform contacts at the elongated anterior and posterior surfaces. (B) Schematic of intercalating cells. The cells exert traction on each other by their lamellipodia (red), the short filiform protrusions (stiffening adhesions, green) hold the cells together to provide stiffness but they can also slide in the membrane and turn over to allow movement. Adapted from (Keller, 2002).

Another example of a coordinated movement in fish embryos is the migration of myocardial precursor cells to the midline where they fuse to form the primitive heart tube (McFadden and Olson, 2002). The myocardial precursors do not migrate as individuals but become intimately connected and move in a coordinated way as an epithelium. If the formation of apicobasal polarity is disturbed as in *natter* embryos, mutant for the ECM molecule Fibronectin, myocardial precursors migrate abnormally (Trinh and Stainier, 2004). This causes cardia bifida (the formation of two separate hearts) (Chen et al., 1996).

Although different organisms acquire very different shapes and the exact pathway and factors involved depends on the context, the basic cellular machinery they use is similar. Rho GTPases for example are involved in establishing asymmetry in a variety of tissues and cells in organisms ranging from yeast to mammals (Etienne-Manneville and Hall, 2002). Other examples are the planar cell polarity pathway (PCP) that is involved in tissue polarity during CE in vertebrates and in polarization of the wing or eye epithelium in *Drosophila* (Mlodzik, 2002). PDGF guides mesodermal cells in *Xenopus* as well as border cells in *Drosophila*, and similarly, the JAK/STAT pathway has been implicated in both processes (Montero and Heisenberg, 2004).

In summary, morphogenesis is a tightly controlled process that involves the modulation of adhesion between cells or to the ECM and dynamic changes in the cytoskeleton. Both processes are necessary both, for the cell to change shape and to migrate. Proliferation contributes to the shaping of an organ or embryo either by means of localized centers of proliferation, asymmetric divisions or control of spindle orientation. In some cases it is also necessary to inhibit proliferation to allow shape changes or movement to occur.

1.2 The embryonic origin of the eye

In embryonic development, organ formation can be traced back to gastrulation when the three germ layers, (neuro)ectoderm, mesoderm and endoderm separate and patterning events give rise to specific fields that will later form the organs. A good example for this is vertebrate eye development. The eye is essentially a highly complex and specialized extension of the brain that signals via the ganglion cells to the visual centers of the brain, allowing us to see and integrate signals from our environment. It originates from the neuroectoderm and the eyes fail to develop without the evagination of optic vesicles from the anterior forebrain. Eye development can thus be traced back to gastrulation, when in the course of neural patterning an eye field is established within the anterior neural plate. The following chapters will outline the embryonic origin of the eye. First neural induction specifies neural fate prior to and during gastrulation opposed to epidermal fate. Subsequently the anterior-

posterior axis within the neuroectoderm is established and the eye field is specified within the anterior neural plate. Special emphasis will be given on cell and tissue rearrangements that accompany or are the consequence of the patterning events during eye development.

1.2.1 Specification of the anterior neural plate and induction of the eye field

The forebrain including the eyes arises from anterior neuroectoderm during gastrulation. The earliest step in neural development is a fate choice within the ectoderm between epidermal and neural, also called neural induction. In addition to the acquisition of neural identity, rostral neural tissue has to adopt anterior identity and the neural plate must be regionalized along its anterior-posterior (AP) axis. Regionalization results in distinct subdivisions: adjacent to the anterior borders of the neural plate are the telencephalic precursor cells that encircle the eye field at its anterior and lateral sides. Posterior to the eye field are prospective diencephalic cells followed by midbrain and hindbrain precursors (Hirose et al., 2004; Rubenstein et al., 1998; Varga et al., 1999; Woo and Fraser, 1995). The eye field is demarcated by the expression of several regulatory genes, such as the homeodomain transcription factors *Pax6*, *Six3* and *Rx*.

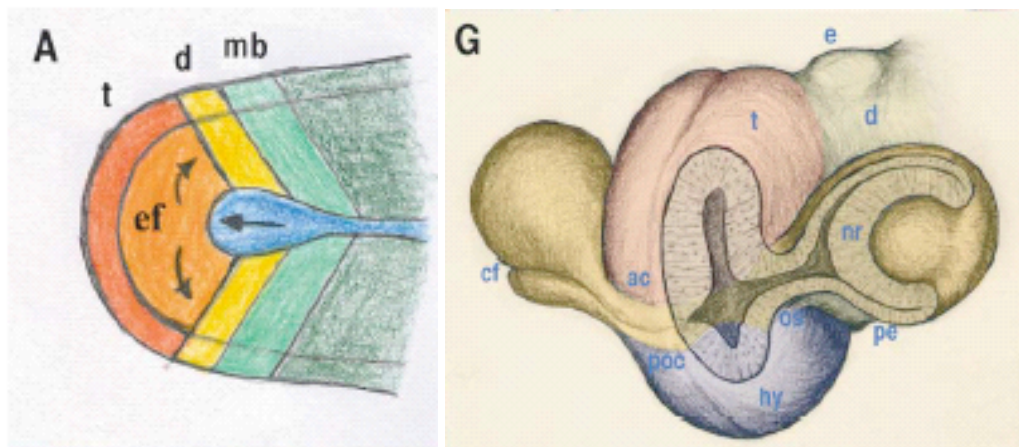


Figure 4. The left picture shows the organization of the anterior neural plate with telencephalon (t) being anterior and lateral to the eye field (ef). Posterior to it are diencephalic (d) and midbrain (mb) precursors. Midline tissue (blue) is shown migrating anteriorly. The right panel shows the organization of the fish forebrain and eye. Abbreviations: ac, anterior commissure; cf, choroid fissure; d, diencephalon; e, epiphysis; hy, hypothalamus; nr, neural retina; os, optic stalk; pe, pigment epithelium; poc, postoptic commissure; t, telencephalon; Adapted from (Wilson and Houart, 2004)

1.2.1.1 Neural induction

Despite being a field of intensive study, there is still no consensus about the mechanism of neural induction (Munoz-Sanjuan and Brivanlou, 2002; Stern, 2002; Wilson and Edlund, 2001). Bmp, Wnt and Fgf signaling take a central role in this process. Evidence mainly obtained from *Xenopus* showed that inhibition of Bmp signaling by the organizer is necessary to inhibit epidermal fates and allow neural induction to occur (Grunz and Tacke, 1989; Hawley et al., 1995; Hemmati-Brivanlou and Melton, 1994; Xu et al., 1995). In agreement with this, several secreted inhibitors of Bmp signaling were found to be expressed in the organizer such as *noggin* (Lamb et al., 1993; Smith and Harland, 1992; Zimmerman et al., 1996), *folliculin* (Hemmati-Brivanlou et al., 1994), *chordin* (Piccolo et al., 1996; Sasai et al., 1995), *Cerberus* (Bouwmeester et al., 1996; Piccolo et al., 1999) and *Xnr3* (Hansen et al., 1997). Misexpression of these Bmp inhibitors in animal caps induces neural tissue, while Bmps can antagonize neural induction in ectodermal explants (Wilson and Hemmati-Brivanlou, 1995). Together these findings lead to the proposition of the ‘default model’ of neural induction (Munoz-Sanjuan and Brivanlou, 2002). The model proposes that ectodermal cells are fated to become neural by default unless they are exposed to Bmp signaling that imposes an epidermal fate. Thus to allow neural induction to occur Bmp signals have to be inhibited in the anterior neural plate by Bmp antagonists that are secreted from the organizer. However, evidence from other species (especially mouse and chick) suggests that inhibition of Bmp signaling is not sufficient for neural induction but might rather be required to maintain neural fate (eg. (Davidson et al., 1999; Klingensmith et al., 1999; Shih and Fraser, 1996; Streit et al., 1998)). Earlier signals are necessary to confer sensitivity to Bmp (Wilson and Edlund, 2001). Recently, Fgf has been identified to constitute this signal in chick and fish (Londin et al., 2005; Streit et al., 2000; Wilson et al., 2000). A requirement for Fgf in neural induction has also been demonstrated in the ascidian *Ciona*, where it appears to be the main neural inducing signal (Bertrand et al., 2003; Hudson et al., 2003). These findings are in agreement with earlier studies in *Xenopus* that Bmp antagonists are unable to induce neural fates when Fgf signaling is blocked using a dominant-negative version of the Fgf receptor-1 (Launay et al., 1996; Sasai et al., 1996). A dominant negative version of Fgfr4, can block neural development on its own (Hongo et al., 1999) and Fgfr4 in combination with Bmp inhibition induces neural marker

genes (Linker and Stern, 2004). In chick, Fgf alone or in combination with Bmp antagonists is not sufficient to induce neural fate in prospective epidermal ectoderm (Streit et al., 2000; Wilson et al., 2000) and it has been suggested that inhibition of Wnt signalling cooperates with Fgf in the suppression of Bmp and induction of neural fate (Wilson et al., 2001). In *Xenopus*, simultaneous inhibition of Wnt and Bmp signaling is sufficient to induce a secondary head (Glinka et al., 1997).

Thus, Fgf and Wnt and maybe other signals (Linker and Stern, 2004) seem to confer a “pre-neural” state to prospective neural tissue prior to gastrulation that is later cemented by Bmp antagonists. Interestingly, the same signals will act later in neural development as posteriorizing factors.

1.2.1.2 Establishment of anterior identity

The induction of neural tissue is often accompanied by the expression of marker genes that are later confined to anterior (forebrain including telencephalon, eyes and diencephalon) fates. This suggested a link between neural induction and the acquisition of anterior identity and that subsequently part of the neural plate is transformed to posterior fates to get the full range of the mature CNS (activation-transformation model) (Foley and Stern, 2001). The candidates for posteriorizing signals are Fgfs, Wnt proteins, retinoic acid, Nodals and Bmps that are secreted by the late organizer, paraxial mesoderm or local organizing centers such as the isthmic organizer at the mid-hindbrain boundary (Wilson and Houart, 2004). Anterior neural tissue develops in regions that are protected from the influence of posteriorizing signals. This is accomplished by a combination of different mechanisms: the localized expression of posteriorizing and anti-posteriorizing signals and the morphogenetic movement of anterior tissue away from posteriorizing signals (see Figure 5).

1.2.1.2.1 Movement away from posteriorizing signals

The organizer and its early derivatives such as prechordal plate mesoderm are initially a source of antagonists of posteriorizing signals and express Wnt and Bmp antagonists (Kiecker and Niehrs, 2001b). But at later stages, when the organizer is contributing to more posterior tissue it becomes a source of caudalizing signals such as Wnt and Fgf proteins. In addition to the early derivatives of the organizer other tissues help to

protect the anterior neural plate from the influence of caudalizing signals. In chick, the hypoblast, an early extraembryonic endodermal layer, directs cell movements in the overlying epiblast away from the caudalizing signals emanating from the organizer (Foley et al., 2000). A similar mechanism acts in mouse but in this case the extraembryonic endoderm moves itself. The anterior visceral endoderm (AVE) migrates from the distal tip of the blastula rostrally during gastrulation and comes to underlie the presumptive anterior neural plate where it is an important source of anti-caudalizing signals (Thomas et al., 1998) (Perea-Gomez et al., 2001a) (Kimura et al., 2000) (Perea-Gomez et al., 2001b). Both, movement and induction of anterior fate depend on *Otx2* function in the AVE (Perea-Gomez et al., 2001a) (Kimura et al., 2000) but anterior fate is only maintained if *Otx2* is also expressed in the anterior neuroectoderm and axial mesendoderm (Acampora et al., 1998; Rhinn et al., 1998). The mechanism of AVE migration seems to involve both, active cell migration (Srinivas et al., 2004) and differential proliferation (Yamamoto et al., 2004). Nodal, a TGF- β related factor, is expressed in the node and is essential for mesoderm specification and anterior-posterior (AP) patterning (Schier and Shen, 2000). The expression domains of the Nodal antagonists *Lefty1* and *Cerl* are shifted towards the anterior part of the AVE before the onset of migration, creating thus lower Nodal activity on the future anterior side. Nodal stimulates proliferation and the AVE cells seem to migrate away from the site of active proliferation. The inhibition of proliferation by *Lefty1* and *Cerl* thus directs the AVE to migrate to the anterior side while Nodal signalling creates the driving force (Yamamoto et al., 2004).

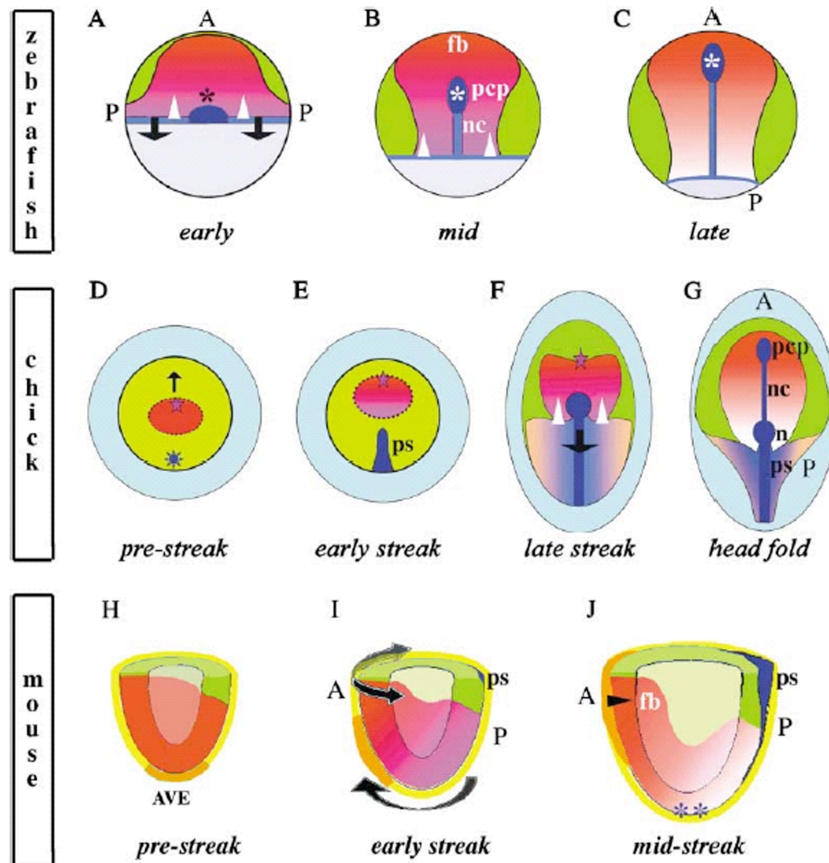


Figure 5. Cell movements separate the prospective forebrain from sources of caudalizing signals.

Epiblast/nonneural ectoderm is shown in green, neural ectoderm in red/pink. (A-C) Dorsal view of fish embryos during gastrulation. The germ ring (blue) is a source of posteriorizing signals (white arrowheads). As epiboly moves the germ ring vegetalwards (black arrows) the prospective forebrain becomes positioned further distant from these signals. The prechordal plate, a source of antagonists of posteriorizing signals moves anteriorly underneath the neural plate along with hypothalamic precursors (asterisk). (D-G) Dorsal view of chick embryos prior to and during gastrulation. At early stages (D-E) the prospective forebrain moves rostrally in response to signals from the underlying hypoblast bringing it further away from the primitive streak and organizer (blue star). Later (F) also the node regresses posteriorly as in fish. (H-J) Lateral views of sagittally bisected mouse embryos prior to and during gastrulation. The AVE (orange) in the extraembryonic layer (yellow) moves rostrally and emits signals that protect the overlying forebrain from posteriorizing signals. The Node is marked by a double asterisk.

Abbreviations: AVE, anterior visceral endoderm; fb, prospective forebrain; n, node; nc, prospective notochord; pcp, prechordal plate mesendoderm; ps, primitive streak; A, anterior; P, posterior.

Adapted from (Wilson and Houart, 2004).

1.2.1.2.2 A Wnt signaling gradient defines anterior and posterior

An important mechanism for defining anterior-posterior positional values is the establishment of a gradient of secreted Wnt activity. This is achieved by anteriorly localized Wnt antagonists that inhibit posteriorly localized Wnt signaling. (Wilson

and Houart, 2004; Yamaguchi, 2001). Ectopic Wnt signaling results in the lack of forebrain and eyes as in *masterblind* mutant zebrafish (*mbl*), that carry a mutation in the intracellular Wnt pathway scaffolding protein Axin1 (Heisenberg et al., 2001; Masai et al., 1997; van de Water et al., 2001) or in *headless* (*hdl*) fish, mutant for *Tcf3*, a transcriptional repressor of Wnt target genes (Kim et al., 2000). The source of Wnt is the mid-hindbrain boundary that expresses *Wnt8b* in fish (Houart et al., 2002). Wnt antagonists are secreted within the anterior neuroectoderm and adjacent anterior mesoderm, also from the AVE and anterior axial mesendoderm in mouse (Finley et al., 2003; Mukhopadhyay et al., 2001; Yamaguchi, 2001) or by the anterior neural border (ANB) in fish (Houart et al., 2002; Houart et al., 1998). In *Xenopus*, mouse (Glinka et al., 1998) and fish (Hashimoto et al., 2000) the secreted Wnt antagonist *Dickkopf* (*Dkk*) is expressed in the organizer and axial mesendoderm. Overexpression of *Dkk* results in an enlarged head and shortened trunk in both, frog (Glinka et al., 1998) and fish (Hashimoto et al., 2000) and anteriorizes the neural plate (Hashimoto et al., 2000; Kazanskaya et al., 2000). Similarly, the ANB in fish expresses *Tlc*, a member of the secreted Frizzled-related protein (sFRP) family (Houart et al., 2002). sFRPs share homology with the extracellular domain of the Frizzled receptors but lack the membrane-spanning and intracellular domains (Kawano and Kypta, 2003). They antagonize Wnt activity by sequestering secreted Wnts (Uren et al., 2000). *Tlc*-expressing cells can restore telencephalic fate in embryos lacking the ANB and can also induce telencephalic gene expression in diencephalic or midbrain domains (Houart et al., 2002) while activation of the canonical Wnt pathway suppresses anterior forebrain markers (Braun et al., 2003; Houart et al., 2002; Kiecker and Niehrs, 2001a; Nordstrom et al., 2002). Neural explants in chick that would normally develop posterior character *in vitro* acquire forebrain fate in the presence of a Wnt antagonist. Anterior explants, in contrast, acquire increasingly more posterior character the higher the Wnt concentration they experience, demonstrating the action of graded Wnt activity (Nordstrom et al., 2002). The same has been observed in *Xenopus* animal caps where treatment with Wnt8 leads to progressive posteriorization and repression of anterior markers (Kiecker and Niehrs, 2001a). Direct evidence for a Wnt morphogen gradient in the neural plate came from expression of a GFP-Wnt8 fusion in zebrafish. The protein was found in the extracellular space at a distance of 2-3 cell diameters, although the actual distribution might be wider but invisible due to

being under the detection threshold (Rhinn et al., 2005). Also in *Xenopus* an AP gradient of nuclear localization of β -catenin has been found (Kiecker and Niehrs, 2001a). Canonical Wnts stabilize β -catenin that then translocates to the nucleus and acts as co-activator of Tcf/LEF target genes (Kawano and Kypta, 2003). However, fish lacking *Tcf3* show no enhanced expression of a β -catenin activated transgene (Dorsky et al., 2002), although the anterior neural plate is posteriorized. It was thus suggested that the primary role of Wnt signaling lies in relieving a *Tcf*-mediated repression of posterior neuroectoderm genes but not in their activation (Dorsky et al., 2003).

Wnt8 in zebrafish, originating from the blastoderm margin also regulates the position of the organizer at the midbrain-hindbrain boundary (MHB) (Rhinn et al., 2005). Wnt8 directly represses *Otx2* and activates *Gbx1* in a concentration-dependent manner and thus establishes the interface of these two genes. Mutual repressive interaction between *Otx2* and *Gbx1* sharpens the boundary (Rhinn et al., 2003). Similarly, Wnt represses *Six3* and activates *Irx3* in chick and fish (Braun et al., 2003; Itoh et al., 2002) and the interface between these two gene expression domains determines the position where the zona limitans intrathalamica (zli) later forms (Braun et al., 2003; Kobayashi et al., 2002). The zli divides the rostral forebrain (telencephalon, eyes, hypothalamus and prethalamus) from caudal diencephalon (thalamus, pretectum) (Wilson and Houart, 2004). Again, the expression boundary is sharpened by mutual repressive interactions between *Six3* and *Irx3* (Kobayashi et al., 2002). Thus a Wnt gradient in the anterior neural plate establishes a crude AP pattern. This is cemented and sharpened by the induction and mutual repressive activities of genes within it.

1.2.1.3 Induction of the eye field

As discussed before, increasing the activity of Wnt antagonists in the ANB drives telencephalic gene expression into the eye field whereas the local activation of canonical Wnt signaling abolishes the formation of telencephalon and eyes (Houart et al., 2002). The eye field develops thus in a region with moderate Wnt activity at a level intermediate between that which promotes posterior diencephalon and that required for the telencephalon (Wilson and Houart, 2004). As mentioned earlier, the

eye field transcription factor *Six3* is repressed by Wnt signaling (Braun et al., 2003; Kim et al., 2000), while *Six3* in turn directly represses Wnt in the anterior neural plate (Braun et al., 2003; Lagutin et al., 2003). Ectopic expression of mouse *Six3* restores normal *Wnt1* expression and rescues the forebrain and eye phenotype of zebrafish *headless (hdl)* embryos (Lagutin et al., 2003). The rescue involves probably a dual role for *Six3*, the repression of ectopic Wnt and additional functions downstream of Wnt signaling.

1.2.1.3.1 Homeobox transcription factors pattern the eye field

Besides *Six3*, several transcription factors expressed in the anterior neural plate are required for eye development such as *Otx2*, *Pax6* and *Six6* genes.

1.2.1.3.1.1 *Six3*

Six3 and the closely related *Six6/Otx2* are members of the SIX-homeodomain family (Loosli et al., 1998; Oliver et al., 1995; Toy et al., 1998). *Six3* is expressed in the anterior neuroectoderm, including the eye field and telencephalon and abutting surface ectoderm and later in the optic vesicle in all vertebrates analyzed so far (Bovolenta et al., 1998; Granadino et al., 1999; Loosli et al., 1998; Oliver et al., 1995; Seo et al., 1998; Zhou et al., 2000) and mutually interacts with Wnt signaling as outlined before. *Six3* and *Pax6* activate each other in a crossregulatory interaction (Chow et al., 1999; Loosli et al., 1999). *Six3* has a critical role in the formation of eyes and forebrain. Knock-down of *Six3* in medaka results in loss of the forebrain and eyes (Carl et al., 2002). Mouse embryos lacking *Six3* function lack most of the head structures anterior to the midbrain including eyes and nose (Lagutin et al., 2003). In humans, mutations in SIX3 cause holoprosencephaly (Pasquier et al., 2000; Wallis et al., 1999). Overexpression of *Six3* (or *Six6*) results in expanded and ectopic retinal primordia in more posterior neural tissue in medaka (Loosli et al., 1999) and *Xenopus* (Zuber et al., 1999) and in ectopic optic vesicles in mouse (Lagutin et al., 2001). In zebrafish, *Six3* overexpression leads to an expansion of the rostral forebrain and an enhanced expression of *Pax2* in the optic stalks while moderate knock-down in medaka causes loss of proximal fates and *Vax1* expression and cyclopia, demonstrating a role in proximo-distal patterning of the eye (Carl et al., 2002; Kobayashi et al., 1998). *Six3* and the closely related *Six6/Otx2* play a pivotal role in

controlling the proliferation of retinal precursor cells (Bernier et al., 2000; Li et al., 2002; Loosli et al., 1999; Zuber et al., 1999). *Six6* acts as a transcriptional repressor (Li et al., 2002; Zuber et al., 1999) and both, *Six3* and *Six6* interact with TLE1 (transducin-like enhancer of split) a transcriptional repressor of the *Groucho* family (Kobayashi et al., 2001; Lopez-Rios et al., 2003). Moreover, *Six6* has been shown to repress cyclin-dependent kinase inhibitors such as *p27Kip1*, *p19Ink4d* and *p57Kip2* and thereby to regulate proliferation (Li et al., 2002). Interestingly, *Six3* can control the proliferative capacity of retinal precursor cells in a transcription-independent manner (Del Bene et al., 2004). Geminin inhibits DNA-replication by sequestering Ctd1, the key component of the pre-replication complex (Tada et al., 2001; Wohlschlegel et al., 2000). *Six3* competes with Ctd1 directly to bind to Geminin and thereby antagonizes its activity allowing retinal precursor cells to proliferate (Del Bene et al., 2004).

1.2.1.3.1.2 Pax6

Pax6 is a *paired* box and *paired*-like homeobox gene expressed in the anterior neural plate and eye field (Grindley et al., 1995; Hirsch and Harris, 1997; Li et al., 1997; Walther and Gruss, 1991). It is extremely well conserved throughout evolution (Callaerts et al., 1997), and plays an essential role in eye formation. Mutations in *Pax6* result in eye malformations known as Aniridia, Peter's anomaly, and cataracts in humans (Glaser et al., 1992; Hanson et al., 1994; Jordan et al., 1992; Ton et al., 1991) and the *Small eye* (*Sey*) syndrome in mice and rats (Fujiwara et al., 1994; Hill et al., 1991). The *Sey* mutation is semidominant, heterozygous mice have smaller eyes (Hill et al., 1991). Homozygous mouse or rat *Sey* mutants are anophthalmic and die at birth (Grindley et al., 1995; Hogan et al., 1986; Matsuo et al., 1993). The *Drosophila* homologue of *Pax6*, *eyeless*, is essential for eye formation (Quiring et al., 1994) and misexpression of *Drosophila* or mouse *Pax6* can induce ectopic eyes in non-eye imaginal discs (Halder et al., 1995). *Pax6* can also induce fully differentiated ectopic eyes in *Xenopus* (Chow et al., 1999). *Pax6* has been proposed as the 'master control gene' of eye development (Gehring, 2002). However, although the eyes are absent in *Sey/Sey* mutant embryos, the optic vesicle form but fail to constrict proximally and degenerate later (Grindley et al., 1995) In addition, *Pax6* only induces ectopic eyes in *Xenopus* when injected into the dorsal blastomeres that give rise to neural and

ectodermal tissues (Chow et al., 1999), suggesting that other genes are involved in parallel or upstream of *Pax6*. *Pax6* has also an essential role in lens development (Grindley et al., 1995; Lang, 2004).

1.2.1.3.1.3 Otx2

Otx2, a member of the *orthodenticle*-related family of homeobox proteins (Simeone et al., 1993), is expressed in the anterior neuroectoderm and essential for anterior neural development. Mice lacking *Otx2* function lack forebrain and midbrain and consequently also the eyes (Acampora et al., 1995; Ang et al., 1996; Matsuo et al., 1995). In *Xenopus*, anterior structures are lost when *Otx2* fused to the engrailed transcriptional repressor is expressed in embryos (Isaacs et al., 1999). *Otx2* is repressed by *Wnt8* originating from the lateral mesendodermal precursor at the blastoderm margin in fish and thereby *Otx2* expression is restricted to the anterior neuroectoderm (Rhinn et al., 2005). Consistent with this finding, Tcf4-binding sites have been found in the enhancers driving *Otx2* expression in the mouse anterior neural plate (Kurokawa et al., 2004). Evidence for the requirement of *Otx2* in eye formation comes from overexpression studies, where eye field transcription factors such as *Pax6*, *Six3*, *Six6/Optx2* or *Rx* lead to ectopic eye formation. As Chuang and Raymond pointed out, ectopic eye development appears to occur only within the *Otx2* expression domain (Chuang and Raymond, 2002). *Otx2* thus plays rather a permissive role in eye development. At the beginning of neurulation, *Otx2* is downregulated in the presumptive eye field concomitant with the onset of expression of many eye field transcription factors indicating that it might be regulated by these (Andreazzoli et al., 1999; Zuber et al., 2003). Indeed, it was shown earlier that *Rx* misexpression at early neurula stages can repress endogenous *Otx2* (Andreazzoli et al., 1999).

1.3 Morphogenetic movements shape the embryo

The specification of the eye field occurs within the context of the gastrulating embryo. Here I will briefly outline early embryonic development and morphogenesis in fish and then discuss morphogenetic movements occurring in the eye field and optic vesicles, if known.

1.3.1 General early morphogenesis

1.3.1.1 Gastrulation and convergent extension in zebrafish

The inductive events described in the previous chapters occur within a developmental window from blastula to the early neurula stage and are thus happening in the context of extensive cell migration and rearranging tissues. Zebrafish and medaka embryos undergo meroblastic cleavage, leading to the formation of a blastoderm cap on top of a big yolk cell. Initially, the cap is comprised of a surface enveloping layer (EVL) consisting of flattened large epithelial cells and a deep layer of more loosely associated blastodermal cells (DEL). The EVL is a simple embryonic epithelium that later forms the periderm (Kimmel et al., 1990). Epiboly starts with the thinning of the blastoderm driven by radial cell intercalation within the DEL (Warga and Kimmel, 1990; Wilson et al., 1995). Gastrulation begins with mesendodermal cell internalization, also called involution in the germ ring. These cells form the hypoblast layer, which gives rise to the mesodermal and endodermal germ layers. Positioned above the hypoblast is the layer of non-involuting ectodermal progenitor cells (epiblast), that will form the (neuro-) ectodermal germ layer. A second movement, convergent extension (CE) of the mesendodermal and neuroectodermal layer leads to the formation and elongation of the embryonic body axis. Mesendodermal and ectodermal precursors converge towards the dorsal side of the embryo and then undergo medio-lateral cell intercalations. This leads to a thinning of the forming body axis along its medio-lateral extent and a concomitant elongation along the anterior-posterior axis. Anterior migration is restricted to the early internalized cells whereas later internalized cells move towards the vegetal pole (Warga and Kimmel, 1990).

As mentioned earlier, CE in *Xenopus* depends on cell rearrangements within a tissue as a whole and consequently, gastrulation movements are interdependent and inhibition of CE also interferes with epiboly and mesoderm internalization (Shih and Keller, 1994). In zebrafish the movements are independent from one another. Strong impairment of CE does not interfere with mesoderm internalization and epiboly (Myers et al., 2002b; Solnica-Krezel et al., 1996; Wallingford et al., 2002). Extension can occur without convergence in the mesoderm of *no tail* (Glickman et al., 2003) or *somitabun* mutants (Myers et al., 2002a). There are thus apparently two components of CE in fish, first a migratory event: ‘dorsal convergence’, meaning the directed migration cells towards the dorsal midline and second, a cell rearrangement event: mediolateral intercalation at the midline that drives extension (Myers et al., 2002b; Wallingford et al., 2002).

Mediolateral intercalation is driven by polarized protrusive activity (Keller, 2002). Before mediolateral cell intercalation starts, cells extend protrusions in all directions, but when intercalation begins, cells form medially and laterally directed bipolar lamelliform protrusions that appear to attach to and crawl on adjacent cells. As a result of this traction cells elongate and intercalate (Shih and Keller, 1992a). Neural cells can intercalate using bipolar protrusive activity, or they can be secondarily induced by midline-generated signals to intercalate using a monopolar, medially directed protrusive activity (Elul and Keller, 2000; Ezin et al., 2003; Keller, 2002).

1.3.1.2 Wnt/PCP and Wnt/Ca²⁺ signaling in CE

The polarization of cells along their mediolateral axis and directed migration during CE is controlled by Wnt signaling in *Xenopus* and zebrafish. In both organisms, interfering with the Wnt ligands or components of the downstream signaling cascade leads to defects within the orientation and stabilization of cellular protrusions and CE (Jessen et al., 2002; Kilian et al., 2003; Marlow et al., 2002; Topczewski et al., 2001; Ulrich et al., 2003; Wallingford et al., 2000). Wnt11 and Wnt5 act as ligands (Heisenberg et al., 2000; Kilian et al., 2003; Moon et al., 1993; Rauch et al., 1997) and transmit through the non-canonical signaling pathway that is molecularly similar to the planar cell polarity pathway (PCP) in *Drosophila*, which regulates cell polarity within the plane of an epithelium (Adler, 2002; Mlodzik, 2002). The downstream effectors in the case of CE include the serpentine, seven-pass transmembrane receptor

Frizzled (Fz) (Djiane et al., 2000; Sumanas and Ekker, 2001; Sumanas et al., 2001) and the intracellular signaling protein Dishevelled (Dsh) (Tada and Smith, 2000; Wallingford et al., 2000). The small GTPases RhoA and Rac (Habas et al., 2003; Habas et al., 2001) signal through the Rho effector Rho kinase 2 (Rok2) (Marlow et al., 2002) or the Jun-N-terminal kinase (JNK) downstream of Rac (Habas et al., 2003; Park and Moon, 2002; Yamanaka et al., 2002) to regulate the actin cytoskeleton, cell polarity and protrusive activity. The transmembrane protein Strabismus/Trilobite/van Gogh (Stbm/Tri/Vang) (Darken et al., 2002; Goto and Keller, 2002; Jessen et al., 2002; Park and Moon, 2002) interacts with Dishevelled and localizes it to the membrane (Park and Moon, 2002). Knypek (Kny), a member of the glypican family of heparan sulfate proteoglycans (Topczewski et al., 2001) probably binds and stabilizes Wnt11.

Although CE has been most extensively studied in mesendodermal cells, it appears that the same signaling pathways are active and responsible for CE movements in posterior neuroectodermal cells (eg. (Darken et al., 2002; Gong et al., 2004; Goto and Keller, 2002; Kilian et al., 2003; Park and Moon, 2002; Wallingford and Harland, 2001; Wallingford and Harland, 2002)).

Wnt signaling is clearly required for the polarization of the cells once a polarity signal has been received but it is less clear what provides the asymmetry/polarity at the first place. *Xenopus* explants converge and extend autonomously in culture (Keller, 2002) and ubiquitously expressed components of the Wnt/PCP pathway can rescue the defects caused by loss of Wnt signals (Heisenberg et al., 2000; Kilian et al., 2003; Marlow et al., 2002). This suggests that the Wnt/PCP pathway is necessary to react to an earlier signal that confers directionality. There is recent evidence that a significant contribution comes from anterior-posterior patterning of chordamesoderm by activin-like signals (Ninomiya et al., 2004).

Genes required for CE such as *Prickle1*, *Scribble*, and *Strabismus*, are also involved in mediating branchiomotor neuron migration in the CNS, probably independent of the noncanonical Wnt pathway (Bingham et al., 2002; Carreira-Barbosa et al., 2003; Jessen et al., 2002; Wada et al., 2005). Moreover, the PCP pathway also plays a role in the migration of neural crest cells (De Calisto et al., 2005).

Wnt signaling can be transduced through a third branch independent of Dishevelled, called the Wnt/Ca²⁺ pathway. It is mediated by Ca²⁺ release, protein kinase C (PKC),

and Cdc42. This pathway seems to affect mainly adhesion and germ layer separation during gastrulation (Choi and Han, 2002; Djiane et al., 2000; Winklbauer et al., 2001).

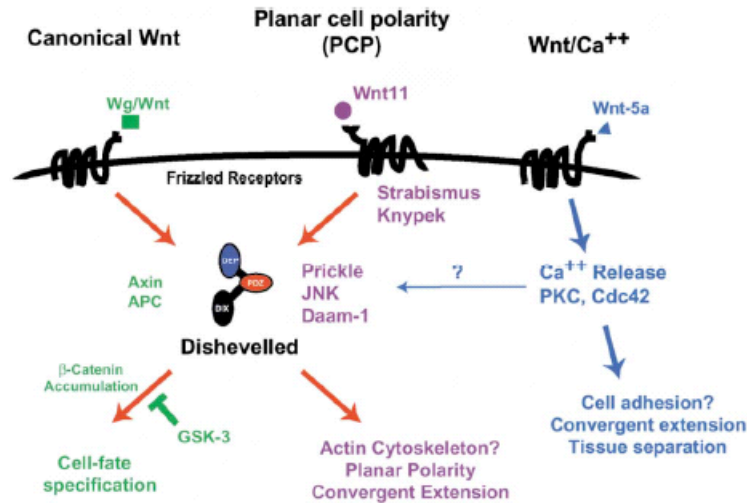


Figure 6. Canonical Wnt, PCP, and Wnt/Ca²⁺ signaling pathways.

PCP pathway members are shown in purple, Wnt components in green, and Wnt/Ca²⁺ components in blue. Adapted from (Wallingford et al., 2002).

1.3.2 Morphogenesis of the eye field and optic vesicle

1.3.2.1 The eye field

As outlined before, also the neural ectoderm undergoes CE, but this is limited to the hindbrain and spinal cord. The anterior neural ectoderm is excluded from convergence movements (Keller et al., 1992) and *Wnt11* for example is not expressed in the anterior neuroectoderm encompassing the *Six3* expression domain. It is only expressed in the lateral neuroectoderm posterior to the eye field (Heisenberg et al., 2000). *Otx2* inhibits CE of the posterior body when overexpressed and leads to reduced trunk and tail structures (Morgan et al., 1999; Pannese et al., 1995). As it is expressed in the anterior neuroectoderm and thus the region that is excluded from CE (Pannese et al., 1995), Morgan and co-workers concluded that it mediates that exclusion (Morgan et al., 1999). However, an *Otx2*-null mutation in mouse does not cause a narrowing of the head (Ang et al., 1996). Similarly, overexpression in *Xenopus* does not expand the head (Morgan et al., 1999; Pannese et al., 1995). The

defects lie rather in maintenance of anterior fate (Acampora et al., 1998; Rhinn et al., 1998) and the lack of suppression of posterior fate mediated by *Otx2* in the neural ectoderm or the AVE, respectively (Kimura et al., 2000; Perea-Gomez et al., 2001a; Perea-Gomez et al., 2001b). Nevertheless, *ClpH3*, the *Xenopus* homologue of the mammalian *Calponin* gene is a direct target of *Otx2* and is expressed in the anterior neural plate and mesendoderm and later in the forebrain and eyes. Loss-of-function of *ClpH3* rescues the phenotype resulting from overexpression of *Otx2* and blocks convergence extension movements of mesoderm in Keller explants (Morgan et al., 1999). Calponin binds actin and myosin and can prevent the sliding of actin filaments over a myosin substrate by inhibiting the ATPase activity of myosin (Shirinsky et al., 1992). A mutant form of *ClpH3* that is unable to inhibit the Mg-ATPase activity of myosin does not induce a phenotype (Morgan et al., 1999). *Otx2* has also been shown to upregulate nonmuscle tropomyosin in the mouse (Zakin et al., 2000). Furthermore, *Otx2* has been implicated in the control of other movements in the embryo, such as the movement of the AVE in mouse (Kimura et al., 2000; Perea-Gomez et al., 2001a). Moreover, *Otx2* controls the adhesive properties of cells in the midbrain (Rhinn et al., 1999). *Otx2*-mutant cells in chimeric mouse embryos are excluded from fore- and midbrain and tend to cluster and sort from WT cells. The effect in the midbrain is presumably due to the positive regulation of *R-Cadherin* and *Ephrin-A2* by *Otx2* in midbrain cells.

As discussed earlier the eye field forms by inductive signals that regionalize the anterior neural plate. In addition to cell fate specification, it becomes obvious that cellular movements are important. Ectopic expression of the eye field transcription factors *Rx1*, *Pax6*, or *Otx2* in a *Xenopus* ventral midline blastomere that normally gives rise to epidermis transfects its descendants to retina. Their gastrulation movements are altered and the cells dispersed and moved ectopically into the neural plate (Kenyon et al., 2001). A similar phenomenon was observed when interfering with Fgf signaling in *Xenopus* (Moore et al., 2004). *EphrinB1* and *Fgfr2* expression overlap along the anterolateral margin that borders the eye field, low levels of *EphrinB1* alone are expressed in the eye field. B-type ephrins have a cytoplasmic domain through which they transmit signals into the cell (reverse signaling). Fgf receptors can associate with this domain and induce its phosphorylation, resulting in enhanced cell adhesion (Chong et al., 2000). Constitutive activation of Fgf signaling

(cFgfr2) in the dorsal blastomeres that contribute to the retina blocks their retinal fate and instead causes the descendants to adopt a ventral neural fate. The effect is due to altered gastrulation movements of these cells. While wild-type descendants of the dorsal blastomeres are dispersed and populate the eye field, the cells are found closer to the midline after ectopic activation of Fgf signaling, populating the area of the presumptive neural tube. Co-expression with *Otx2*, *Pax6* and *Rx1* rescued the morphogenetic phenotype to some extent in agreement with their ability to alter cell movements in an earlier study (Kenyon et al., 2001). Increased EphrinB1 signaling in dorsal blastomeres fully rescues the phenotype caused by cFgfr2 injection and ectopic expression of EphrinB1 in ventral blastomeres caused them to populate the eye field at a higher incidence. Thus Fgf modulation of EphrinB1 signaling controls the morphogenetic movements of presumptive anterior neural plate cells and EphrinB1 reverse signaling is required to promote cellular movements into the eye field (Moore et al., 2004).

1.3.2.2 The optic vesicle

During late gastrulation/early neurulation, the single eye field condenses to a domain in the forebrain. Vertebrate eye morphogenesis starts at early neurula stage with the evagination of two bilateral optic vesicles from the forebrain. Eye morphogenesis has been analyzed in zebrafish by electron and light microscopy with special emphasis on optic cup formation (Li et al., 2000; Schmitt and Dowling, 1994). Early eye morphogenesis in fish is overall very similar to that of other vertebrates. A major difference is that the vesicles in fish evaginate as a solid mass of cells because the neural tube itself also forms initially as a solid mass and is usually referred to as neural keel. The lumen of both, the optic vesicles and the neural keel forms secondarily by cavitation (see (Schmitt and Dowling, 1994)). The optic pit and vesicle of mammals in contrast, is a hollow vesicle that originates from the lateral wall of the cephalic neural tube while the neural folds are closing (Svoboda and O'Shea, 1987). After the initial evagination, the optic vesicles (OV) flatten and extend further along the AP-axis assuming a wing-like shape in zebrafish (8-9 somites stage, SS). Only the most anterior part is now connected with the forebrain and will give rise to the optic stalk. Subsequently, the vesicles bend ventrally and rotate slightly in an anterior direction (10-12 SS). This rotation occurs in parallel with the cephalic flexure that

also brings the anterior forebrain in a more ventral position. The former dorsal and now lateral surface of the OV will give rise to the neural retina (NR), while the former ventral and now medial layer will form the retinal pigmented epithelium (RPE). The optic stalk is still at the anterior end of the primordia. Subsequently the vesicles start to invaginate distally, starting from the center of the primordium to form the eye cups. The choroid fissure, through which the optic nerve will later project to the visual centers in the brain, forms by an involution along the anterior region of the eyecup. After the eye cups are well formed (>30 SS) they undergo an anterior-directed rotation, so that the choroid fissure comes to lie ventrally. Due to the rotations that the optic vesicle and eye undergoes, the initial anterior-posterior orientation of the vesicle ultimately becomes the ventral-dorsal one of the eye (Schmitt and Dowling, 1994). The earliest process of morphogenesis, evagination itself, has not been analysed.

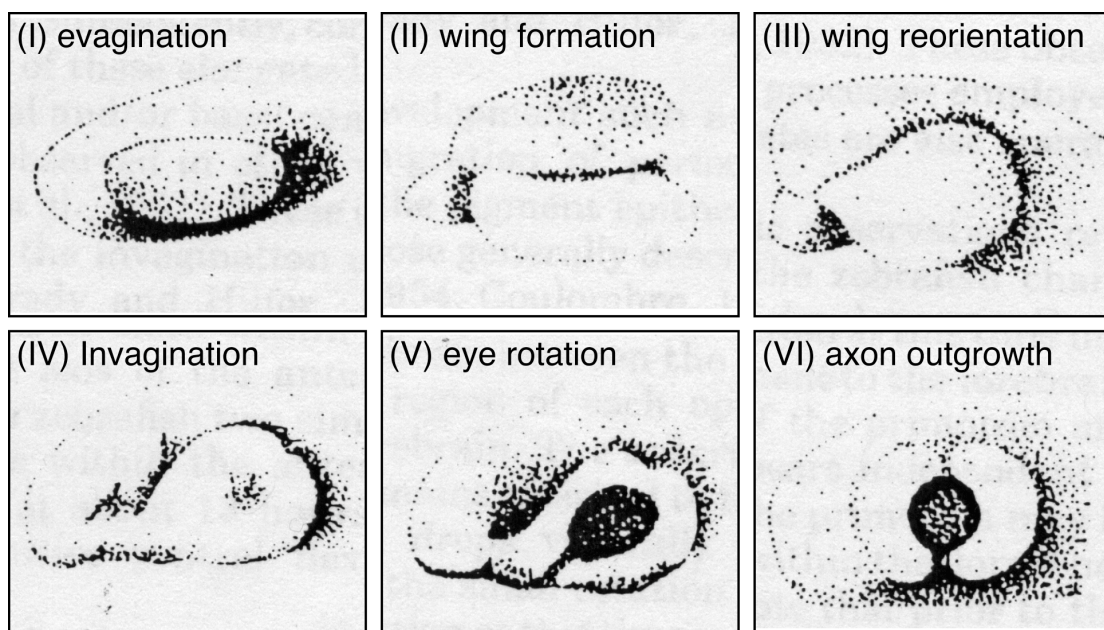


Figure 7. Eye morphogenesis in zebrafish. Adapted from (Schmitt and Dowling, 1994).

1.3.2.2.1 Rx is indispensable for optic vesicle formation

The *paired*-like homeobox genes of the *Rx* family (for Retinal homeobox) play an essential role in eye development. *Rx* genes have been identified in several vertebrate and invertebrate species, including chicken, mouse, *Xenopus*, medaka, zebrafish, humans and *Drosophila* (Casarosa et al., 1997; Chuang et al., 1999; Deschet et al., 1999; Eggert et al., 1998; Furukawa et al., 1997; Loosli et al., 1999; Mathers et al.,

1997; Ohuchi et al., 1999). The number of *Rx* genes varies between different species and ranges from one in mouse, two genes in *Xenopus* and chicken to three in medaka and zebrafish. The homeodomains are extremely well conserved and are identical between *Xenopus*, *Drosophila* and zebrafish *Rx1* and *Rx2* proteins and differ only in two amino acids between the *Xenopus* *Rx1/2* and the more divergent zebrafish *Rx3* (Mathers et al., 1997). The expression pattern of *Rx* genes in different species is similar but not identical, one conserved aspect however, is their early expression in the eye field within the anterior neural plate followed by expression in the optic vesicles/retina and ventral forebrain (see (Bailey et al., 2004). Teleost fish have three *Rx* genes, and as mentioned earlier, *Rx3* is more divergent from *Rx1* and *Rx2* (Chuang et al., 1999; Deschet et al., 1999; Mathers et al., 1997). In medaka only *Rx3* is expressed in the eye field and optic vesicles while *Rx1* and *Rx2* are expressed only in the fully evaginated vesicle (Furutani-Seiki and Wittbrodt, 2004; Loosli et al., 2003; Loosli et al., 2001). In zebrafish all three genes are expressed in the eye field and optic vesicles (Chuang et al., 1999) but *Rx1* and *Rx2* seem not to be able to compensate for loss of *Rx3* function (see later). *Rx3* becomes later restricted to the hypothalamus and excluded from the retina while *Rx1* and *Rx2* are exclusively expressed in the retina (Chuang et al., 1999; Deschet et al., 1999; Loosli et al., 1999; Mathers et al., 1997). The combined expression pattern of teleost *Rx* genes is thus equivalent to the expression domain of the single mammalian *Rx*, suggesting that the multiple roles of the ancestral *Rx* gene in forebrain development might have been split into separate roles among the teleost paralogues (Bailey et al., 2004; Chuang and Raymond, 2002).

Targeted elimination of *Rx* in mouse embryos results in the absence of eyes and forebrain (Mathers et al., 1997). The eye phenotype is characterized by a failure to form the indentations (optic sulci) that will give rise to optic vesicles. *Pax6* and *Six3* were expressed normally in the anterior neural plate but retina specific upregulation of these genes was not detected at the optic vesicle stage (Zhang et al., 2000a). The mutation of *Rx3* leads to a complete absence of eyes both in medaka and zebrafish. The phenotype is due to a defect in optic vesicle evagination despite the specification and presence of retinal precursor cells and very specifically affects only retinal precursor cells (Kennedy et al., 2004; Loosli et al., 2003; Loosli et al., 2001; Winkler et al., 2000). *Rx3* thus controls the morphogenesis and growth of the optic vesicle

independent of earlier retinal specification. The *eyeless* mutation in medaka is due to a large intronic insertion that affects the expression of *Rx3*. The mutation is temperature sensitive, at the restrictive temperature of 18°C no transcript is detected, while low levels are transcribed at the permissive temperature of 26°C. In agreement with this, small optic vesicles form under permissive conditions, correlating expression levels and optic vesicle evagination (Loosli et al., 2001). Also in mouse, the hypomorphic *ey1* allele causes a reduction in Rx protein levels and a variable size of the optic vesicle (Tucker et al., 2001). In both fish species *Pax6* and *Six3* expression is not altered in the eye field and during optic vesicle stages (Kennedy et al., 2004; Loosli et al., 2003; Winkler et al., 2000) indicating that specification of retinal precursor cells is not affected. At stages when the optic cup has formed in wild-type, retinal precursors that failed to evaginate are found in the ventral diencephalon in the mutant (Winkler et al., 2000). These cells are identified by their expression of genes specific of early retinal cells such as *Six3.1*, *Rx1*, and *Pax6* in zebrafish (Kennedy et al., 2004; Loosli et al., 2003) and by *Rx1*, *Rx2*, and *Pax6* in medaka ((Winkler et al., 2000), F.L. and J.W., unpublished data). At late somitogenesis stage an optic stalk-like structure positive for *Vax1* and *Fgf8* is found indicating that proximal-distal patterning is maintained in the absence of morphogenesis. The misplaced retinal cells fail however to differentiate as shown by the lack of *Vsx2* expression, specific for retinal cells just prior to differentiation or *Vsx1* expression, specific for differentiated neurons of the retina (Loosli et al., 2003; Winkler et al., 2000), and superfluous cells are eliminated by apoptosis occurring in two waves, at optic vesicle stage and during somitogenesis (Winkler et al., 2000).

Also in *Xenopus*, a functional inactivation of *Rx* by using dominant-negative *Rx* constructs or *Rx*-specific morpholinos leads to a reduction or loss of eyes and the anterior head. In contrast to mutation of *Rx3* in fish also anterior gene expression domains (*Otx2*, *BF-1*, *Six3* and *Pax6*) in the neural plate are affected (Andreazzoli et al., 1999; Andreazzoli et al., 2003). In humans, *RX* has an important function in eye formation as well. Mutations in human *RX* cause anophthalmia and sclerocornea (Voronina et al., 2004).

1.3.2.2.1.1 Rx genes and proliferation

Rx genes have been implicated in the control of proliferation. In *Xenopus*, overexpression of *Rx1* causes hyperproliferation of the neuroretina, the RPE and the neural tube and in some cases duplication of the neural tube (Andreazzoli et al., 1999; Casarosa et al., 2003; Mathers et al., 1997). *Rx1* has been shown to inhibit expression of *Ngnr-1* and the cell cycle inhibitor *p27Xic1* (Andreazzoli et al., 2003) and to activate transcription of *BF-1* in *Xenopus* (Andreazzoli et al., 1999; Andreazzoli et al., 2003). *BF-1* at high doses supports proliferation and inhibits *p27Xic1* (Hardcastle and Papalopulu, 2000). As a consequence of these interactions *Rx1* expressing cells proliferate but do not differentiate. Overproliferation of the optic vesicle is also observed with *Rx3* in medaka but only after their evagination from the forebrain (Loosli et al., 2001). No effect on the early eye field in the anterior neural plate can be observed, as the size of the expression domain of *Six3* and *Pax6* seems unaltered.

1.3.2.2.2 Other factors involved

Only very limited information is available about the earliest steps of OV morphogenesis and – apart from *Rx3* – the genes involved in this process. A role for the orphan nuclear receptor *tailless (tll)* in OV formation was suggested in *Xenopus* (Hollemann et al., 1998). In contrast, inactivation of the mouse homologue *Tlx* causes no defects in OV formation but later degeneration of the retina and optic nerve resulting in blindness (Yu et al., 2000). Another factor is the LIM/homeodomain protein *Islet-3*. Antagonizing *Islet-3* function by overexpression of a dominant negative form caused a failure of OV evagination in zebrafish despite the presence of *Pax2*-positive tissue in the forebrain indicating the presence of proximal/ventral retinal tissue. In contrast to the eye specific phenotype observed by loss of *Rx3*, also the formation of the isthmus, the boundary between mes- and metencephalon is defective where *Islet-3* function is non-cell autonomously required for maintenance of *Wnt1* expression. In the optic vesicles *Islet-3* is required cell autonomously as rescued eyes in mosaic analysis consist exclusively of wild-type cells (Kikuchi et al., 1997). Even less is known about the players controlling the earliest steps of OV morphogenesis at the cell biological level. Recently it has been shown that both, β -catenin as well as p120 catenin are necessary for the morphogenesis of the optic

vesicles in rat and *Xenopus*, respectively (Ciesiolka et al., 2004; Matsuda and Keino, 2001). Cadherins are a family of transmembrane cell-cell adhesion receptors. The intracellular catenin-binding domain (CBD) of Cadherins interacts with β -catenin or plakoglobin (γ -catenin). These proteins bind to α -catenin that links them to the cytoskeleton, which is required for strong adhesion (Anastasiadis and Reynolds, 2000). β -catenin accumulates at the luminal surface of the sulcus, the early evaginated optic vesicle in rat embryos, during its transition to a distally flattened fully evaginated vesicle. Treatment with Lithium-chloride abolishes this accumulation of β -catenin, and inhibits the shape change during transformation of the sulcus to the optic vesicle. Early evagination and the formation of the sulcus per se was however unaffected by Lithium treatment (Matsuda and Keino, 2001). A second highly conserved domain of the intracellular tail of Cadherins, the juxtamembrane domain (JMD) interacts with p120 catenin family members, including p120 catenin, ARVCF and δ -catenin/NPRAP. p120 does not bind to α -catenin but acts via the small GTPases RhoA, Cdc42 and Rac1 (Anastasiadis and Reynolds, 2000). *p120 catenin* is among other regions highly expressed in the optic vesicles in *Xenopus*. Knockdown of p120 in dorsal blastomeres or expression of p120 uncoupled E-Cadherin result in smaller or absent eyes, defects in the craniofacial cartilage and migration of the cranial neural crest. The phenotype is due to defective or impaired evagination of the optic vesicle as well as anterior neurulation defects (Ciesiolka et al., 2004). The phenotype observed with *Rx3* loss-of-function is thus the only one that is specific for OV morphogenesis.

1.4 Generating two eyes

The single eye field has to be split in two and thus separated along the midline to give rise to two bilaterally symmetrical optic vesicles. The signals responsible for the separation of the eye field in two and also the proximo-distal patterning of the eye emanate from the underlying axial tissue, the prechordal plate. Already in the 1930s it was found that in the absence of axial tissues the eye field never separates into two bilateral domains and the optic stalks fail to develop, resulting in cyclopia (Adelmann, 1936). Nodal signaling from the axial tissue is responsible for the bisection of the

single eye field and many zebrafish mutants exhibiting cyclopia affect this pathway such as *Cyclops* (*cyc*) or *squint* (*sqt*), both coding for a Nodal-related member of the TGF- β family (Feldman et al., 1998; Hatta et al., 1991; Rebagliati et al., 1998; Sampath et al., 1998) or *one-eyed pinhead* (*oep*), coding for the extracellular co-factor EGF-CFC (Gritsman et al., 1999). It has been proposed that Nodal is required for the anterior movement of prospective hypothalamic cells from a position posterior to the eye field. The anterior movement displaces more medially located cells and thus leads to a separation of the eye field (Hirose et al., 2004; Varga et al., 1999). A failure of this anterior movement in *cyclops* mutants (Varga et al., 1999) or in embryos with defective gastrulation movements (Heisenberg and Nusslein-Volhard, 1997; Heisenberg et al., 2000) results in cyclopia. An alternative proposition is that eye field specific gene expression is downregulated at the midline under the influence of signals from the prechordal plate (Li et al., 1997). A second function of the axial midline is the production of signals that direct proximo-distal patterning. Shh is induced by Nodal signaling (Muller et al., 2000) and specifies proximal cells to adopt optic stalk identity rather than retinal. Loss of hedgehog activity results in a failure to induce optic stalk specific genes. The presence of ectopic retinal tissue at the midline results in cyclopia (Chiang et al., 1996; Ekker et al., 1995; Macdonald et al., 1995; Varga et al., 2001). Conversely, overexpression of hedgehog results in expanded optic stalk tissue at the expense of retina (Ekker et al., 1995; Macdonald et al., 1995). In agreement with this, Shh has been reported to induce optic stalk and proximo-ventral eye markers such as *Vax1*, *Vax2* (Take-uchi et al., 2003) and *Pax2* (Ekker et al., 1995; Macdonald et al., 1995). In addition to Shh other signals, such as Fgf are involved in regulating *Vax* expression and proximal patterning (Take-uchi et al., 2003). The interaction of Shh and Fgf signaling pathways in proximo-distal patterning had been demonstrated earlier (Carl and Wittbrodt, 1999). Fgf signaling is required to induce Shh target genes. If Fgf signaling is blocked, Shh is unable to induce expression of a target gene *Spalt* (*sal*) in the proximal optic vesicle (and at the MHB) (Carl and Wittbrodt, 1999). Surprisingly, also *Six3* has proximo-distal patterning activity and is involved in the regulation of *Vax1* expression (Carl et al., 2002).

1.5 Dorso-ventral patterning of the optic vesicle

The dorso-ventral patterning of the optic cup depends on ventrally derived Shh signalling and dorsally derived Bmp signalling. Shh from the ventral midline of the neural tube promotes the expression of proximal-ventral genes such as *Vax1*, *Vax2* (Take-uchi et al., 2003) and *Pax2* (Ekker et al., 1995; Macdonald et al., 1995). At the same time, *Pax6* expression defines the dorsal-distal fates of neural retina and RPE (Schwarz et al., 2000).

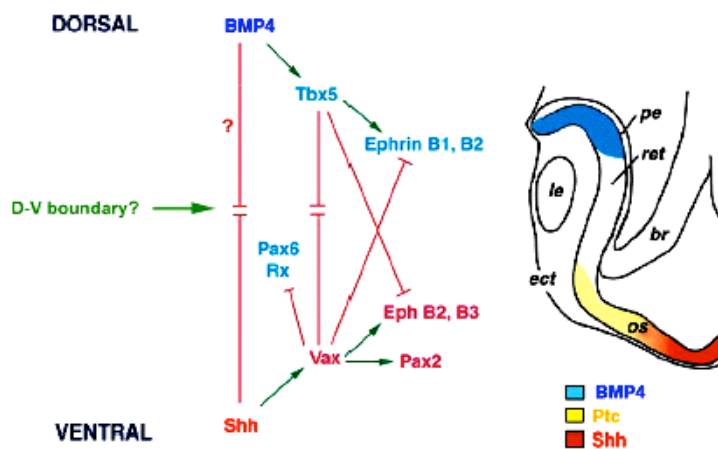


Figure 8. A model for the roles of Shh and BMP4 in D-V pattern formation of the vertebrate eye. The schematic drawing depicts a section plane through the optic fissure of an early optic cup. The optic cup is patterned by Shh emanating from the ventral forebrain and Bmp signals from the dorsal retina. Antagonistic interactions between the induced genes establish a DV boundary. Arrows and bars indicate promoting and repressing activities, respectively. *le*, lens; *pe*, pigmented epithelium; *ret*, retina; *br*, forebrain; *os*, optic stalk; *ect*, ectoderm. Adapted from (Yang, 2004).

Mice lacking *Pax2* function display optic nerve defects, including coloboma (a failure to close the optic fissure) and an extension of the RPE into the optic nerve (Torres et al., 1996). A similar phenotype is seen upon inactivation of *Vax1* (Bertuzzi et al., 1999; Hallonet et al., 1999). Recently, a double-mutant of *Vax1* and *Vax2* has been reported that displays extreme coloboma and a complete transformation of the optic stalk into retina (Mui et al., 2005) similar to zebrafish embryos injected with morpholinos against *Vax1* and *Vax2* (Take-uchi et al., 2003).

Ectopic expression of *Shh* at the optic vesicle stage abolishes dorsal *Bmp4* expression and expands ventral *Vax* and *Pax2* expression (Zhang and Yang, 2001b). In contrast, ectopically expressed *Bmp* acts antagonistically to *Shh*, suppresses *Vax* and *Pax2*

expression and induces genes of the dorsal retina such as *Tbx5* (Koshiba-Takeuchi et al., 2000). These findings demonstrate the antagonistic action of Shh and Bmp in the dorso-ventral specification of the optic cup. *Tbx5* and *Vax2* negatively regulate each other to sharpen the dorso-ventral boundary (Koshiba-Takeuchi et al., 2000; Schulte et al., 1999). The differential expression of dorsal *Tbx5* and ventral *Vax* genes controls the graded expression of the EphB family of receptors and the ephrinB ligands in the optic cup that is important for establishing the retinotectal topographic map. The dorso-ventral patterning of the optic cup is thus translated in dorso-ventral identity of the projecting axons (Barbieri et al., 2002; Bertuzzi et al., 1999; Hallonet et al., 1999; Koshiba-Takeuchi et al., 2000; Mui et al., 2002; Schulte et al., 1999).

Retinoic acid (RA) has been implicated in ventral patterning. RA treatment upregulates *Pax2* expression in zebrafish (Hyatt et al., 1996) and loss-of-function of the RA receptor RXR alpha in mouse reduces the ventral part of the optic cup (Kastner et al., 1994). Recently it has been found that Retinoic acid and Fgf signaling synergize with Shh in dorso-ventral patterning (Lupo et al., 2005).

1.6 Creating the diverse cell types of the neuroretina

During neurogenesis retinal ganglion cells (RGCs) are those that differentiate first in the retina. Neurogenesis in the eye begins within a small cluster of cells located adjacent to the optic stalk and then spreads throughout the retina resembling an advancing wavefront. Shh is required for the spreading of the wave (Neumann and Nüsslein-Volhard, 2000; Zhang and Yang, 2001a) but the initiation is independent of Shh (Neumann, 2001; Neumann and Nüsslein-Volhard, 2000). If the optic stalk is removed or fails to form as in *oep* mutants, neurogenesis is not initiated (Masai et al., 2000). It has been shown recently, that indeed Fgf is the signal that triggers the onset of retinal ganglion cell differentiation in fish and chick (Martinez-Morales et al., 2005). Implantation of Fgf-soaked beads induces neurogenesis and is able to rescue the retina differentiation in *oep* in the absence of an optic stalk. Neurogenesis is also absent in mutants for both *Fgf3/lia* and *Fgf8/acerebellar* (Martinez-Morales et al., 2005). In agreement with this several Fgf family members are expressed in the optic stalk, among which are *Fgf3* and *Fgf8* (Crossley and Martin, 1995; Herzog et al.,

2004; Martinez-Morales et al., 2005; Vogel-Hopker et al., 2000; Walshe and Mason, 2003) and Fgf signaling is required for optic stalk development itself (Shanmugalingam et al., 2000; Take-uchi et al., 2003).

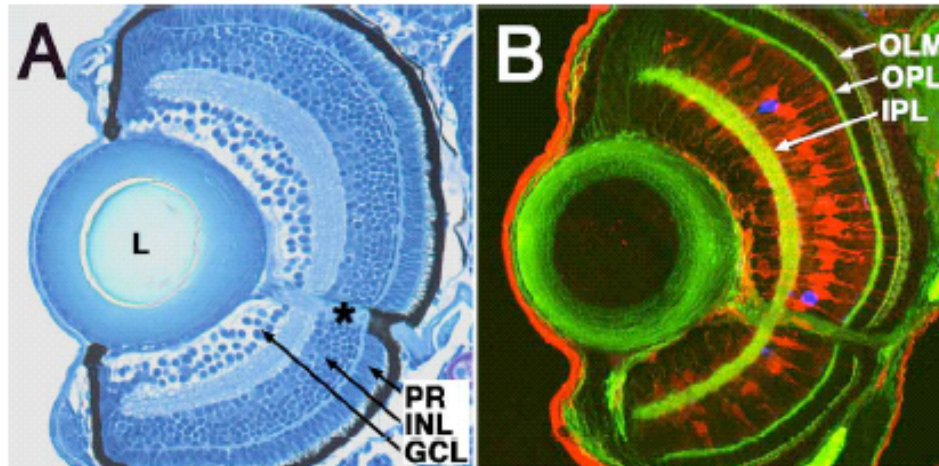


Figure 9. Pattern formation and cell types in the retina. Panel A shows a plastic section through a zebrafish eye with the ganglion cell layer (GCL), the inner nuclear layer (INL) containing interneurons, namely amacrine, Müller glia, bipolar and horizontal cells and the photoreceptor layer (PR). The asterisk marks the optic nerve. L, lens. The darkly pigmented layer is the retinal pigmented epithelium (RPE). Panel B shows F-actin staining in green, marking the axons of the inner plexiform layer (IPL) and the outer plexiform layer (OPL). OLM, outer limiting membrane. Adapted from (Pujic and Malicki, 2004).

The 7 major cell types of the retina are generated in a timely ordered fashion: ganglion and horizontal cells differentiate first, followed in overlapping phases by cone-photoreceptors, amacrine cells, rod-photoreceptors, bipolar cells and Müller glia cells last (Marquardt and Gruss, 2002). Retinal progenitor cells are multipotent and can generate several cell types up to their final cell division (Holt et al., 1988; Turner et al., 1990; Wetts and Fraser, 1988) but they are limited in a way that a particular progenitor can only generate a subset of retinal cell types at a given time. Extrinsic factors can only change the relative proportion of a particular cell type made (Austin et al., 1995; Belliveau and Cepko, 1999; Belliveau et al., 2000). These observations lead to the competence model that proposes that progenitors pass through a series of competence states during which they are able to generate a specific subset of retinal cell types. The competence state is determined by intrinsic factors such as bHLH transcription factors and the generation of specific cell types within a certain competence state by extrinsic factors (reviewed in (Livesey and Cepko, 2001; Marquardt and Gruss, 2002)).

1.7 Aim of the thesis

The vertebrate eye has been extensively studied as a model for induction, patterning, cell fate specification and differentiation. The major component of the eye that gives rise to neural retina, retinal pigmented epithelium (RPE) and the optic stalk and nerve originates from the neuroectoderm and the eyes fail to develop without the evagination of optic vesicles from the anterior forebrain. Amazing progress has been made in unraveling the mechanisms and signals underlying early morphogenesis of the zebrafish embryo. In these studies however, the neuroectoderm has been rarely looked at and very little is known about the movement of cells within the eye field or during optic vesicle evagination. The process of evagination, although of crucial importance remains completely obscure. Optic vesicle morphogenesis requires the function of the *paired*-like homeodomain gene *Rx3* as loss-of-function of *Rx3* causes a failure of optic vesicle evagination (Loosli et al., 2003; Loosli et al., 2001). In contrast to other eye mutants the evagination process is very specifically affected with no other phenotypes. A 4 kb promoter element upstream of *Rx3* had been isolated earlier by Felix Loosli in the lab. It is sufficient to recapitulate endogenous *Rx3* expression if driving GFP and was used to follow the fate of *Rx3*-positive eye field cells during optic vesicle formation. The aims of the thesis were first to establish a 4D imaging set up for medaka. Subsequently, I aimed at the analysis of the cellular movements and forces that drive optic vesicle evagination by *in vivo* 4D imaging in the wild-type and *Rx3*-mutant background to get insight into the link between cell fate specification and the induction of a specific cellular behaviour.

2 RESULTS

2.1 *In vivo* time-lapse imaging in medaka – n-Heptanol blocks contractile rhythmical movements

Microscopic time-lapse imaging is an important and powerful technique to follow the development of cells and organs *in vivo*. Recent advances in imaging techniques, the development of confocal and two-photon laser-scanning microscopes combined with the use of green fluorescent protein (GFP) has opened new possibilities (Megason and Fraser, 2003). The number of fluorescent proteins with different spectral properties is steadily growing (Lippincott-Schwartz and Patterson, 2003; Matz et al., 2002; Tsien, 2005). Taking into account recent advances in transgenesis and enhancer-trapping (Grabher et al., 2003; Grabher et al., 2004; Thermes et al., 2002), different structures in the fish embryo can be marked by GFP expression under the control of specific promoters or enhancer elements. Subsequently, their development and morphogenesis can be followed in real-time. The killifish medaka (*Oryzias latipes*) is an ideally suited genetic model organism that has been used to study embryogenic development and sex determination (Wittbrodt et al., 2002). Due to the transparency of embryo and yolk, development can easily be observed by light microscopy. However, from mid-epiboly stages onwards (Iwamatsu stage 14/15) (Iwamatsu, 1994) rhythmic contraction waves propagate across the periderm of the embryo. The amplitude of the contractions peaks around stage 18 and ceases after the onset of the heart beat (stage 26) (Cope et al., 1990; Fluck et al., 1983; Robertson, 1979; Yamamoto, 1975). Rhythmical contractile movements are known for other teleost species, such as goldfish (*Carassius auratus*), pike (*Esox lucius*) and sticklebacks (*Gasterosteus* and *Pygosteus*) (Yamamoto, 1975). Their function is unknown but they occur predominantly in embryos with a high yolk to cytoplasm ratio and simple vitelline vessels. It has thus been proposed that the movements might aid the transport and adsorption of yolk components to the blastoderm (Yamamoto, 1975).

After completion of epiboly in medaka, the waves move over the entire surface of the embryo causing it to rotate within the chorion. These vivid movements and rotations preclude microscopic time-lapse observation that requires the immobilization of the specimen. For long-term microscopic time-lapse imaging we intended thus to block the contractile movements over long periods.

As mentioned before, the embryo is covered by the enveloping layer (EVL), a simple epithelium that serves as a protective shield but is not incorporated into the body tissues of the adult animal (Fleig, 1993; Warga and Kimmel, 1990). A thin layer of stellate-like cells beneath the EVL is responsible for the contractile movements (Cope et al., 1990). The contraction waves depend on extracellular calcium (Fluck et al., 1984; Sguigna et al., 1988) and are preceded by intercellular Ca^{2+} waves and intracellular Ca^{2+} oscillations within the stellate cell layer, indicating a role for gap junctional communication (Fluck et al., 1991; Simon and Cooper, 1995). It had been demonstrated previously that bathing of embryos for 40 minutes in either of the gap-junction inhibitors *o*-nitrobenzylacetate (*o*-NBA), *n*-heptanol or *n*-octanol blocks pulsing activity for 10 – 60 minutes, followed by a complete recovery from the block (Cope et al., 1990). In order to analyze the effect of these substances on development we tested them by bath application. *o*-NBA in a concentration of 1 mM immediately arrested development (data not shown). It has been shown, that *o*-NBA at concentrations of 1- 5 mM reduces gap junction conductance by drastically acidifying the cytoplasm (Spray et al., 1984). This decrease in pH_i might well be responsible for the negative effects on the embryos. *N*-heptanol and *n*-octanol, however, uncouple gap junctions without decreasing the intracellular pH or affecting the Ca^{2+} concentration (Meda et al., 1986). In medaka embryos neither octanol nor heptanol affected early development when applied in a concentration of 1 mM and 3.5 mM, respectively (Fig. 11f). Only a minor slowdown of the rate of development was observed. While untreated embryos developed from early gastrula stage (st 16) to the 9-somite stage within 28 hours at 18°C, siblings treated with 3.5 mM 1-heptanol developed to the late 8-somite stage. Careful morphological examination showed no difference in the extent of development compared to control embryos at the 8-somite stage. Further experiments were performed only with 1-heptanol.

Embryos were dechorionated and incubated in balanced salt solution (BSS) containing 3.5 to 7 mM 1-heptanol depending on the developmental stage. As the amplitude of the contractions is highest at stage 18 (Cope et al., 1990), higher concentrations were needed for inhibition at this stage, whereas 3.5 mM is sufficient for gastrula stages (st 16) or later than stage 18. Embryos were incubated for at least 1 hour to stop all contractile movements before embedding them in 0.5 to 1 % low melting point agarose in glass-bottom petri dishes. All media contained 1-heptanol

(3.5-7 mM) as the embryos otherwise recover rapidly from the effect of the drug. Subsequently, the embryos were analyzed under a light microscope. Figure 10 shows still images from a short time-lapse sequence covering 12.5 minutes. Without heptanol treatment the embryos exhibit contractile movements and rotate even in stringent embedding medium of 1 % agarose. One contractile wave runs across the yolk within one minute at 25°C (Fig. 10b-d, see figure legend; see also supplementary movie S1). Eventually, the embryo turns and disappears from the field of view. Heptanol-treated embryos show reduced contractions that are not spreading as a wave over the time period observed (Fig. 10f-j and supplementary movie S2). The embryo is thus immobilized in the embedding medium and amenable to microscopic observation.

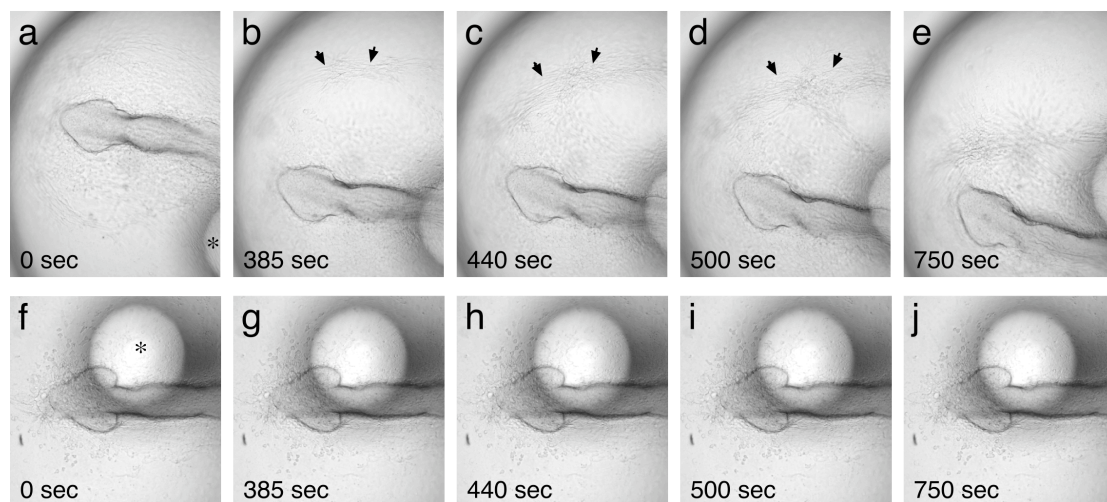


Figure 10: *n*-heptanol inhibits rhythmical contractile movements.

Still images of a short time-lapse sequence of 12.5 minutes with images taken every 5 seconds. The upper panel (a-e) shows a stage 18 embryo embedded in 1% agarose without the addition of 1-heptanol. The embryo contracts rhythmically, one contractile wave travels across the yolk within one minute (see arrows in b-d, the images are 1 min apart). The embryo rotates and eventually disappears from the camera field. The embryo presented in the lower panel (f-j) has been treated with 7 mM 1-heptanol. Contractile events are still seen (see supplementary information, movie 2) but they are not spreading as waves over the time period observed. The asterisks in (f) marks the oil droplet.

The images were recorded at a Leica DM ASW workstation with a magnification of 10x. Taken from (Rembold and Wittbrodt, 2004).

Long-term imaging over 21 hours showed that the embryo develops normally in the presence of 7 mM heptanol (Fig. 11 and supplementary movie S3). The embryo was embedded in 1 % agarose at the optic vesicle stage (stage 18) and observed until early somitogenesis (stage 22). The contractions were not completely inhibited but strongly reduced; the embryo was prevented from rotating in the agarose.

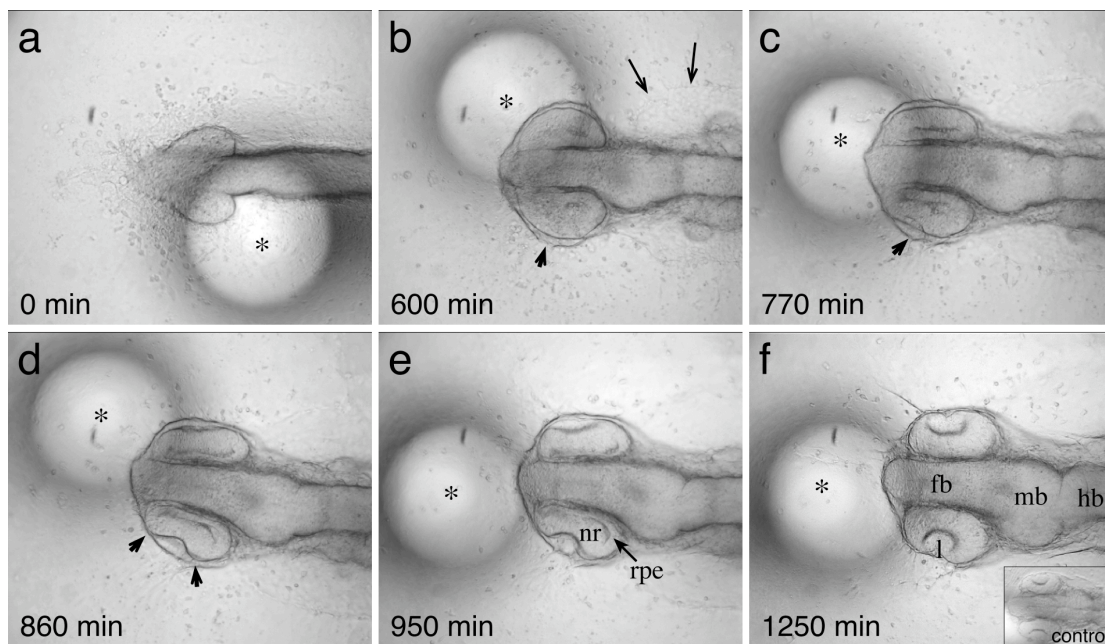


Figure 11: *In vivo* time-lapse of the development of anterior structures.

The sequence covers 21 hours of development at an ambient room temperature of 24°C. The embryos were treated with 7 mM heptanol and embedded in 1 % agarose. **(a)** The sequence starts at stage 18, the optic vesicles are already evaginated from the forebrain. **(b)** The optic vesicles have grown in size, two layers can be seen. The arrowhead marks the lens ectoderm, the arrows delimitate the developing body cavity. **(c)** Optic cup morphogenesis started with the distal infolding of the optic vesicle. The arrowhead points at the thickening lens placode. **(d)** The optic cup further invaginates and the lens is forming. **(e)** Two layers can be distinguished in the retina, the thickened neural retina (nr) and the thin retinal pigmented epithelium (rpe). **(f)** The last frame shows a stage 22 embryo, the neurocoel has differentiated to forebrain, midbrain and hindbrain. The inset shows an untreated control embryo. Fb, forebrain, hb, hindbrain, l, lens, mb, midbrain. The asterisk marks the oil droplet. The images were recorded with a Leica DM ASW workstation, magnification is 10x. Taken from (Rembold and Wittbrodt, 2004).

Time-lapse imaging of immobilized embryos was used for a detailed analysis of optic cup morphogenesis starting from the late neurula stage (st 18). During the first hours the optic vesicle is growing in size, two layers of equal width can be distinguished (Fig. 11b). Moreover, the body cavity has formed on the surface of the yolk sphere (see arrows in Fig. 11b). Subsequently, the vesicle starts to fold distally, concomitantly with the thickening of the lens placode. Upon further invagination, the cells in the outer cell layer of the optic cup change shape and cause the layer to flatten; it will later give rise to the retinal pigmented epithelium. The inner layer that will differentiate to the neural retina, enlarges (Fig. 11e). At the same time the lens develops from the lens placode. The neurocoel is formed into fore-, mid- and hindbrain (Fig. 11f).

In order to study morphogenetic processes in more detail I used confocal microscopy in combination with fluorescent proteins. Histone H2BdiHcRed mRNA (Gerlich et al., 2003) was injected at a concentration of 200 ng/ μ l into one-cell stage embryos, to fluorescently label all nuclei. The embryo was treated with 3.5 mM heptanol, embedded at late gastrula stage in 0.5 % agarose and subjected to confocal time-lapse microscopy on a Leica TCS SP2 setup. Z-stacks were recorded every 10 minutes over 138 μ m at an interval of 3 μ m. The images were 3D reconstructed over time using the Volocity software (Improvision, UK). The sequence (Fig. 12 and supplementary movie S4) shows the convergent extension movements of neural plate cells and the formation of the neural keel. Subsequently, the optic vesicles evaginate from the forebrain. Again, residual contractile activity was observed exerting only minor influence on the position of the embryo and did not interfere with imaging at a single cell resolution.

In summary the method allows imaging of early stages of medaka development by continuous treatment of embryos with heptanol. Even though residual minor movements remain, single cell resolution can be obtained in time-lapse analysis. We did not observe an influence on development at the concentrations used (3.5 to 7 mM). In early medaka embryos heptanol has no detrimental effect on the cells, although we have not tested stages prior to gastrulation. The residual contractile activity indicates that gap junctional conductance is not blocked, but only reduced which might also account for its lack of a negative effect on development. The establishment of *in vivo* imaging conditions for medaka, allowed the subsequent analysis of optic vesicle morphogenesis at subcellular resolution.

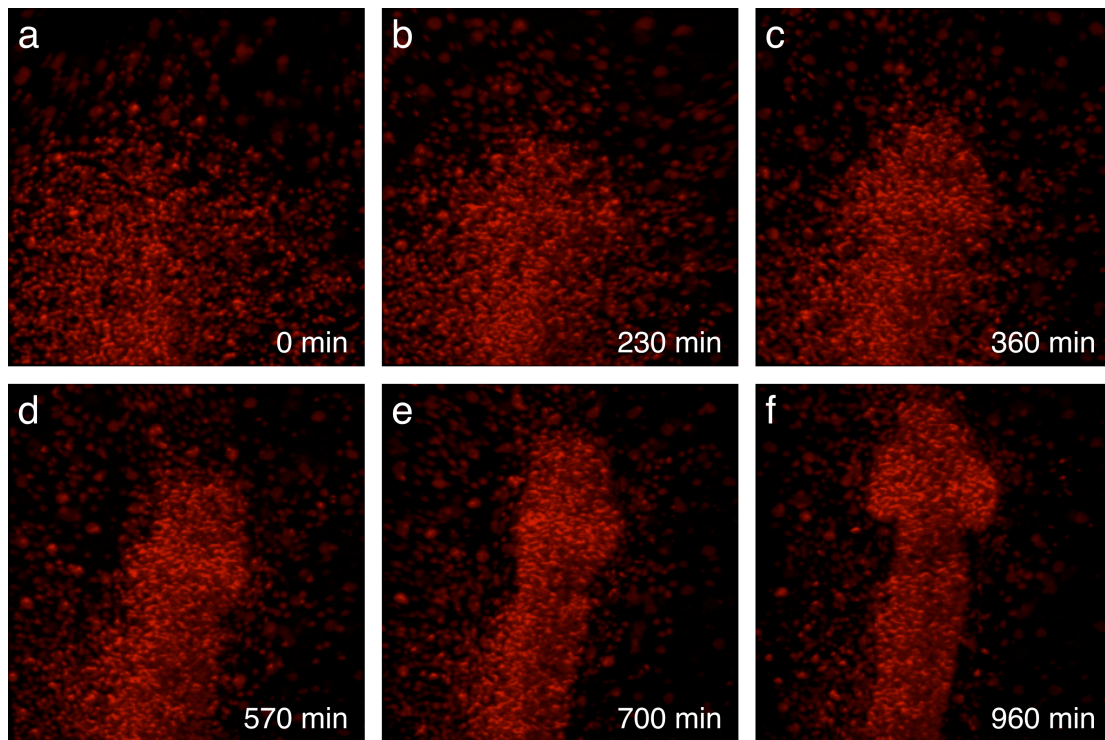


Figure 12. 3 D reconstruction of anterior development.

Embryos were injected with H2BdiHcRed mRNA (Gerlich et al., 2003) at one-cell stage and treated with 3.5 mM 1-heptanol. The embedding medium consisted of 0.5 % agarose. **(a-d)** The initially dispersed cells at neural plate stage converge and form the neural keel. **(e-f)** Optic vesicles evaginate from the forebrain. The images were acquired on a Leica TCS SP2 confocal microscope with a 10x/0.3 NA immersion objective. Taken from (Rembold and Wittbrodt, 2004).

2.2 *In vivo* analysis of optic vesicle morphogenesis

The eye originates from a single eye field in the anterior neural plate, which condenses during neurulation to a domain located in the prosencephalon. The first morphological sign of eye development is the evagination of two bilateral optic vesicles from the forebrain (Chow and Lang, 2001; Chuang and Raymond, 2002). The complex 4-dimensional movements that take place during the formation of the neural system in fish have been addressed by fate mapping using single cell labelling (Hirose et al., 2004; Varga et al., 1999; Woo and Fraser, 1995). Fate mapping studies and lineage analysis can however not address the dynamics of cell movement or cell shape changes and have to deduce the behaviour of cells in between two developmental stages used for map construction. In particular, the cellular rearrangements, movements and cell shape changes that occur during optic vesicle evagination have remained elusive. Therefore we chose a live-imaging approach taking advantage of the transparency of the medaka fish (*Oryzias latipes*) to investigate the morphogenesis of the optic vesicles.

2.2.1 *Rx3* modulates the movement of eye field cells

To identify retinal precursor cells in the early eye field, *Rx3* expression was used as a fate marker. The homeobox transcription factor *Rx3* is expressed in the eye field of gastrula stage embryos (st 16) and later in the evaginated optic vesicles (Chuang et al., 1999; Deschet et al., 1999) and marks thus all retinal precursor cells. An 11 kb genomic fragment containing the genomic locus of the medaka *Rx3* gene was used by Felix Loosli to insert GFP into the second exon of *Rx3* by homologous recombination in *E. coli* (F. Loosli and J. Wittbrodt, unpublished). Transcription from this construct gives rise to a fusion protein consisting of the N-terminus of *Rx3* up to amino acid 166 fused to the N-terminus of GFP. As the homeodomain is disrupted, the protein is non-functional and neutral with respect to development. The *Rx3*-GFP plasmid was used to establish a stable transgenic line (ET19, F. Loosli, unpublished). The expression of GFP faithfully recapitulates the expression pattern of the endogenous gene (Fig.14). Interestingly, the N-terminus of *Rx3* seems to contain an element that regulates protein stability, as fluorescence from the *Rx3* Δ HHD-GFP fusion is lost in the

posterior part of the optic cup from early somitogenesis (st 20) onwards, similar to expression of endogenous *Rx3* (Deschet et al., 1999). GFP alone has a half-life of more than 24 hours and the loss of fluorescence in the posterior optic cup is not observed if a 4 kb promoter fragment (F. Loosli and J. Wittbrodt, unpublished) is used to drive GFP or mYFP expression (see *Rx3mYFP* line).

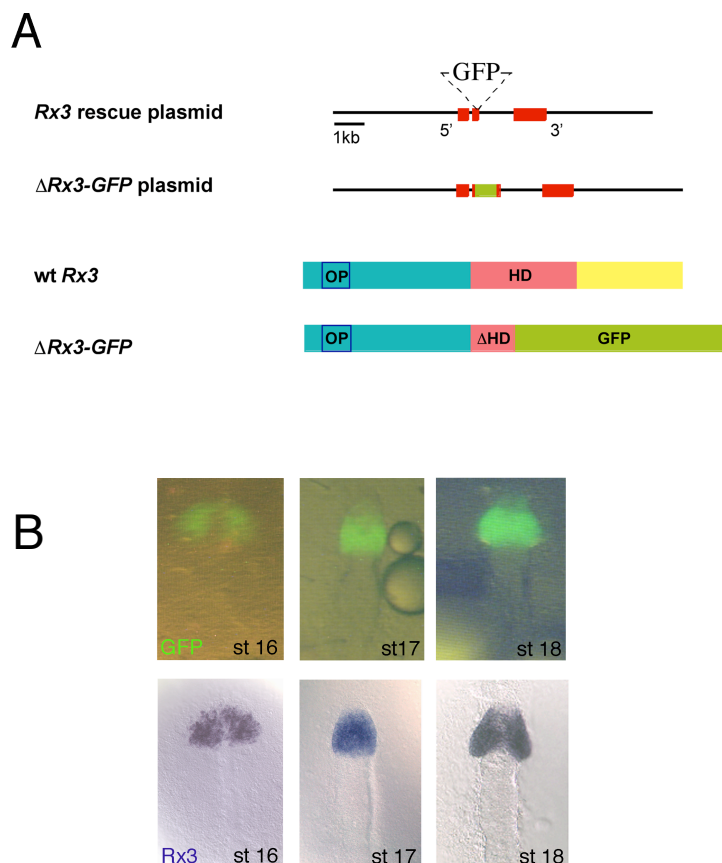


Figure 14. Construction of an *Rx3*-GFP (ET19) transgenic line.

(A) The *Rx3*-GFP BAC clone used to establish the ET19 transgenic line. The upper line shows the *Rx3* rescue plasmid that contains the *Rx3* genomic locus used to rescue the *eyeless* phenotype (Loosli et al., 2001). The red boxes represent the three exons of *Rx3*, GFP was inserted into the second exon ($\Delta Rx3$ -GFP plasmid). This gives rise to a fusion protein of 166 amino acids of *Rx3* to the N-terminus of GFP ($\Delta Rx3$ -GFP). (B) The expression pattern of $\Delta Rx3$ -GFP (shown in the upper panel) recapitulates the expression of endogenous *Rx3* shown by *in situ* hybridization (lower panel). (F. Loosli, unpublished)

To monitor the dynamic behaviour of individual cells during optic vesicle morphogenesis, ET19 embryos were injected with histone H2B-mRFP mRNA (Campbell et al., 2002; Megason and Fraser, 2003) and imaged at high spatial ($2 \mu\text{m}$)

and temporal (2 min interval) resolution by confocal time-lapse microscopy. The nuclear label was used to track individual cells in the acquired 4D sequences. A single confocal plane of a time-lapse sequence in Figure 15 illustrates the formation of the optic vesicles (see supplementary movie S5). The recording begins at late gastrula stage (stage 16) and covers 10 hours of development at 20°C. The wide eye field in the anterior neural plate at st 16 (Fig. 15b), identified by GFP expression, condenses to a more compact domain in the forebrain during the formation of the neural keel (Fig. 15c). Optic vesicle evagination starts with a small outbulging (Fig. 15d, arrows) that subsequently enlarges as optic vesicles form (Fig. 15e-f). After 10 hours of development most retinal precursor cells have moved from the forebrain into the growing vesicles that are now separated by diencephalic cells that moved anteriorly from positions posterior of the eye field (Fig. 15h, asterisk).

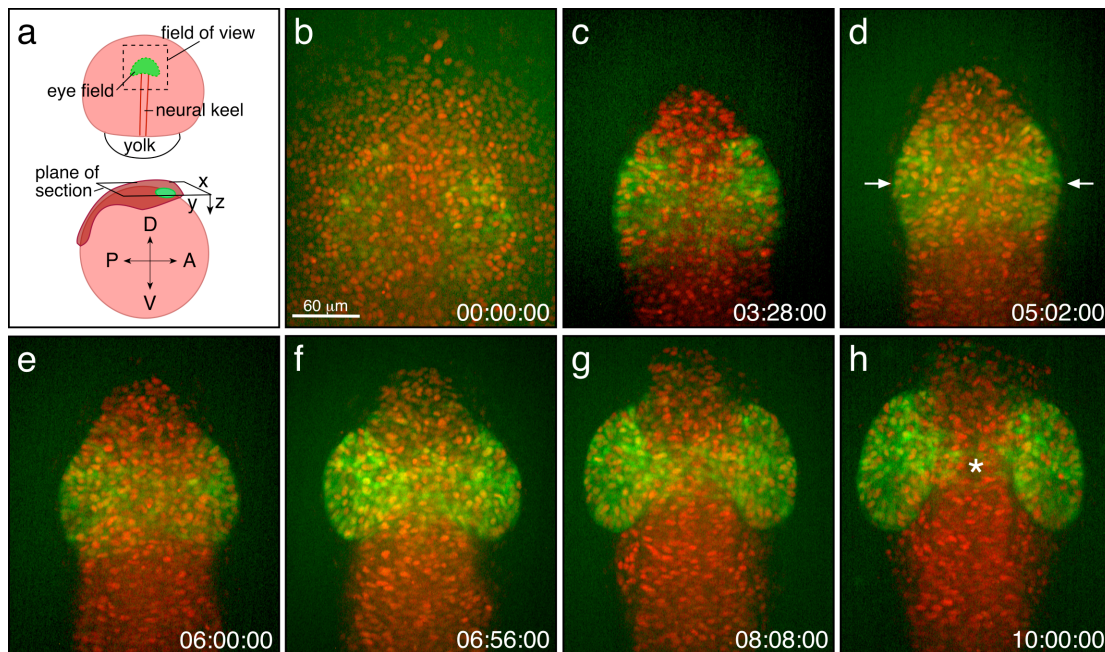


Figure 15. Time-lapse sequence of optic vesicle formation. The panel shows single confocal sections of a recording covering 10 hours of development, viewed from dorsal, anterior is to the top. The embryos express GFP under the control of the *Rx3* promoter (green, ET19), nuclei are labelled by histone H2B-mRFP (red). Time is given in hours:minutes:seconds in all figures. **(a)** Overview of the experimental setup. **(b)** The early eye field at late gastrula stage (st 16), identified by GFP expression, is a wide domain in the anterior neural plate. **(c)** During neural keel formation the eye field condenses to a domain located in the forebrain. **(d)** A first outbulging marks the onset of optic vesicle formation (arrows). **(e-g)** During the next 5 hours the optic vesicles grow as more GFP-positive retinal precursor cells move from the forebrain into the vesicles. **(f)** After 10 hours of development most retinal precursors have evaginated, the two eyes are separated by forebrain cells that moved anteriorly (asterisk).

Magnification: 20x

To elucidate the cell movements during optic vesicle morphogenesis I tracked the position of single nuclei in time-lapse recordings from gastrula to early somitogenesis stage in collaboration with Richard Adams from the University of Cambridge who wrote and provided the code for tracking and analysis (Fig. 16 and supplementary movies S6, S7). Figure 16 shows representative 3D reconstructions of the positions of tracked cells in dorsal (a-f) as well as frontal views (g-l). The eye field is surrounded at its anterior-lateral and posterior borders by telencephalic and diencephalic precursor cells (Hirose et al., 2004; Woo and Fraser, 1995), shown in blue. In the course of neural keel formation the laterally located forebrain cells along with cells from the lateral border of the eye field (Fig. 16, cells 5, 6, 7 and 8 represent forebrain cells, cell 1 is lateral eye field; see also double-arrows in g-l) converge stronger towards the midline as the more medioventrally located retinal precursor cells that lag behind (Fig. 16a-f, cells 3 and 4). Lateral (forebrain) cells move thus over more ventral cells (see Fig. 16c-d) in a process resembling an upfolding of the neural plate. This slow movement of medioventral eye field cells gives rise to a widened eye domain in the neural keel that primes the site of evagination (Fig. 16b-c, h-k, arrows). The widening is supported by an initial ventrally-directed movement/displacement of eye field cells (Fig. 16h-j, arrows), that later move laterally into the growing optic vesicles (Fig. 16k-l), again representing an upfolding-like movement of the neural plate and eye field and ventral/lateral displacement of medially located cells. The initially laterally located eye field cells that move first towards the midline (Fig. 16a-f, cell 1) later change direction and move first ventrally then laterally into the optic vesicles. The dorsal forebrain cells continue their medially-directed movement. Cells that are located in the posterior-lateral eye field (Fig. 16a-f, cell 2) move towards the midline and then anteriorly in the opposite direction to cells that had already evaginated. The latter move towards the posterior within the vesicle, resembling a ‘rolling-out’ – mechanism: posterior movement in the vesicle, anterior movement at the midline (Fig. 16d-f, cells 3, 4, and 1, compare to cell 2). The optic vesicles then grow by the movement of retinal precursors from the forebrain into the vesicles, while posterior forebrain cells continue to move towards the midline (Fig. 16d-f, compare 3,4 and 8).

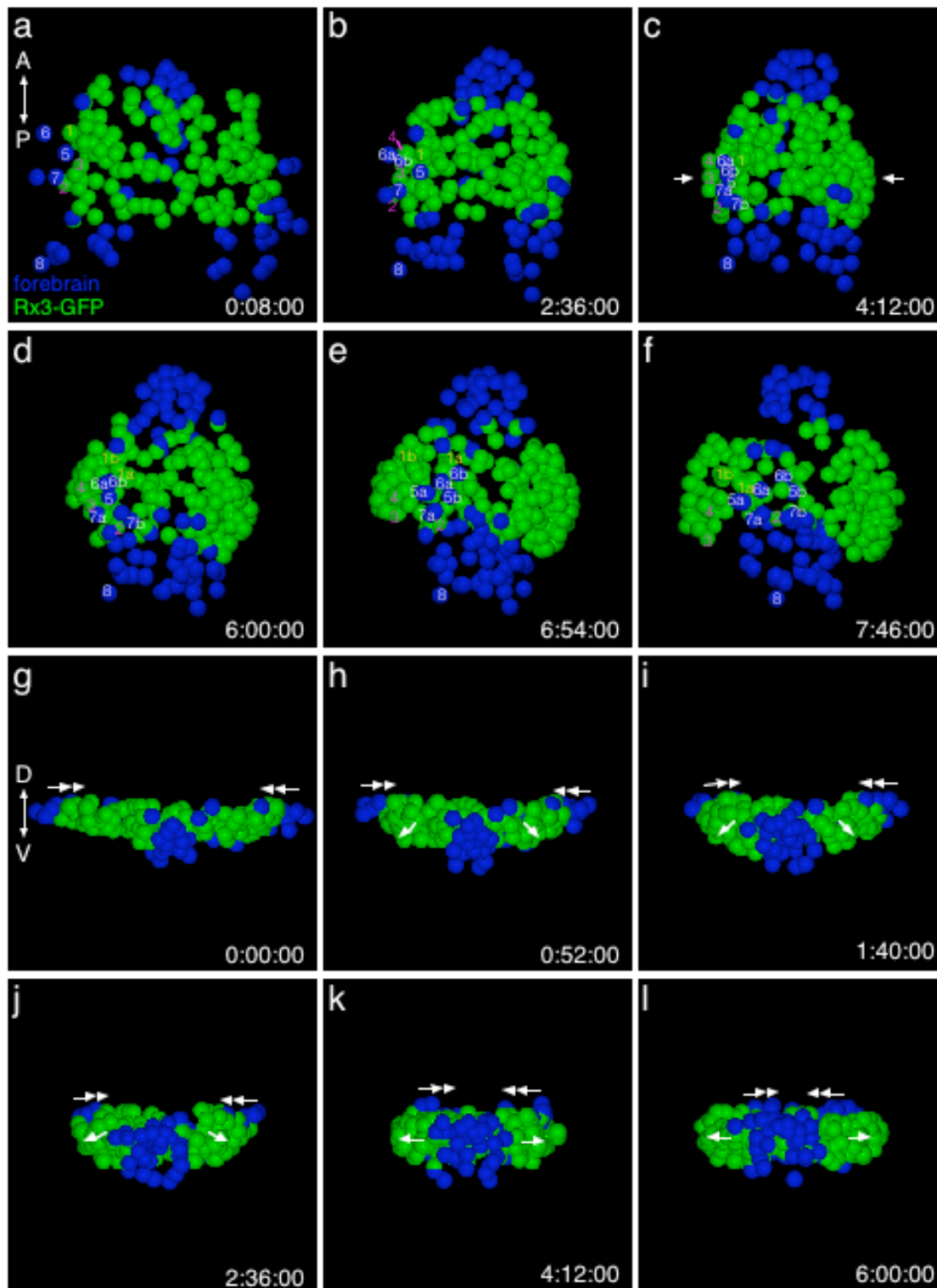


Figure 16. Modulation of midline-directed movements within the eye field.

Single cells were tracked in time lapse recordings from early eye field to optic vesicle stage. The 3D positions of individual cells are depicted as balls in 3D renderings (POVray). Rx3 positive cells are shown in green, forebrain cells in blue. **(a-f)** Dorsal view, anterior is to the top, **(g-l)** frontal view, dorsal is to the top. Several representative cells are numbered to follow their path. **(a-f)** Cells of the dorsal forebrain (white, cells 5, 6, 7) move faster towards the midline than underlying eye field cells (pink, cells 3, 4), keeping the eye domain wide before actual evagination starts. Note that the dorsal-lateral cell 1 (yellow) moves first towards the

midline, before it moves into the vesicles. Cells from the posterior eye field move towards the midline and anteriorly (cell 2), while the cells which evaginated first (3, 4, 1) move posteriorly within the vesicle, resembling a ‘rolling-out’-movement.

(g-l) Forebrain cells located laterally to the eye field move faster and over eye field cells located ventrally to them (double arrows) to form the dorsal forebrain **(l)**. By their medial movement, more medially located eye field cells get displaced and move ventrally (arrows in **h-j**). The combination of these processes gives rise to a wide eye domain that precedes evagination **(k-l)**. A, anterior; P, posterior; D, dorsal; V, ventral.

In summary, the slower medial movement of lateral-ventral eye field cells along with the ventral displacement of medial eye field cells gives rise to a widened eye domain in the forebrain, that precedes evagination. Later, lateral and posterior movement of retinal precursor cells leads to the growth of the optic vesicles. Cells of the prospective telencephalon in contrast move only towards the midline to form the dorsal telencephalon. The prospective diencephalic cells located posteriorly to the eye field also initially follow a midline-directed movement and subsequently move anteriorly. They eventually come to lie between the two optic vesicles. This movement might aid in the separation of the eye field cells at the midline and the establishment of two separate optic vesicles. A mechanical ‘push’ could potentially contribute to the late evagination process, i.e., the movement of medial retinal precursor cells from the neurula stage eye field into the vesicles. Thus anterior and posterior cells of the forebrain form a neural keel by convergence towards the midline, while eye field cells stop and modulate this midline-directed movement.

2.2.2 Neurulation-like behaviour in *Rx3* mutant cells

The analysis of mutant phenotypes is important in understanding developmental and morphogenetic processes in the wild-type organism. The medaka mutant *eyeless* has been found to specifically affect the morphogenesis of the optic vesicle downstream of patterning (Loosli et al., 2001; Winkler et al., 2000). It lacks eyes due to a failure of optic vesicle evagination although retinal precursor cells are present and specified as judged by unaltered *Pax6* and *Six3* expression in the eye field and during optic vesicle stages. At stages where the optic cup has formed in wild-type, mutant retinal precursors are found in the wall of the ventral diencephalon. These cells are characterized by expression of early retinal genes such as *Rx2* and *Pax6* (Winkler et al., 2000).

We have thus a mutant that has a specific defect in the morphogenetic movements that retinal precursors normally undergo, such that they remain within the forebrain and integrate into the diencephalon. To get insight into the cellular basis of the morphogenetic defect and the role of *Rx3* in this process, I applied the same *in vivo* imaging and tracking analysis as in the wild-type. The ET19 line was crossed to the *eyeless* background (ET;*el,B*), embryos were injected with histoneH2B-mRFP and imaged by confocal microscopy, as described before. By light microscopic observation the phenotype becomes visible only after the onset of evagination in wild-type (st 18). Confocal time-lapse analysis of mutant embryos revealed however, that the phenotype is evident already during early neurulation (st 17) by a more complete movement of the eye field towards the midline (Fig. 17, arrows, compare to Fig. 15d; and supplementary movie S8).

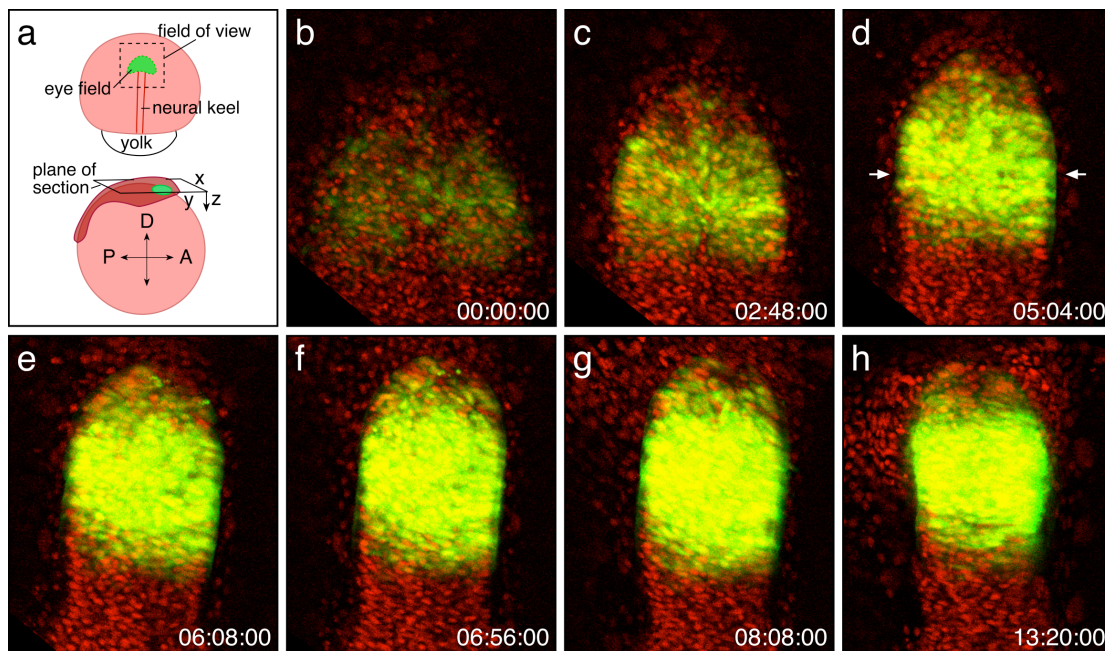


Figure 17. Time-lapse sequence of *eyeless* embryos.

The panel shows single confocal sections of a recording covering more than 13 hours of development, viewed from dorsal. Anterior is to the top. The embryos express GFP under the control of the *Rx3* promoter (green, ET;*el,B*), nuclei are labelled by histone H2B-mRFP (red). (a) Overview of the experimental setup. (b) The early eye field at late gastrula stage (st 16) is indistinguishable from wild-type. (c-g) During neurulation the eye field condenses much stronger as in wild-type (d, arrows) to a domain as narrow as the neural keel posterior to it. Even after more than 13 hours (h) no sign of evagination can be seen, and the mutant retinal precursor cells are packed very densely in the forebrain. Magnification: 20x

Tracking of individual eye field and forebrain cells revealed no difference of the late gastrula stage eye field of *eyeless* and wild-type (Fig. 18b) but subsequently retinal cells continue to move towards the midline to the same extent as forebrain cells (Fig. 18b-f, g-l and supplementary movie S9, S10). The lateral widening that primes evagination in wild-type is not present (Fig. 18d, and 18j compare with Fig. 16c and 16j), instead a narrow neural keel-like structure is formed. This is also evident in frontal views, that show a continuous narrowing of the eye domain (Fig. 18g-k, compare with respective images in Fig. 16) to almost the same width as the anterior forebrain (Fig. 18l). Moreover, the ventrally-directed movement of eye field cells observed in the wild-type seems absent in the mutant. After 6 hours of development, when optic vesicles have formed in wild-type, the mutant eye domain is continuous with the posterior forebrain at its lateral extents (Fig. 18f, arrow heads). This is also visible in the original time-lapse images, showing a compaction of GFP-positive retinal precursors within and continuous with the forebrain (Fig. 17). The ‘default’ movement of the anterior neural plate towards the midline and the formation of a neural keel has thus to be modulated among retinal precursor cells to prime and allow optic vesicle formation.

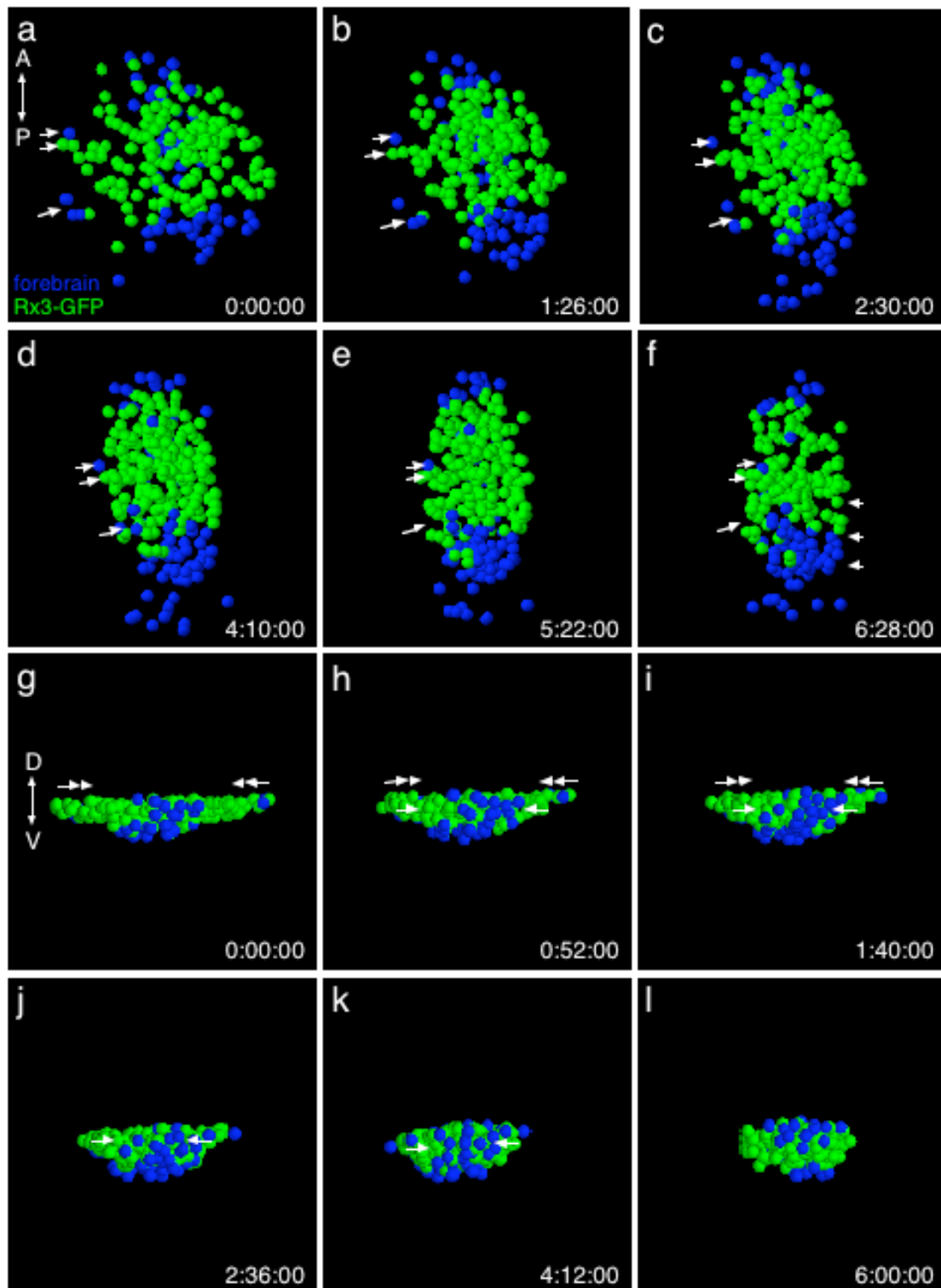


Figure 18. Cell tracks from *eyeless* reveal enhanced movement to the midline.

Single cells were tracked in time lapse recordings from early eye field to optic vesicle stage. The positions of individual cells are depicted as balls in 3D renderings. GFP-positive but *Rx3*-mutant cells are shown in green, forebrain cells in blue. **(a-f)** Dorsal view, anterior is to the top, **(g-l)** frontal view, dorsal is to the top. **(a-f)** Cells of the eye field move at the same pace towards the midline as laterally located forebrain cells (arrows). The eye field continues to condense to the same width as the posteriorly located forebrain (**f**, arrowheads). No anterior-directed movement of posterior-lateral eye field cells can be observed in contrast to wild-type.

(g-l) Also the frontal view shows the medial directed movement and narrowing of mutant retinal precursor cells. Ventral-directed movement of medial eye field cells is absent. A, anterior; P; posterior; D, dorsal; V, ventral.

The forebrain-like behaviour within the *Rx3*-mutant eye field cells can also be observed in time-lapse images using a transgenic line, that expresses membraneYFP under the control of the 4 kb *Rx3*-promoter in the wild-type and mutant background (see also next paragraph). Figure 19 shows 3D reconstructions of confocal z-stacks. A section was cut through the eye domain in the 3D renderings to reveal the process of unfolding, priming and evagination in wild-type and its failure in the mutant. In wild-type embryos, the eye field condenses towards the midline (Fig. 19a-b), but medial movement is not complete. Consequently, the eye field remains wide (Fig. 19c-d, arrows), followed by evagination of the optic vesicles (Fig. 19i-k). In the absence of *Rx3* function, the eye field cells display a cellular behaviour that is similar to the surrounding tel- and diencephalic precursor cells. Along with these cells, the mutant cells move further towards the midline and a neural keel-like structure is formed. As a consequence of the ‘neural-like’ behaviour, the mutant eye field is similar in width to the neural keel itself (Fig. 19e-h, l-n).

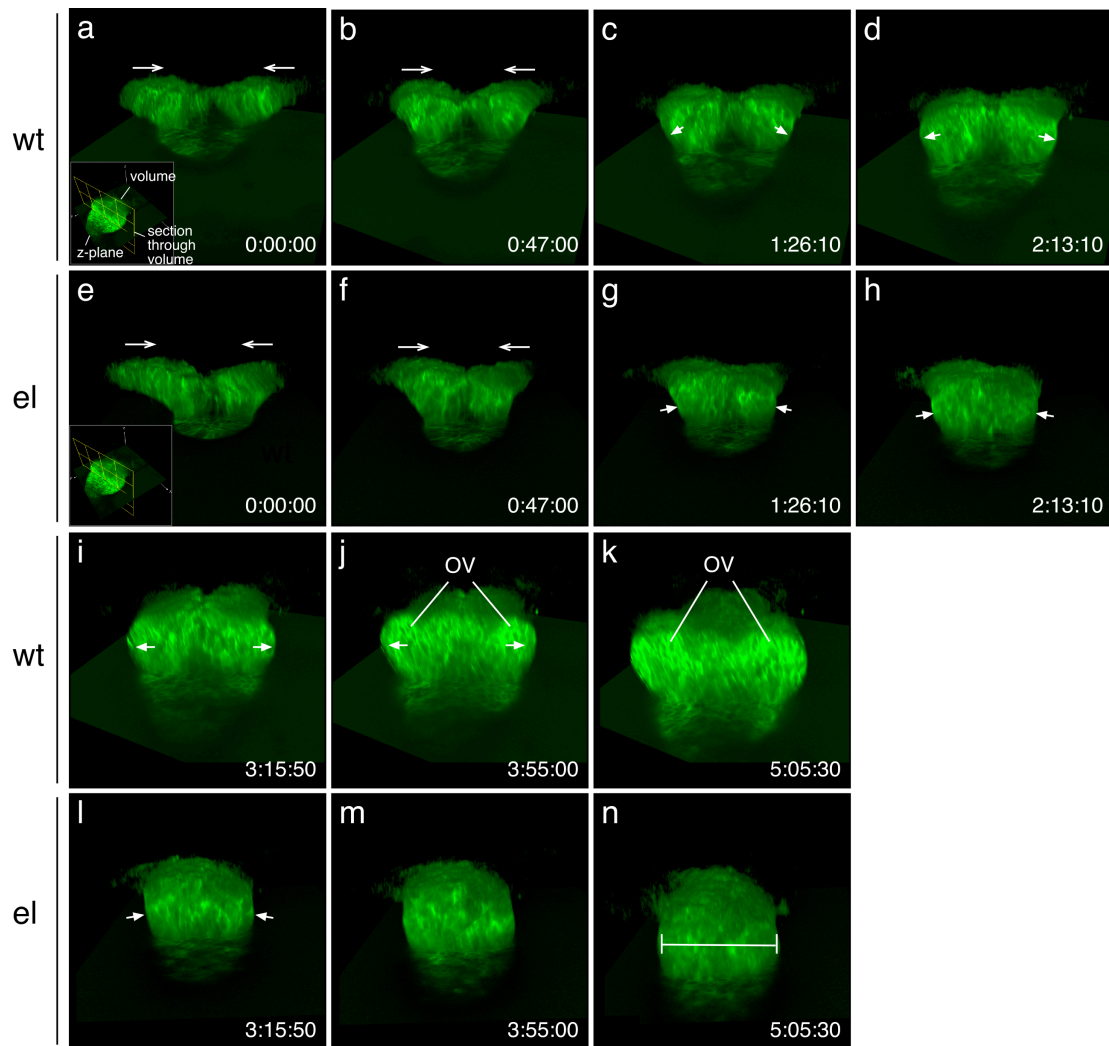


Figure 19. Virtual cross-section through the eye field.

Embryos expressing membraneYFP under the control of the *Rx3*-promoter were imaged at 7 minutes intervals, at a spatial resolution of 3 μ m. The individual timepoints were 3D rendered using Imaris imaging software and a virtual cross-section was cut through the eye region (see inset in a and e). An individual z-plane is shown to outline the missing anterior eye domain (z-plane). **(a-d, i-k)** Formation of optic vesicles in the wild-type. **(e-h, l-n)** Formation of a neural-keel like structure in *eyeless*. **(a-b)** Upfolding: the eye field moves towards the midline (arrows). **(c-d)** Convergence is not complete within the eye domain (arrows). **(e-f)** In *eyeless* the eye field also condenses towards the midline but in the absence of *Rx3* function, the cells continue their midline-directed movement **(g-h, arrows)**. **(i-k)** Optic vesicles form in the wild-type (arrows) while the mutant eye domain condenses further in *eyeless* and forms a domain comparable in width to the neural keel **(l-n, see line in n)**. OV, optic vesicles.

2.2.3 Analysis of cell shape changes during optic vesicle formation

Cell shape changes have been discussed as driving force of tissue morphogenesis as well as cell movements, as outlined before. I used a membrane-tethered form of YFP expressed under the control of a 4 kb *Rx3* promoter element to monitor shape changes during optic vesicle morphogenesis (Fig. 20). Again, the construct was used to establish stable transgenic lines in the wild-type and mutant background (*Rx3*-mYFP and *Rx3*-mYFP;el,B). During the midline-directed movement of the anterior neural plate also the eye field cells move medial as the neural keel forms (Fig. 20a-b). This movement is however attenuated within the eye field while more posterior cells of the forebrain still move towards the midline (Fig. 20b-c), as was also observed with single cell tracks. This process gives rise to a wider eye domain and primes the site of evagination (arrows in Fig. 20b). During further development, cells within the eye domain elongate medio-laterally as they stream into the optic vesicles (Fig. 20g-i, yellow arrows), while posterior cells still converge and move anteriorly (Fig. 20c, white arrows). As movement of *Rx3*-mutant cells towards the midline is not attenuated, convergence is as complete as that of the posteriorly located future diencephalic cells (Fig. 20d-f, arrows in e) and a neural keel-like structure with laterally located elongated columnar cells forms in the eye region (Fig. 20e, red asterisks). 2 hours later, when optic vesicles have already evaginated in wild-type (Fig. 20c), the qualitative difference of laterally located cells becomes more apparent. An epithelialized structure containing elongated, columnar-shaped cells has formed, reminiscent of the epithelium of the forming neural tube (Fig. 20f, red bars). At medial positions mutant cells appear trapped, exhibiting a round morphology in contrast to the elongated cells in wild-type (Fig. 20f, yellow arrows) suggesting a defect in cell polarization.

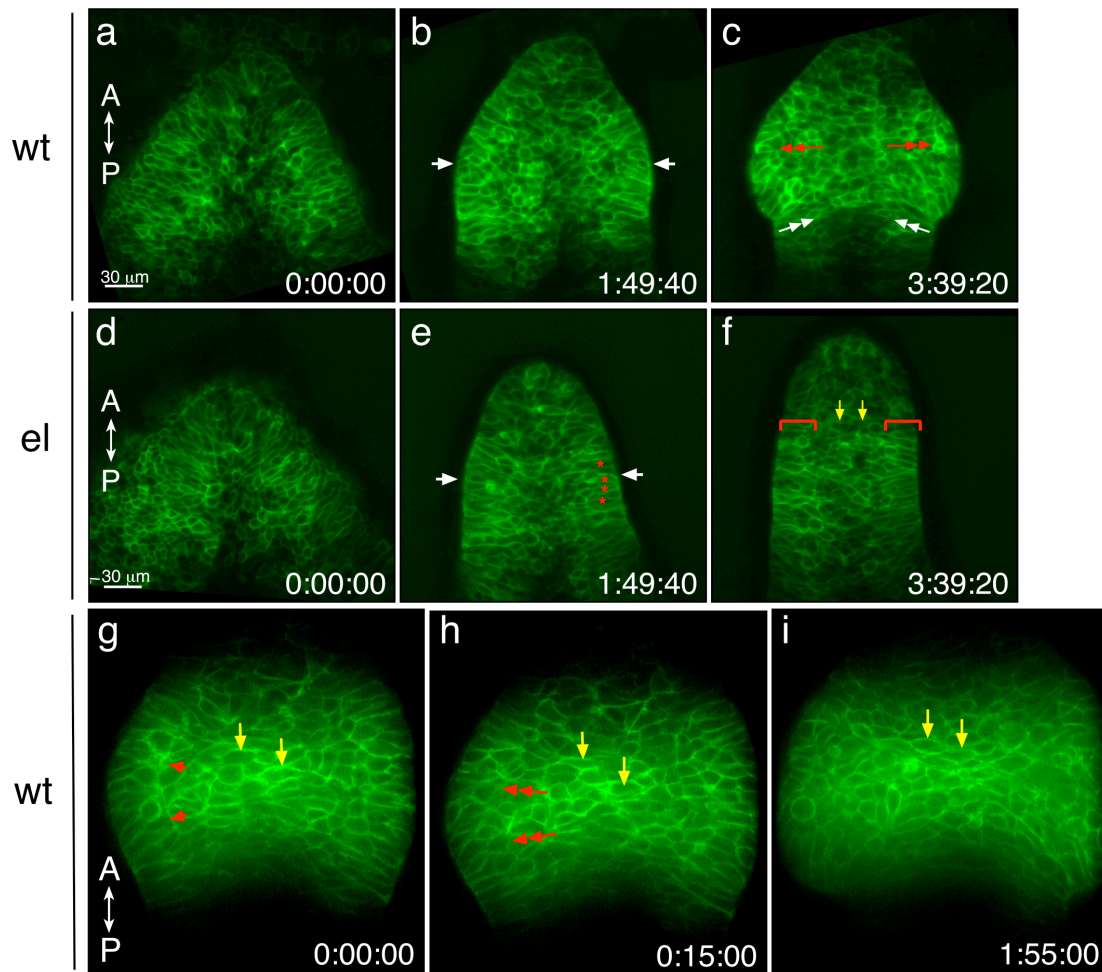


Figure 20. Analysis of cell shape changes during optic vesicle morphogenesis.

Embryos expressing membraneYFP under the control of the *Rx3*-promoter were imaged by confocal microscopy. A single confocal plane of time-lapse sequences from wild-type (**a-c**) and *eyeless* (**d-f**) is shown, anterior is to the top. During neural keel formation the wild-type eye field converges incompletely, resulting in a wide domain that precedes evagination (**b**, arrows). Subsequently, cells move into the optic vesicles (**c**, red arrows indicate migrational direction), while more posterior cells still move towards the midline (white arrows). Without *Rx3* function, the eye field condenses stronger (**e**, arrows) and cells at the lateral border of the eye field start to elongate (asterisks in **e**). At st 18 (**f**), the lateral border of the eye domain in the mutant exhibits an epithelial-like appearance, with elongated, columnar-like cells (red bars), trapping rounded cells (yellow arrows). Magnification: 32x

(g-i) Short sequence showing the medio-lateral elongation of medial retinal precursor cells as they move laterally into the growing vesicles (yellow arrows). A transient boundary between medial versus lateral cells (g, red arrowheads) is lost as cells move laterally (h, red arrows). Magnification: 40x

This is confirmed by staining for α -tubulin and *Rx3* expression on transversal sections through the eye region (Fig. 21). Late gastrula stage embryos can not be distinguished phenotypically and were thus genotyped by *in situ* hybridization for *Rx3*. Mutant embryos were identified by the absence of *Rx3* expression (see figure

legend). Wild-type retinal precursor cells elongate mediolaterally during their movement from the neural keel (Fig. 21b, arrows) while mutant retinal precursor cells have adopted a shape typical for neural keel cells and are stacked in the epithelialized lateral wall of the forebrain (Fig. 21d). This epithelium surrounds non-migratory cells within the neural keel that have failed to elongate and remain rounded (Fig. 21d, arrows). Thus the correct polarization of cells and dynamic cell shape changes contribute to optic vesicle evagination and prevent epithelialization in wild-type.

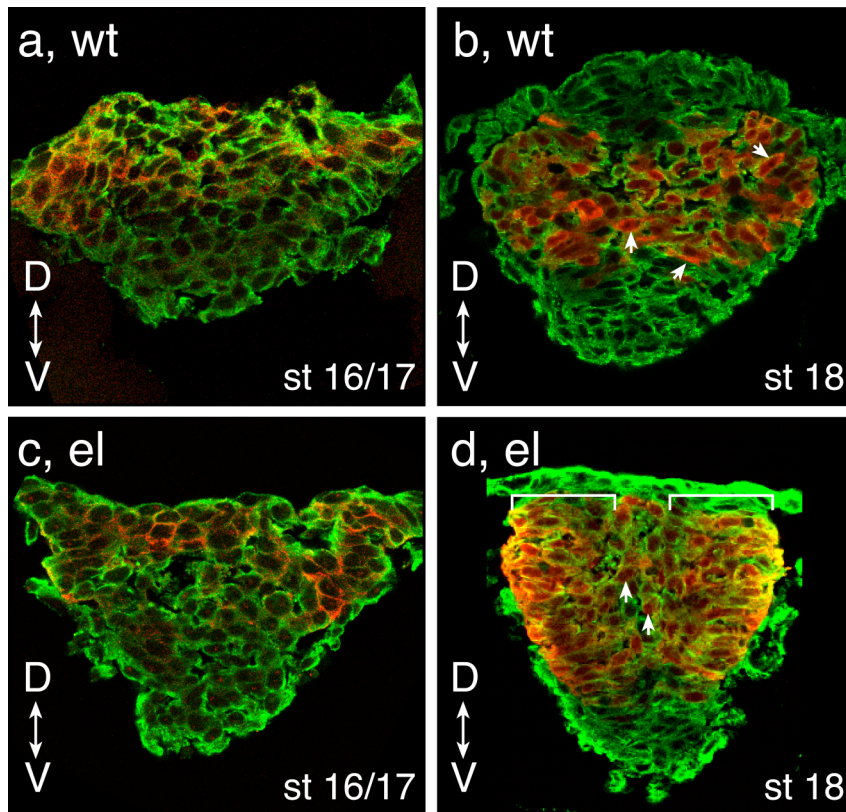


Figure 21. Cell shape revealed by immunostaining.

All images are confocal sections through the eye region with dorsal to the top. Early neurula embryos are *Rx3mYFP;el,B*, and late neurula stage is *ET;el,B*. **(a)** Early wild-type neurula stage (st16/17), stained for *Rx3* expression by *in situ* hybridization (red) and for α -tubulin (green). **(c)** Early *eyeless* neurula stage (st16/17), identified by negative *in situ* hybridization for *Rx3* expression, stained for membraneYFP (red) and for α -tubulin (green). Late neurula stage (st18) in wild-type **(b)** and *eyeless* **(d)**, both stained for α -tubulin (green) and GFP (red). While no gross difference can be detected in the early neurula stage eye field, at the optic vesicle stage (st 18) cell shapes differ between mutant and wild-type. **(a)** In wild-type, retinal precursor cells elongate mediolaterally. **(d)** In *eyeless*, mutant retinal precursors arrange in an epithelialized manner resembling a neural keel (white bar), surrounding round cells (arrows).

2.2.4 Optic vesicle formation involves single cell migration

As outlined before, the formation of an organ is either the result of a concerted action of a cell population that moves within an unbroken cluster or sheet or alternatively, it can be the result of individual cell migration (see (Wallingford et al., 2002)). In this case an individual cell has to break away from its surrounding tissue and modulate its contacts to other cells and the extracellular matrix. To distinguish between these two possibilities and to monitor single cell behaviours during optic vesicle formation, I performed mosaic analysis using cell transplantation. Wild-type cells from embryos ubiquitously expressing a membrane-tethered mRFP (Campbell et al., 2002; Megason and Fraser, 2003) were transplanted at blastula stage to the animal pole of an *eyeless*-intercross expressing membraneYFP under control of the *Rx3* promoter to identify the eye field. Transplantation of cells to the animal pole results in preferential contribution of these cells to the forebrain and the eye. Several embryos were imaged simultaneously (Rabut and Ellenberg, 2004) at 18°C to follow the behaviour of donor cells. Transplanted wild-type cells in a wild-type eye field intermingled with the host cells and participated normally in the developing optic vesicle (Fig. 22a-e and supplementary movie S11). No cluster formation of transplanted cells is observed. Wild-type cells in a mutant eye field rescue optic vesicle evagination (Fig. 22f-j and supplementary movie S12), but the evaginated vesicles consist exclusively of wild-type cells, whereas mutant cells reside within the forebrain (Fig. 22j). At the early neurula stage a large fraction of wild-type cells is located at the lateral border of the eye field in agreement with the observed modulation and delay of convergence within retinal precursors (Fig. 22f). However, part of the wild-type cells was also found in the medial part of the eye field (Fig. 22f, k). Within the next 5 hours almost all of the wild-type cells move from medial to lateral and join the wild-type cell clusters already located there. Moreover, the evaginated cell clusters also fuse with each other by posterior movement of the anterior patches as also observed by cell tracking, gradually merging to a single vesicle. Mutant cells that were positioned initially at the lateral side of the eye field are displaced during this process (see asterisks in Fig. 22f-j) which results in small optic vesicles composed of wild-type cells exclusively (Fig. 22j). 3D reconstruction of rescued optic vesicle evagination suggested that individual wild-type cells from the medial part of the mutant eye field actively migrated laterally

through the surrounding mutant cells and merged with the wild-type cells that had primed the evagination laterally (Fig. 22k-n).

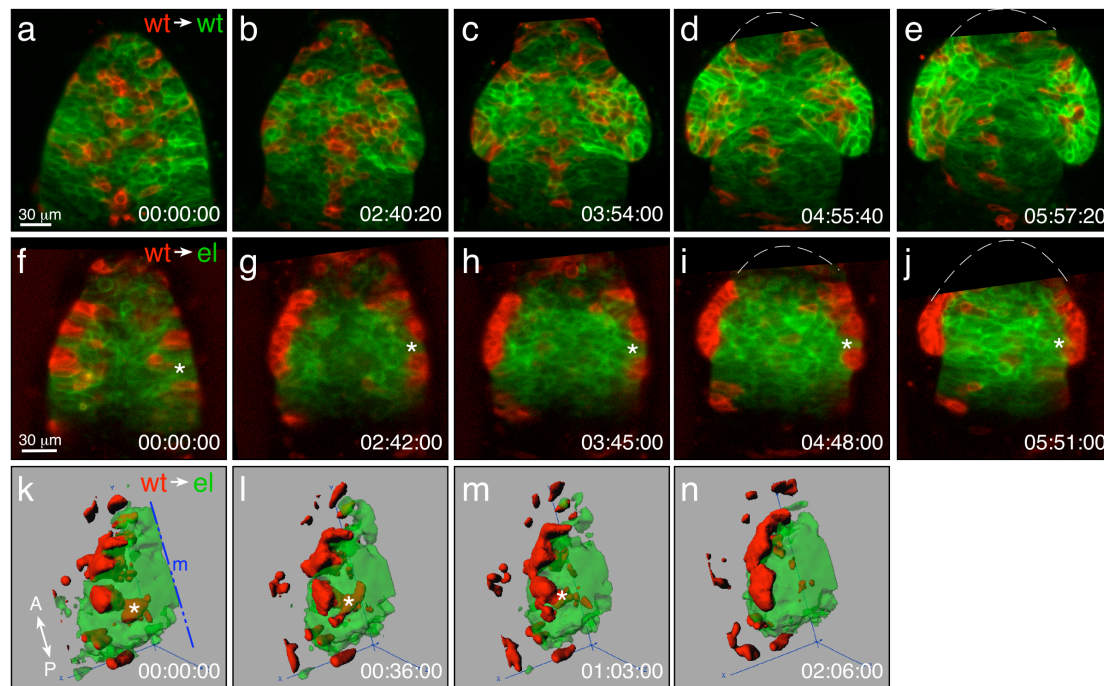


Figure 22. Wild-type cells rescue the evagination defect in *eyeless*.

Wild-type cells expressing membrane-mRFP (red) were transplanted to the animal pole of embryos expressing membraneYFP (green) in the eye field, either in a wild-type (a-e) or an *eyeless* (f-j) background. Anterior is to the top in all images, one confocal section of a 3D time-lapse sequence from early neurula to somitogenesis stages is shown. The broken white lines indicate the anterior border of the forebrain that moved out of the field of view during the recording. (a-e) WT cells (red) transplanted into a WT eye field (green) intermingle with the host cells and participate normally in optic vesicle formation. (f) WT cells (red) in an *Rx3*-mutant eye field (green) are found at the lateral border of the eye field due to altered convergence movements in contrast to mutant cells. Part of the WT cells however are still located in the medial part of the eyefield (see also k). (g-j) During the next 5 hours small optic vesicles develop, consisting exclusively of WT cells, whereas mutant cells remain in the forebrain (see asterisk). (k-n) 3D-reconstruction of the left half of the mutant embryo, the blue stippled line indicates the midline (m). Anterior is to the top-left. (k-l) The WT patches on the left side of the eye field fuse by posterior movement of the anterior part. At the same time the cluster of cells in the more medial part of the eye field marked by an asterisk, leaves the forebrain and becomes part of the optic vesicle.

I therefore analyzed the behaviour of single wild-type cells in the mutant within the time-lapse recordings of two independent experiments. Wild-type retinal precursor cells migrate either as clusters of several cells or individually from the medial part of the neurula stage eye field through the *Rx3*-mutant tissue (Fig. 23 and supplementary movie S13). Cells in a small cluster of approximately 4 cells (Fig. 23a, arrow) elongate medio-laterally and migrate from an anterior-medial position within the neurula eye field laterally. They eventually integrate in the already preformed small

optic vesicle (Fig. 23e). A second cluster in the same embryo consisting of two cells moves through the mutant tissue into the forming vesicles (Fig. 23a-b, arrowheads). Besides migration of cell clusters I also observed single cell migration from cells located within the medial forebrain into the rescued optic vesicles (Fig. 23f-i). Sometimes, the cells divided during their movement (Fig. 23j-m). In summary, optic vesicle morphogenesis involves the migration of single cells rather than the movement of a tissue as a whole.

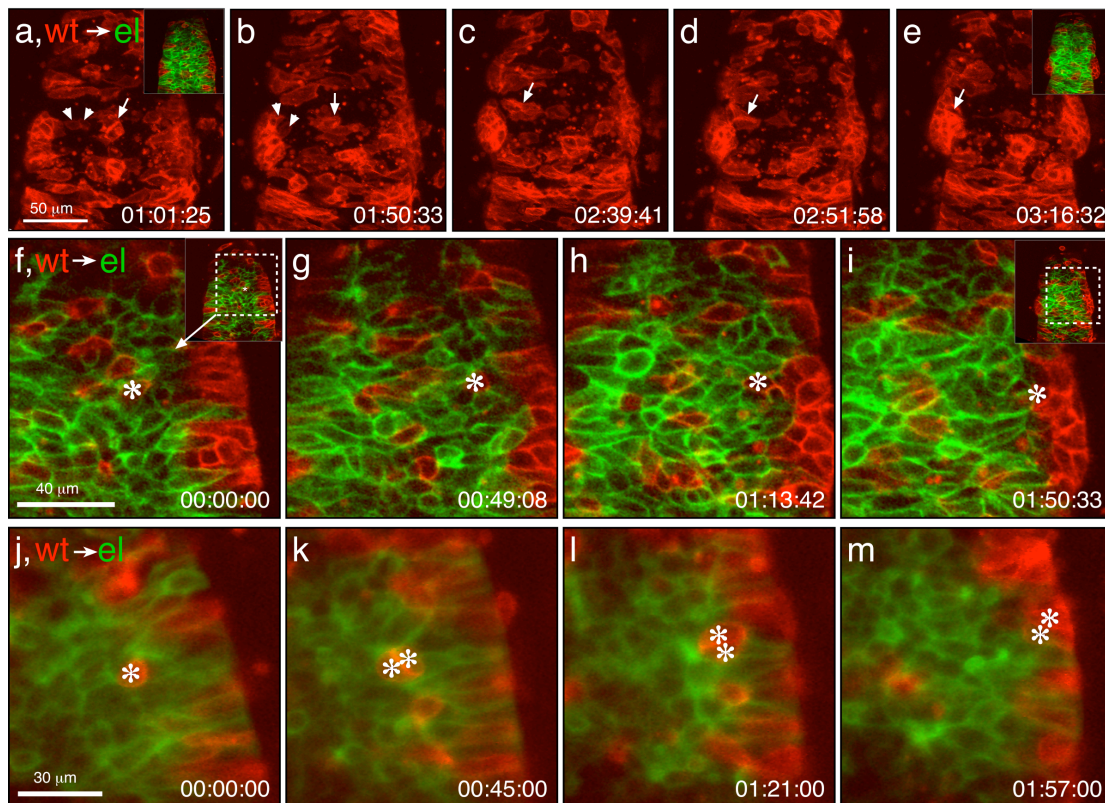


Figure 23. Optic vesicle evagination involves single cell migration.

WT cells (red) were transplanted on *eyeless* embryos (mutant cells in green) as in figure 22. Single cell movements within mosaic mutant eye fields were analyzed. (a-e) The panel shows a maximum intensity projection of several confocal planes of a 4D time-lapse sequence. For clarity only the red channel (wt) is shown, the insets in (a) and (e) show an overlay of both channels. A cluster of 4 cells in the medial part of the mutant eye field (a, arrow) elongates mediolaterally (b) and migrates to the lateral side of the eye field where it joins the optic vesicle (e). Another smaller cluster of 2 cells (a-b, arrowheads) also moves laterally and becomes part of the optic vesicle. (f-i) A single cell (asterisk) migrates laterally and leaves the *Rx3*-deficient forebrain to participate in the optic vesicle. (j-m) A single cell that divides as it moves out of the forebrain.

2.2.5 A model for optic vesicle formation

Taken together my data strongly supports a two-step model of optic vesicle formation (Fig. 24). In a first step, the anterior neural plate and eye field undergoes a movement that resembles an upfolding as the neural keel is formed. Prospective tel- and diencephalic cells laterally to the eye field and cells from the lateral border of the eye field move over the underlying eye field cells towards the midline. The midline movement of more ventral eye field cells is slower and along with the ventral-lateral directed movement of medial eye field cells, the eye domain remains wide and is not condensing, which is essential for priming of optic vesicle evagination. In a second step, cells elongate medio-laterally and move from medial positions laterally, leading to growth of the vesicles. The process of morphogenesis depends on the coordinated movement and migration of single cells, not the movement of the tissue as a whole. Moreover, proliferation seems to control rather the size of the optic vesicle than its evagination as no gross difference in the number of divisions was found between wild-type and mutant. In the *eyeless* mutant, the medial movement of the eye field is not affected, these cells move at the same speed as forebrain precursors towards the midline. Also the ventral-lateral directed movement of medial eye field cells is blocked. In the absence of *Rx3*-function, cells apparently follow a 'default' behaviour of forebrain cells and form a neural keel-like structure. The lateral borders of the mutant eye field adopt a columnar epithelial shape typical of the neural tube. This epithelialization along with the failure of medial cells to elongate medio-laterally, further inhibits evagination.

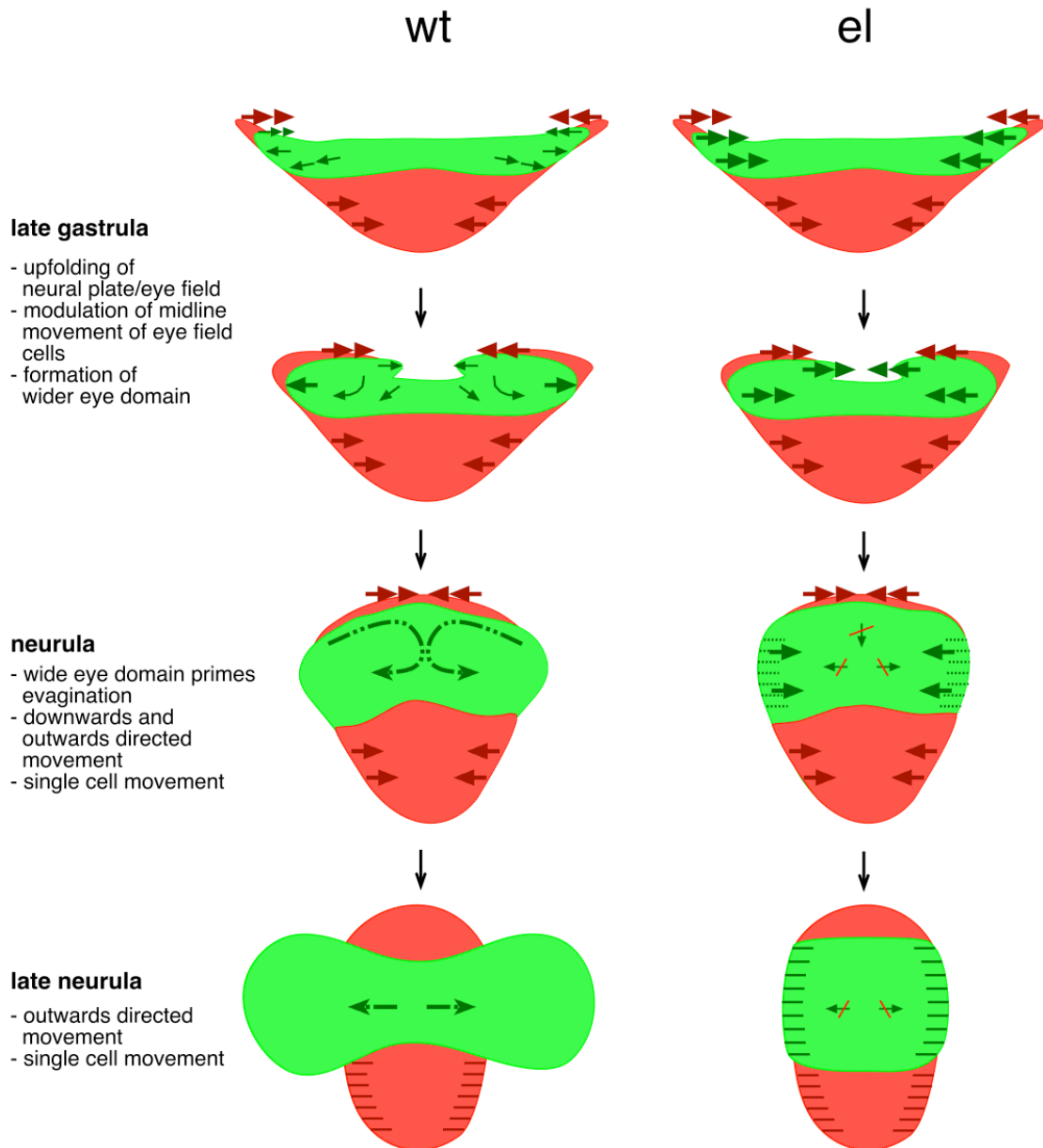


Figure 24. A model for optic vesicle morphogenesis. The arrows indicate cell movements, the lines indicate the formation of an epithelium. Wt, wildtype; el, eyeless.

2.3 Appendix

Index of movies found in the supplementary material on CD:

Movie S1 Contractile movements. Time-lapse covering 13 minutes showing the contractile movements of a neurula stage embryo (st18) that cause it to rotate and eventually disappear from the field of view. Anterior is to the left.

Movie S2 Block of contractile movements by heptanol. Time-lapse of a neurula stage embryo (st18) that was treated with 7 mM 1-heptanol. The contractions are blocked and the embryo is immobilized in the embedding medium over the 12.5 minutes observed. Anterior is to the left.

Movie S3 Long term imaging of anterior development. Time-lapse covering almost 21 hours of development starting from late neurula stage (st18). The embryo was treated with 7 mM heptanol and embedded in 1 % agarose. The sequence covers the development of the optic cup from the optic vesicle and the differentiation of the neural keel to fore-, mid- and hindbrain. (The bright round structure moving through the field of view is an oil droplet.) Anterior to the left.

Movie S4 4D-reconstruction of an embryo expressing histone H2BdiHcRed ubiquitously. The embryo was treated with 3.5 mM heptanol. The movie covers 16 hours of development and shows the formation of the neural keel from the neural plate and the evagination of optic vesicles from the neural keel. Anterior is to the top.

Movie S5 Optic vesicle evagination in wild-type. Single confocal section of a WT embryo expressing *Rx3*-GFP (green) in the eye field and histone H2B-mRFP (red) ubiquitously. The sequence covers 11 hours of development at 20°C. Dorsal view, anterior to the top.

Movie S6 Dorsal view of a 3D reconstruction of tracked cells in WT. Cells of the eye field are shown in green, tel- and diencephalon in blue. Anterior is to the top.

Movie S7 Frontal view of a 3D reconstruction of tracked cells in WT. Color-coding as in movie S6. Dorsal is to the top.

Movie S8 Optic vesicle evagination in *eyeless*. Single confocal section of an *eyeless* embryo expressing GFP in the eye field (green) and histone H2B-diHcRed (red) ubiquitously. The sequence covers about 15 hours of development. Dorsal view, anterior is to the top-left.

Movie S9 Dorsal view of a 3D reconstruction of tracked cells in *eyeless*. Color-coding as in movie S6. Anterior is to the top.

Movie S10 Frontal view of a 3D reconstruction of tracked cells in *eyeless*. Color-coding as in movie S6. Dorsal is to the top.

Movie S11 Mosaic analysis in a WT background. Membrane-tethered mRFP expressing WT cells were transplanted on a WT embryo. The eye field is marked by membraneYFP expression. Transplanted cells intermingle with host cells and participate normally in optic vesicle formation. Dorsal view of a single confocal section, anterior is to the top.

Movie S12 Mosaic analysis in a mutant background. The setup is the same as in movie S11, but the host is *eyeless*. WT cells accumulate at the lateral borders of the eye field and rescue optic vesicle evagination. Dorsal view of a single confocal section, anterior is to the top. The anteriormost part moves out of view during imaging.

Movie S13 WT cells migrating in a cluster (marked with a dot) through a mutant eye field in a transplantation experiment. Dorsal view of a z-projection over 30 μm , anterior is to the top. For better view on the migrating cells only the red channel recording WT cells is shown. The green channel showing the mutant eye field has been omitted.

Movie S14 The setup is the same as in movie S13. Here two WT cells (marked by dots) migrating individually through the mutant eye field are shown,

3 DISCUSSION

There was only very limited knowledge about the early morphogenesis of the optic vesicle when this project was started although it is a crucial process for eye development in all vertebrates and a paradigm for vertebrate organ morphogenesis. Taking advantage of the transparency of fish embryos I aimed at elucidating the cell behaviours and mechanism underlying the evagination of the optic vesicle from the forebrain using *in vivo* imaging techniques. *Rx* genes were shown to be essential for this process, in particular *Rx3* in fish (Loosli et al., 2001; Mathers et al., 1997). Analysis of the morphogenetic behaviour elicited after acquisition of retinal identity in the eye field shows that *Rx3* has a crucial function in modulating the midline directed movement of eye field cells to prime evagination. Unexpectedly, cells evaginate by migration as single cells rather than in an unbroken tissue and the elongation of cells during their outward movement implicates that they have to be correctly polarized to migrate.

3.1 Imaging in Medaka

So far high resolution imaging of medaka embryos was severely compromised by rhythmical contractile movements that travel across the periderm as a wave. The movements start at mid-epiboly stages and stop after the onset of the heart beat (Fluck et al., 1983; Robertson, 1979; Yamamoto, 1975). The amplitude of the contraction wave peaks at the late neurula stage (st 18) when one wave travels across the entire yolk in one minute (Fig. 10) and decreases afterwards (Cope et al., 1990; Iwamatsu, 1994). These contractions cause the embryo to rotate within its chorion and also in quite stringent embedding medium of 1 % agarose used for microscopic observation, hampering time-lapse imaging. Using 1-heptanol the movements could be considerably diminished allowing to establish conditions for the live observation of the embryo with subcellular resolution in 4D. I followed development from the late neurula (st 18) to the somitogenesis stage (st 22). Development during this time period was normal, the embryo developed optic cups from the optic vesicles and the neural keel differentiated to forebrain, midbrain and hindbrain. Only a minor slowdown of development was observed as compared to control embryos. The fact that the contractions are diminished but not completely abolished might also be responsible for the neutral effect on development. This method was thus a crucial

development towards the live imaging of early medaka embryos and to observe and follow the movement of individual cells.

The contractile movements stop soon after the onset of heart beat. All rhythmic activity ceases at the 22-somite stage (stage 26) (Cope et al., 1990). Blood circulation starts 4 hours earlier at 26°C. Addition of heptanol to embryos with circulating blood leads to an immediate collapse of the blood vessels although the heart beat is not affected. Gap junctions are ubiquitously distributed among vascular wall cells and involved in contraction and relaxation (Christ et al., 1996). Heptanol can therefore not be used during these developmental stages. Thus, with the exception of a short developmental time window of about 8 hours (st 24 –26) medaka development is fully amenable to high resolution 4D imaging. To overcome that limitation, embedding medium of 1 % agarose or higher can be used to immobilize the embryo at these late stages, as the contractile movements are not as regular and efficient anymore. Later in development the anesthetic MS-222 efficiently blocks muscle contractions and thus prevents the embryos from moving.

3.2 *Eyeless* exhibits a unique phenotype

The *eyeless/Rx3* mutant in medaka was incorporated into this study as it exhibits a unique phenotype. Loss of *Rx3* function affects very specifically the morphogenetic behaviour of cells that is elicited downstream of patterning (Loosli et al., 2001; Winkler et al., 2000). Early specification of retinal progenitor cells is normal, yet they fail to evaginate and incorporate into the forebrain instead (Winkler et al., 2000). As a consequence, the *Emx1*-positive domain representing the dorsal telencephalon extends further posteriorly at somitogenesis indicating a retained movement of these cells. The hypothalamus forms normally (Winkler et al., 2000). The function of *Rx3* is very well conserved, as mutations of *Rx3* in zebrafish *chokh* result in the same phenotype (Kennedy et al., 2004; Loosli et al., 2003). Moreover, 4D imaging in zebrafish revealed that the formation of the optic vesicles is very similar to medaka (data not shown). The phenotype is specific to cells of the eye field. Other eye mutants affect also other aspects of development and patterning. The *Pax6* mutant *small eye (sey)* in

mouse for example displays defects in the lens and nose as well as in forebrain patterning in addition to the eye defect. Moreover, the initial steps of optic vesicle evagination are not affected, but the vesicles fail to constrict proximally and degenerate subsequently (Grindley et al., 1995; Hill et al., 1991; Hogan et al., 1986; Stoykova et al., 1996). *Masterblind (mbl)* or *headless (hdl)* zebrafish lack eyes but also the forebrain due to defective Wnt signaling (Heisenberg et al., 2001; Kim et al., 2000; Masai et al., 1997; van de Water et al., 2001). Overexpression of a dominant-negative form of the LIM/homeodomain protein Islet-3 results in a failure of optic vesicle formation, but also in defects in the formation of the isthmus (Kikuchi et al., 1997). Medaka *eyeless* is thus a unique mutant in that it uncouples patterning and morphogenesis of the eye very specifically. Detailed analysis of the mutant morphogenetic phenotype in addition to the wild-type gives thus important insights into the mechanism by which optic vesicle evagination occurs in wild-type.

3.3 Modulation of convergence by Rx3

The medaka *Rx3*-promoter was used to specifically label all retinal precursor cells of the eye field with GFP. This enabled me to follow the movement and fate of these cells during the formation of the optic vesicles from late gastrula to early somitogenesis stages as opposed to surrounding tel- and diencephalic progenitor cells. Earlier analysis of eye formation by light and electron microscopy concentrated on the formation of the optic cup from the optic vesicles (Li et al., 2000; Schmitt and Dowling, 1994) ignoring the transition of the eye field to the optic vesicles. Fate mapping experiments of the anterior neural plate can not give information on the dynamics in between individual timepoints (Hirose et al., 2004; Woo and Fraser, 1995). Therefore, the mechanism underlying evagination remained obscure. Using an *in vivo* imaging approach I followed the behaviour of cells at a temporal resolution of 2 minutes at 20°C in wild-type and *eyeless* embryos. In wild-type embryos the eye field converges as the neural keel forms. The anterior neural plate is excluded from convergent extension movements which is thought to be mediated by *Otx2* and *Calponin* (Keller et al., 1992; Morgan et al., 1999), and neither *Wnt11* nor *Wnt5* are expressed in the anterior neuroectoderm (Heisenberg et al., 2000; Kilian et al., 2003).

Indeed it does not undergo extension, but medial movement towards the midline does occur. Tracking of single cells within time-lapse sequences showed that this medial movement is attenuated within the eye field as compared to cells located laterally to the eye field that will give rise to the dorsal telencephalon. The lateralmost cells of the eye field do move at the same speed towards the midline as telencephalic precursors, but then move ventrally and laterally into the forming optic vesicles. The more ventral-medial part of the eye field however does not move medially and together with ventrally directed movement of dorsal-medial eye field cells, the eye domain never converges as extensive as the posterior diencephalon but instead is kept wide. The dorsal telencephalic precursors coming from the lateral borders of the eye field move thus over the underlying eye field cells in a process that resembles the unfolding of the neural tube in other vertebrates. This retained movement keeps the eye domain in the early neurula stage embryo (st 17) widened and seems a prerequisite for the priming of evagination as it is absent in *Rx3/eyeless* embryos. Instead in *eyeless* the mutant retinal progenitor cells converge towards the midline at the same extent as telencephalic and also posteriorly located diencephalic cells. Ventrally directed movement was not observed. These movements result in the formation of a neural keel-like structure instead of eyes highlighting the importance of the modulated movement within the eye field for evagination to occur. The movement of telencephalic cells over the eye field had been suggested earlier (Chuang and Raymond, 2001; Chuang and Raymond, 2002). Cells lateral and rostral to the eye field at bud stage (9.5 hrs) express *Emx1* and *BF-1* in zebrafish, both expressed in telencephalic cells (Chuang and Raymond, 2001; Varga et al., 1999). At a stage where the optic vesicles have started to evaginate (11.5 hrs) *Emx1* and *BF-1*-positive cells are found dorsal to the optic vesicles constituting the dorsal telencephalon. This suggested their movement to the midline superficial to the underlying eye field cells (Chuang and Raymond, 2001). The dorsal telencephalic cells have to move thus on the eye field cells. On transversal sections a boundary can be seen between retinal progenitor cells in the optic vesicles and the forebrain cells between which they are sandwiched (Chuang and Raymond, 2001). This is also evident in immunostainings on the early optic vesicle stage, where a clear delineation between *Rx3*-positive cells and cells of the forebrain is visible. A boundary is however not visible at the late gastrula stage when the telencephalic precursors are actually moving over the

underlying eye field. In any case, a possible additional role for *Rx3* might lie in the control of differential adhesion between eye field and forebrain cells to allow different migratory behaviours to develop. An interesting downstream candidate is signaling via ephrins/Eph receptors. Eph-ephrin signaling mediates cell-contact dependent repulsive interactions that mediate cell sorting and boundary formation eg. in the hindbrain rhombomeres (Cooke and Moens, 2002) or the in the dorso-ventral patterning of the optic vesicle (Peters, 2002). A member of the Eph RTK family, *EphA4/rtk1* is expressed in the anterior forebrain but excluded from the eye field. Misexpression of a dominant-negative EphA4 resulted, however, in transformation of forebrain tissue to eye rather than changes in adhesive properties (Xu et al., 1996). *EphrinB1* is expressed at low levels in the eye field in *Xenopus* and at high levels in the neuroectoderm surrounding it. In the anterior and lateral neuroectoderm bordering the eye field it is co-expressed with and phosphorylated by *Fgfr2* (Moore et al., 2004). Reverse ephrinB1 signaling in the eye field is necessary for cells to move into the eye field. In contrast, the phosphorylation of ephrinB1 by *Fgfr2* inhibits this movement and causes cells to populate positions closer to the midline. Thus modulation of ephrin signaling seems important in controlling different cellular behaviours in the anterior neural plate. It will be interesting to see if ephrin signaling is downstream of *Rx3* during optic vesicle formation in particular as Eph signaling is also involved in cell migration (reviewed in (Holder and Klein, 1999)). Preliminary experiments have however not shown a difference in *EphA4* or *ephrinB1* expression in the *Rx3* mutant embryos. It is however unlikely that optic vesicle evagination is a simple cell sorting mechanism, as not all of the transplanted wild-type cells found in the early neurula eye field are later also found in the optic vesicles. Moreover, the migratory properties of all cells in the eye field are affected by loss of *Rx3* and not only of these cells that are close to telencephalic or diencephalic cells. In addition, the movement of eye field cells during evagination is quite complex and not easily explainable by cell sorting. Nevertheless, there is extensive crosstalk between adhesion and the cytoskeleton and thus motility of cells. In particular, adhesion via Cadherins feeds back on the cytoskeleton and thus on the migratory ability of cells. Recently, p120 catenin has been shown to be essential for proper optic vesicle evagination in *Xenopus* (Ciesiolka et al., 2004). Knock-down of p120 catenin or overexpression of a mutant form of E-Cadherin unable to bind p120 catenin results in defective optic vesicle formation and

reduced eyes. Interestingly, neural crest cells are also impaired in their migration (see also later section).

The requirement for *Rx3* function within the eye field already at the gastrula stage, thus before evagination actually starts, correlates well with earlier temperature shift experiments (Winkler et al., 2000). The *eyeless* phenotype is due to a large insertion into the second intron of *Rx3* that probably renders transcription from this locus temperature-sensitive (Loosli et al., 2001). At the restrictive temperature of 18°C no transcript can be detected and the phenotype is fully amorph. At 28°C low levels of *Rx3* are transcribed and consequently, 52 % of the mutant embryos develop small optic vesicles (Loosli et al., 2001). To obtain the amorph and fully expressive phenotype the embryos have to be kept at the restrictive temperature between the late gastrula and early neurula stage (st 16 –17), thus before optic vesicle evagination actually occurs (Winkler et al., 2000). A shift to the permissive temperature after early neurula stage cannot rescue OV evagination. This is also evident in time-lapse analysis using membraneYFP to assess cell shape changes. The formation of elongated columnar cells at the lateral border of the eye field is seen already at early neurula stage before evagination starts. If the formation of a neuroepithelium has started it might not be reversible as well as the incorrect polarization of cells during their movement.

The modulation of convergence towards the midline gives rise to a widened eye domain within the forebrain before evagination has actually started. This resembles the formation of the optic pit in mouse. In mouse embryos, optic vesicle evagination starts during the elevation of the cephalic neural folds and thus prior to neural tube closure. Also in fish the earliest signs of the evagination process, the retained movement of eye field cells, happen before the anterior neural keel has actually formed. In the mouse the optic area lags behind as the previously flat neural plate starts to elevate, the optic pit bulges out in the ventral direction, which will later be lateral. During further development the evagination enlarges and forms the optic sulcus (early optic vesicle). The optic vesicle is fully developed after the closure of the anterior headfolds (Svoboda and O'Shea, 1987). In the case of the mouse, the formation of the optic pit has been attributed to changes in cell shape and not the

movement of these cells (see also next section). Nevertheless, the process of evagination, though occurring in a hollow tube in most vertebrates and in a solid keel in teleost fish, might share more conserved features than previously thought. Coordinated shape changes occur in both species, mouse and fish as well as a halted movement towards the midline within the eye field/optic pit. In fish, as solid vesicles evaginate from a solid neural keel, the process also depends on the migration of single cells from the keel into the vesicles. In *eyeless* both processes are affected, the lateral borders of the neurula stage eyefield form a neuroepithelium instead of giving rise to the widened outbulged domain present in wild-type, and the medial cells fail to elongate and to migrate into the optic vesicles.

3.4 *Rx3* modulates cell shape changes

Using a membrane-tethered form of YFP, cell shape changes during optic vesicle evagination were analyzed. Cells of the medial eye field at early neurula stage elongate mediolaterally as they migrate into the optic vesicles. *Rx3*-mutant cells fail to undergo a shape change, remain round and trapped in the neural keel. The mediolateral elongation indicates that the cells become polarized before and during their migration into the optic vesicles. As polarization is a key aspect in cell migration, a failure to do so could cause the nonmigratory phenotype in *eyeless*. A wrong polarization or a failure to respond to extracellular guidance cues could also explain the continued movement towards the midline and the defect in the modulation of this behaviour. It will be interesting to find the molecules involved in this polarization defect. Drastic differences were observed in the lateral borders of the *eyeless* eye field. When in wild-type the modulation of midline-directed movement is visible and the earliest sign of evagination can be seen, lateral cells in the mutant start to adopt a columnar-epithelialized organization. Later during development the difference in cell shape becomes more obvious as the cells adopt a very ordered epithelialized shape reminiscent of the epithelium of the neural tube. The formation of the epithelium might be tightly connected with the nonmigratory phenotype. If the adhesion between the cells in *eyeless* is enhanced in general it could be responsible for the failure to migrate. The cells might not be able to modulate adhesion to allow movement to occur. Also a premature differentiation to an epithelium along with the

formation of tight junctions or adherens junctions would strongly counteract movement. Moreover, cell shape changes per se without movement, especially in the outer (lateral) border of the neurula eye field can be themselves a driving force for evagination. The lateral border of the eye field has to undergo bending or to allow cell intercalation. Again, the formation of an epithelium at this place could enhance the stiffness of the tissue, which would not allow major cell shape changes to occur. In mouse, coordinated cell shape changes seem to be the driving force for the evagination of the optic vesicles without cell movement. The number of apical intercellular junctions appears to increase during evagination. Moreover, the extracellular matrix surrounding the optic vesicle becomes transiently deficient in laminin and type IV collagen around the tip of the vesicle during evagination, which is re-established later (Svoboda and O'Shea, 1987; Tuckett and Morriss-Kay, 1986). Evidence from rat suggests a role for β -catenin in the cell shape changes that accompany the transition from the early optic vesicle (sulcus) to the fully formed optic vesicle, thus the distal flattening and full evagination (Matsuda and Keino, 2001). Information on the extracellular matrix is limited in fish and it is not clear if the transient breakdown of the basal lamina also occurs during evagination. The present study shows that evagination is an active process involving active migration of cells. Coordinated cell shape changes at the lateral wall of the neurula stage eye field do occur. They are however presumably not sufficient for evagination. A combination of these two mechanisms – cell migration and cell shape changes – most likely cooperates in eye formation.

3.5 Single cell migration

Mosaic analysis of optic vesicle evagination clearly shows that retinal precursor cells are migrating as single cells. Wild-type cells transplanted into the mutant eye field can rescue the mutant phenotype. Optic vesicles form that consist solely of wild-type cells demonstrating that *Rx3* acts cell-autonomously as has been reported earlier (Winkler et al., 2000). The mutant cells of the mosaic eye field remain in the neural keel and follow a midline-directed movement. At the early neurula stage, before evagination has started, a large fraction of the wild-type cells can be found at the lateral borders of

the eye field, consistent with the results obtained from single cell tracking. The midline-directed movement of wild-type cells is modulated in contrast to the surrounding mutant cells that converge further and eventually form a neural keel-like structure. Interestingly, not all of the transplanted WT cells are found at the lateral border and many of those that remained initially in the medial eye field will subsequently also move into the vesicles following their normal path of movement. These cells migrate actively through the surrounding mutant tissue either as single cells or as small cell clusters. They also seem to extend protrusions pointing in the direction of their migration (see also movie S13). This process leads to a separation of wild-type from mutant cells not by means of passive sorting but by active movements. The migratory phenotype correlates well with the polarization of the cells along their mediolateral axis as visualized with membrane-tethered YFP and the failure to do so in *eyeless*. Moreover, cells can cross the midline and cells from the left eye field may end up in the right eye as observed in the transplantation experiments and in single cell tracks. This observation has also been made by Varga and co-workers (Varga et al., 1999). Individual cell movement has also been shown during mesoderm internalization in fish. In *Xenopus* the mesendodermal cells involute as a coherent sheet (Winklbauer et al., 1996). In contrast, in zebrafish mesendodermal cells delaminate and move as individuals when they ingress during gastrulation (Carmany-Rampey and Schier, 2001; Montero et al., 2005) and cells of the organizer seem to undergo an epithelial-to-mesenchymal transition that is essential for their anterior migration (Yamashita et al., 2004). The neuroectoderm is thought to move as a coherent sheet of cells during epiboly and cells display contact inhibition of movement. At bud stage the cells lose contact inhibition and start to develop protrusive activity as they begin to engage in medio-lateral intercalation (Concha and Adams, 1998). This is also the time when optic vesicle morphogenesis starts with the medial movement of cells within the eye field. A similar change in adhesive and protrusive properties might occur within the eye field. A function of *Rx3* might thus be the control of cell polarity and adhesion within the retinal precursor cells that allows them to pursue their movement during evagination as opposed to other cells of the anterior neuroectoderm. Optic vesicle evagination is thus most likely the result of locally coordinated but individual movement of retinal progenitor cells.

The migration of cells through a tissue requires that they modulate adhesion between each other and to the extracellular matrix (ECM) and polarize their actin cytoskeleton. Signaling via Rac and Cdc42 at the leading edge as well as Integrin receptors have been shown to be important for directed migration (Ridley et al., 2003). Very little is known about the ECM in early fish embryos. It appears that no ECM is present between endomesoderm and neuroectoderm during gastrulation (Montero et al., 2005) but nothing is known about the anterior neuroectoderm at neurula stage. Fibronectin is expressed in the lateral plate mesoderm and the tailbud but not in the anterior neural plate at the relevant stages of optic vesicle formation (Trinh and Stainier, 2004). A small member of the immunoglobulin superfamily, *secreted immunoglobulin domain 4 (Sid4)*, composed solely of 4 immunoglobulin domains, is expressed ubiquitously throughout gastrulation and later at higher levels in the eye, hindbrain and somites (Diiorio et al., 2005). It is similar to the fibronectin binding Ig domains of mouse *Perlecan/HSPG2* suggesting a role in ECM interactions. Sid4 has diverse roles in morphogenesis as assessed by morpholino knock-down, but no effect on evagination. It causes however coloboma.

Adhesion and migration are tightly linked processes. There is extensive cross-talk between adhesion and the cytoskeleton, for example mediated from Cadherin receptors via catenins (Braga, 2000). p120 catenin has recently been shown to be involved in optic vesicle formation in *Xenopus*. A knock-down of p120 catenin or overexpression of p120-uncopuled E-Cadherin in *Xenopus* causes impaired or defective optic vesicle evagination (Ciesiolka et al., 2004). Cadherins are transmembrane glycoproteins that are involved in a variety of processes like cell-cell adhesion, cell sorting but also migration depending on the cellular context (Wheelock and Johnson, 2003). They interact via their juxtamembrane domain (JMD) with members of the p120 catenin family. p120 does not bind to α -catenin but regulates adhesion and actin crosslinking via the small GTPases Rac, Cdc42 and RhoA (Anastasiadis and Reynolds, 2000). The phenotype in *Xenopus* has been attributed to stronger adhesion mediated by the p120-uncoupled Cadherin. Stronger membrane localization was shown as compared to WT Cadherin which was reduced if a dominant-negative form of Rac1 (DN-Rac) was co-expressed. The mutant form of Cadherin used to demonstrate membrane localization was however a form that had a deletion in the JMD, that removed not only the p120 binding site but also the tyrosine

residues involved in Hakai-mediated endocytosis and degradation. The protein might thus be more stable at the membrane. Nevertheless, enhanced adhesion would also account for the defects in tissue separation and delamination/migration of neural crest cells observed in this study (Ciesiolka et al., 2004). Moreover, the phenotype of *p120* depletion can be rescued by co-expression of a dominant-negative form of Rac1 (DN-Rac), WT-RhoA or a DN-form of the downstream effector LIM-kinase. In contrast, overexpression of constitutively active Rac or DN-RhoA induced smaller eyes and heads (Ciesiolka et al., 2004). Enhanced adhesion would counteract both, the cell shape changes and active migration of cells as demonstrated in this study and could constitute a cellular mechanism by which evagination is controlled. However, p120 can both negatively and positively regulate adhesion and p120 uncoupled E-Cadherin has also been shown to reduce adhesion in cell culture (Thoreson et al., 2000). Though further experiments will clearly be necessary to clarify the exact role of p120 catenin in eye morphogenesis it will be interesting to see if signaling via p120 catenin or the modulation of adhesion is involved in cell migration during optic vesicle evagination. A gross effect on Cadherin expression or distribution per se was not observed in the eye field of *eyeless* mutant embryos (unpublished observation).

3.6 Rx3 and proliferation

Proliferation is an important factor in morphogenetic processes also within the neural plate. Cell divisions are highly oriented within the neuroectoderm during gastrulation and neurulation (Concha and Adams, 1998). During gastrulation cells at the dorsal side of the embryos divide preferentially along the anterior-posterior axis, perpendicular to their long axis (Concha and Adams, 1998; Gong et al., 2004). Interestingly, the most anteriormost cells exhibit rather random divisions at 90 % epiboly just before the onset of eye morphogenesis. After completion of epiboly, when the neural plate begins to form, cells divide preferentially in a mediolateral orientation, which is the predominant orientation in the neural keel. In the keel cells preferentially divide at the midline and generate bilateral progeny (Concha and Adams, 1998). Recently it was shown that the AP-orientation of divisions during gastrulation depends on Wnt/PCP signaling (Gong et al., 2004). Interfering with

Dishevelled or *Strabismus* function leads to a random orientation of cell divisions. Equally, divisions are not oriented in *slb/Wnt11* embryos. Oriented cell division accounts for a significant part but not for the total amount of axis elongation. This indicates that the PCP pathway not only regulates cell elongation and intercalation but also spindle orientation and that both processes collaborate in axis elongation. One could speculate that the absence of Wnt signaling in the anterior neuroectoderm accounts for the random orientation of mitosis.

Rx genes have been implicated in the control of proliferation. In *Xenopus*, overexpression of *Rx1* causes hyperproliferation of retina, retinal pigment epithelium and the neural tube (Andreazzoli et al., 1999; Andreazzoli et al., 2003; Casarosa et al., 2003; Mathers et al., 1997). The effect is mediated partially by enhancing proliferation in the anterior neural plate (Andreazzoli et al., 1999; Andreazzoli et al., 2003). Also *Rx3* controls the growth of the optic vesicles however only after their evagination at somitogenesis stages. No difference in the size of the vesicles can be observed at mid neurula stage if *Rx3* overexpressed. Also the size of the eye field as judged by the unaltered expression domain of GFP expressed under the control of the *Rx3* promoter, does not differ between mutant and wild-type. *Rx3* thus controls the proliferation of retinal precursor cells within the evaginated optic vesicle but not during evagination (Loosli et al., 2001). In agreement with this observation no difference in the rate of proliferation was observed among the tracked cells during evagination (data not shown). Proliferation was not analyzed at later stages. Also the preferentially medio-lateral orientation of the mitotic spindle was not significantly altered. This indicates that proliferation or oriented divisions are not involved in optic vesicle evagination but that the major contribution comes from cell movement. The dense packing of mutant retinal precursor cells within the forebrain visualized by their GFP expression argues against the possibility that reduced proliferation causes a failure of the optic vesicles to evaginate. This is in agreement with earlier studies in *Xenopus* that had indicated that a severe reduction in proliferation by combined treatment with the DNA synthesis inhibitors hydroxyurea and aphidicolin during gastrulation, does not interfere with early morphogenesis and development of the central nervous system (Harris and Hartenstein, 1991). Smaller embryos developed that still proceeded relatively normally through neurulation, neural tube closure and CNS subdivision.

3.7 Cell fate and cell behaviour – future aspects

In recent years progress has been made in unraveling the link between cell fate specification and subsequent cellular behaviour. The analysis of movements underlying eye field formation during gastrulation showed that it is controlled by transcription factors such as *Otx2* or *Pax6*, as well as EphrinB1 reverse signaling (Kenyon et al., 2001; Moore et al., 2004). *Otx2* also prevents convergent extension in the anterior neural plate via Calponin (Morgan et al., 1999). A good example for a link between patterning and behaviour is *Brachyury*: the mesoderm inducing transcription factor controls the morphogenesis of the embryos through convergent extension movements by activating the expression of *Wnt11* (Tada and Smith, 2000). An interesting link between cell fate determination and behaviour has been made recently in a study that demonstrated that AP polarity is required for convergent extension (Ninomiya et al., 2004). While Keller explants with wild-type AP patterning converge normally, explants containing two anterior or two posterior halves fail to converge. AP polarity is not required to activate PCP signaling but it might provide the long-range cue as to how cells orient and move in respect to the axis.

It is thus becoming increasingly clear how the patterning of the embryo results in the activation of specific morphogenetic behaviours within different ‘compartments’ that ultimately shape the embryo. While great strides are being made at the elucidation of these processes during gastrulation, little has been known so far about early eye morphogenesis.

Rx3 can be added to the list of genes that control downstream cell behaviour. Using an *in vivo* imaging approach I analysed the morphogenetic behaviour that is elicited downstream of patterning in the formation of the optic vesicle mediated by *Rx3*. I showed in this study how *Rx3* function is required for an eye field specific behaviour in contrast to tel- and diencephalic cells, for their migration, cell shape changes and polarization in early eye formation. Now that we know how cells move and behave during optic vesicle formation, we can start to tackle the problem of how these migrations and cell shape changes are accomplished on a cell biological level. As optic vesicle evagination involves single cell migration it will be interesting to see what mechanisms drive this migratory behaviour downstream of *Rx3*. One would

expect to find molecules involved in the polarization of the cell, probably acting on the actin cytoskeleton, or genes involved in the signal transduction cascade leading to it. Moreover, modulators of adhesion will contribute to a second group of downstream genes. Using the *eyeless/Rx3* mutant to screen for differentially regulated genes downstream of *Rx3* will thus give important insights in the mechanism by which *Rx3* controls the migration and shape changes elicited in retinal precursor cells of the eye field. As general effectors of the cytoskeleton such as Rho GTPases are not likely to be affected at the transcriptional level but rather at the level of their activation and subcellular localization, it will also be interesting to investigate these factors dynamically by *in vivo* imaging, e.g., by using GFP-tethered proteins. Moreover, identified downstream genes can be expressed using the *Rx3* promoter in the *eyeless* background and examined for their ability to rescue the phenotype, contributing to our understanding of morphogenesis at a cellular level.

4 MATERIALS AND METHODS

4.1 Materials

4.1.1 Fish strains

The Cab strain of wild type medaka (*Oryzias latipes*) from a closed stock of EMBL Heidelberg was kept as described previously (Köster et al., 1997). The *eyeless* stock was as described (Loosli et al., 2001; Winkler et al., 2000). For all experiments, *eyeless* in the Cab background was used, that carried the dominant *B* allele from Kaga in the closely linked (1.32 cM) pigmentation locus *b* (Loosli et al., 2001) due to a recombination event (*eI/+*, *B/b*). The *B* allele results in darkly pigmented melanophores in contrast to the recessive *b* allele, that gives rise to unpigmented melanophores. The mutation is thus genetically marked and carriers can be identified by their dark pigmentation. Embryos were staged according to Iwamatsu (Iwamatsu, 1994).

4.1.2 Buffers and Media

All buffers not specifically described in this section were prepared according to standard protocols (Sambrook et al., 1989) using highly deionized water (Millipore), unless indicated differently. Sterilization was achieved by autoclaving.

BSS (balanced salt solution)

111.5 mM	NaCl
5.37 mM	KCl
0.8 mM	MgSO ₄
1.36 mM	CaCl ₂
1%	PEG 20.000

The pH was adjusted to pH 7 using a 5 % NaHCO₃-solution.

BSS/low melting point agarose

0.5 –1.0 % (w/v) low melting point agarose (SeaPlaque GTG agarose, Cambrex Bioscience Rockland, gelling temperature 26 – 30 °C) was dissolved in BSS without PEG 20.000, aliquoted in Eppendorf tubes, stored at 4°C and melted in an Eppendorf

shaker at 80°C if needed. The agarose was kept liquid at 35°C before the embryo was embedded.

Embryo Injection Plates/Transplantation plates

1.5 % agarose was dissolved in distilled water and poured into 9 cm Petri dishes. Before the agarose had solidified, a plastic mould was put on top to form troughs in the agarose. Finally, the mould was removed and the troughs were used to align and orient the embryos for injection. For transplantation experiments a plastic mould was used that produced small indentations.

ERM (Embryo Rearing Medium)

0.1 % (w/v)	NaCl
0.003 % (w/v)	KCl
0.004 % (w/v)	CaCl ₂ x 2H ₂ O
0.016 % (w/v)	MgSO ₄ x 7H ₂ O
0.0001 % (w/v)	Methylenblue (omitted for GFP-positive fish)

LB Medium (Luria-Bertani Medium)

10 g	Tryptone
5 g	Yeast extract
10 g	NaCl
ad 1 l	Deionized H ₂ O

pH adjusted to 7.0 with 5 N NaOH; sterilized. If necessary, 100 µg/ml ampicillin or 30µg/ml kanamycin were added.

LB Agar

15 g agar were dissolved in 1 l LB medium, allowed to cool down to 60°C, supplemented with antibiotics if necessary, and poured into 9 cm diameter petri dishes.

PBS

10 mM	NaCl
1.95 mM	KCl

5.9 mM Na_2HPO_4
1.1 mM KH_2PO_4
pH adjusted to 7.3

PTW

PBS containing 0.1 % Tween 20

10 x Yamamoto Ringer Solution

7.5 % (w/v) NaCl
0.2 % (w/v) KCl
0.2 % (w/v) $\text{CaCl}_2 \times 2\text{H}_2\text{O}$
adjusted to pH 7.3 with HCl

4.1.3 Enzymes, Kits and Standards

- LaTaq DNA polymerase, TaKaRa Biomedicals
- T4 DNA ligase, Roche
- Restriction enzymes, Roche or New England Biolabs (NEB)
- 100 bp DNA ladder, Invitrogen
- 1 kb DNA ladder, Stratagene
- QIAquick Gel Extraction Kit, QIAGEN
- QIAquick PCR Purification Kit, QIAGEN
- QIAfilter Plasmid Maxi Kit, QIAGEN
- Ambion mMessage machine SP6 Kit, Ambion
- Rneasy Mini Kit, QIAGEN
- T3, T7 or SP6 RNA Polymerase, Roche
- GFX™ PCR, DNA and Gel Band Purification Kit, Amersham Biosciences
- *I-SceI* meganuclease, New England Biolabs
- Alkaline Phosphatase, Roche
- Fast Red Tablets, Roche

4.1.4 Antibodies

Primary antibodies (dilution used indicated in brackets):

Rabbit anti-GFP, A-11122, Molecular Probes (1:200)

Mouse anti- α -tubulin, T9026, Sigma (1:400)

Secondary antibodies:

Rhodamine (TRITC)-conjugated goat anti-rabbit, Jackson ImmunoResearch Lab (1:400)

Alexa Fluor 488 goat anti mouse, A-11001, Molecular Probes (1:500)

Alexa Fluor 488 goat anti rabbit, A-11034, Molecular Probes (1:500)

Alexa Fluor 568 goat anti mouse, A-11004, Molecular Probes (1:500)

4.1.5 Bacteria

DH10B, Stratagene

4.1.6 Vectors and Oligos

pCS2⁺ was used as *in vitro* transcription vector (constructed by D. Turner and R. Rupp, 1993)

***ISceI*-pBSII SK⁺**, a pBSII SK⁺ backbone with the MCS flanked by two inverted *I-SceI* recognition sites (Thermes et al., 2002) was used as basic vector for the construction of transgenic lines.

p13-pCS-H2B-mRFP contains histoneH2B fused to monomeric RFP (Campbell et al., 2002) (gift of S. Megason) and was used for mRNA synthesis from the SP6 promoter.

p13-pCS-membrane-mRFP contains a membrane-tethered version of mRFP (gift of S. Megason) and was used for mRNA synthesis.

pCS-H2B-tandemdimer-HcRed contains histoneH2B fused to td-HcRed (Gerlich et al., 2003) and was used for mRNA synthesis.

Oligos were synthesized by Sigma-Genosys Ltd.

4.1.7 Chemicals

All chemicals not listed were supplied by Sigma-Aldrich or Merck.

- Agarose, Electrophoresis grade, Invitrogen
- SeaPlaque GTG agarose, melting temperature (1.5%) $\leq 65^{\circ}\text{C}$, gelling temperature (1.5%) 26 - 30°C , Cambrex
- 1-Heptanol 98 %, Aldrich
- 1-Octanol 99 %, Sigma
- *o*-nitrobenzylacetate (*o*-NBA) was kindly synthesized by Carlo Dinkel in the lab of Carsten Schultz, EMBL Heidelberg
- Proteinase K, Roche
- Narcotic MS222, Sigma-Aldrich

4.1.8 Additional Materials

- Injection needles: Borosilicate glass capillaries with filament GC100F-10, Clark Electromedical Instruments
- Transplantation needles: Borosilicate glass capillaries without filament GC120T-15, Clark Electromedical Instruments (parameters used for pulling: heat 520, pull 45, vel. 50, time 15).
- 35 mm Glass-bottom Microwell dishes, P35G-1.5-10-C, MatTek
- Cell saver tips, Biozym
- SuperFrost Plus microscope slides, Menzel-Gläser

4.1.9 Equipment

Incubators

Heraeus, Karlsruhe (for embryo breeding at 18°C)

RUMED, Rubarth Apparate GmbH (for 28°C)

Needle puller P-30, Sutter Instruments Co, USA, for injection capillaries

Needle puller P-97, Sutter Instruments Co, USA for transplantation capillaries

Eppendorf Microinjector 5242, equipped with a Leica Micromanipulator and a Zeiss

Stemi 2000 stereomicroscope for injections

Leica cryostat CM3050

Stereomicroscopes

Stemi 2000, Zeiss

MZ FLIII fluorescence stereomicroscope, Leica

Microscopes

(A) **Leica AS MDW workstation** with a **Leica DM IRE2** inverted microscope: used for DIC imaging

(B) **Zeiss LSM 510 META**: used for imaging multiple embryos in transplantation experiments.

(C) **PerkinElmer Spinning Disk Confocal Ultraspin RS**: 4D image acquisition for cell tracking and mYFP imaging.

(D) **Leica TCS SP2** upright microscope: image acquisition on fixed material

4.2 Methods

4.2.1 Transgenic fish

GFP was inserted in-frame by homologous recombination in E.coli into an 11 kb SnaBI fragment containing the entire *Rx3* locus. The PCR primers CCA CAT ACC AGC TCC ACG AAC TGG AGC GGG CCT TTG AGA AAT CCC ACT ATG TGA GCA AGG GCG AGG AGC TG and CGG ACC TCC GGC AGG TTG ACC TTC

AGG GCC AGC TCC TCT CTG CTG TAC TAT TAC TTG TAC AGC TCG TCC A were used to amplify the GFP ORF (2 cycles: 45 s 94°, 45 s 50°, 2 min 72° followed by 23 cycles 45 s 94°, 2 min 68°). The PCR products were DpnI digested and purified (Qiaquick spin columns). The 11 kb genomic *Rx3* fragment was digested with BspEI and cotransfected with the GFP PCR fragment into ET-competent E.coli cells as described (Zhang et al., 2000b). Correct recombination was verified by sequence analysis. The resulting 12 kb *Rx3*-GFP fusion plasmid was then inserted into pBS-IsceI between the flanking IsceI restriction sites using NotI and XhoI respectively. The in-frame insertion of GFP is at position 166 of the protein; the open reading frame of GFP is followed by two stop codons, thus the resulting fusion protein lacks the helix 3 of the homeodomain and the entire carboxy terminal region.

Transgenic lines (ET19) were established by coinjecting the plasmid together with I-SceI enzyme into 1-cell stage medaka eggs as described (Thermes et al., 2002). The ET19 line was crossed into the *eyeless* background to yield ET;el,B.

A 4kb fragment of the *Rx3* promoter was PCR amplified from genomic DNA using primers CCG CTC GAG CTC TGA TGT GAT GTT GAC AA and CCA TCG ATG GTT GTC TAA AAA GGA ACT T (2 cycles: 45 s 94°, 45 s 50°, 4 min 72° followed by 21 cycles 45 s 94°, 4 min 68°), digested with XhoI and ClaI respectively and inserted 5' of a GFP-SV40 polyA cassette in pBS-IsceI using XhoI and ClaI restriction sites respectively. This plasmid was used to construct the *Rx3mYFP* line. The plasmid containing the 4 kb promoter fragment was digested with EcoRI and NotI to release GFP. Instead a membraneYFP cassette taken from pEYFP-mem (Clontech) via EcoRI and NotI was inserted. Transgenic lines were established using the meganuclease protocol as described (Thermes et al., 2002). *Rx3mYFP* was crossed into the *eyeless* background to yield *Rx3mYFP*;el,B.

4.2.2 Transcription of mRNA *in vitro*

Histone H2B-mRFP mRNA, membrane-mRFP mRNA or histone H2B-diHcRed mRNA were generated *in vitro* from the SP6 promoter in pCS2⁺ using the Ambion mMessage machine (SP6) according to the manufacturers protocol. The mRNA was

subsequently purified using the Rneasy RNA purification kit from QIAgen according to the manufacturers protocol and stored at -80°C ..

4.2.3 Microinjection

To collect images for cell tracking experiments, embryos of ET;e1,B intercrosses were injected with 150 ng/ μl H2B-mRFP mRNA at the one-cell stage. Fertilized eggs were collected and placed in chilled Yamamoto's embryo rearing medium to slow down development (Yamamoto, 1975). For injection a pressure injector (Eppendorf 5242) was used with borosilicate glass capillaries (GC100TF10, Clark Electromedical Instruments). The Capillaries were backfilled with the injection solution (mRNA in 1X Yamamoto buffer). The injection solution was injected through the chorion into the cytoplasm of the one-cell stage embryos.

4.2.4 Hatching enzyme

500 μl embryos were collected prior to hatching (7 dpf) in a 2 ml Eppendorf tube and shock frozen in liquid nitrogen. After passing them through 3 successive freeze/thaw cycles (37°C /liquid nitrogen), the embryos were homogenized with a pestle, centrifuged for 5 min and the supernatant was collected. The pellet was again homogenized after addition of 500 μl PBS, centrifuged, and the two supernatants were combined. An additional centrifugation step of 10 minutes was used to purify the hatching enzyme from residual debris and oil. The enzyme was stored at -20°C .

4.2.5 Dechorionisation

Embryos were dechorionated and incubated in BSS (balanced salt solution) consisting of 111.5 mM NaCl, 5.37 mM KCl, 0.8 mM MgSO_4 , 1.36 mM CaCl_2 , 1% PEG 20.000. The pH was adjusted to pH 7 using a 5 % NaHCO_3 -solution. To remove the chorion embryos were incubated for 1 to 2 hour(s) in Proteinase K (10mg/ml in H_2O) with rigorous agitation until the chorion hair disappeared. Embryos were rinsed 3 times with water and incubated in hatching enzyme until the chorion was reduced to a soft skin. The embryos were overlaid with BSS and transferred to a petri dish with BSS

using a Cell Saver tip (Biozym). The chorion was gently removed using watchmaker's forceps.

4.2.6 Heptanol treatment and mounting

Dechorionated embryos were incubated in BSS containing 3.5mM 1-heptanol (Sigma, 3.5M stock in DMSO) for 1 hour to block contractile movements. Embryos were embedded in 0.5% to 1 % low-melting point agarose (SeaPlaque GTG, Cambrex) in BSS (w/o PEG), containing 3.5 mM 1-heptanol using glass-bottom petri dishes (MatTek, Ashland, MA). 1-heptanol was added after cooling the agarose to 35°C to prevent evaporation. After the agarose had solidified, the dish was filled with BSS/3.5 mM 1-heptanol.

4.2.7 Microscopy

Part I, Setting up conditions for imaging in medaka:

Brightfield time-lapse recordings were obtained with a HC PL FLUOTAR 10x 0.3 NA air objective on a Leica AS MDW workstation with a Leica DM IRE2 inverted microscope at an ambient room temperature of 24°C.

Confocal time lapse recordings for Figure 15 were made with a HC PL APO 10x 0.4 NA immersion objective on a Leica inverted confocal microscope TCS SP2 at a temperature of 20.5°C. Z-stacks were recorded every 10 minutes by scanning areas of 499.15 x 499.15 μm (0.975 $\mu\text{m pixel}^{-1}$) with 3 μm steps over a total distance of 138 μm . The images were 3D reconstructed over time using Volocity (Improvision, UK).

PartII, 4D imaging of optic vesicle morphogenesis:

(1) Confocal time-lapse recordings for **cell tracking** were obtained on a PerkinElmer Spinning Disk Confocal Ultraspin RS workstation with a Zeiss FLUAR 20x/0.75 air objective at an ambient room temperature of 20°C. Z-stacks were recorded every 2 minutes by scanning areas of 436.8 x 332.8 μm (0.65 $\mu\text{m pixel}^{-1}$) with 2 μm steps over a total distance of 98 μm . Cells were tracked using a software developed by Richard Adams, University of Cambridge (see below).

(2) **Rx3mYFP images** (g-i) for figure 20 were also obtained on this microscope, using a Plan NEOFLUAR 40x/1.3 oil objective and scanning every 5 minutes an area of $218.4 \times 166.4 \mu\text{m}$ ($0.325 \mu\text{m pixel}^{-1}$) with $2 \mu\text{m}$ steps over a total distance of $98 \mu\text{m}$.

(3) The **mosaic analysis** was done on a Zeiss LSM510 META workstation using a PLAN-NEOFLUAR 40x/1.3 Oil DIC objective at 20°C . Multiple embryos were imaged simultaneously over time using the AutoTimeSeries Macro for LSM3.2, developed by Gwen Rabut in the lab of Jan Ellenberg, EMBL Heidelberg (Rabut and Ellenberg, 2004). The individual images were concatenated into a timeseries lsm-file using the Concatenate macro v1.09 by G. Rabut (Rabut and Ellenberg, 2004). Z-stacks were obtained every $3 \mu\text{m}$ over a total distance of $102 \mu\text{m}$.

(4) The same settings were used for imaging **Rx3-mYFP** embryos but a zoom factor of 0.8 was used, thus an area of $287.93 \times 287.93 \mu\text{m}$ ($0.56 \mu\text{m pixel}^{-1}$) was scanned with $3 \mu\text{m}$ steps over a total distance of $102 \mu\text{m}$ every 7 minutes.

4.2.8 Image analysis

Images were analyzed in ImageJ (<http://rsb.info.nih.gov/ij/>), which was also used for the generation of Quicktime movies. Volume reconstruction over time was either done using the software Imaris (Bitplane AG) or Volocity (Improvision, UK).

Time-lapse images of the mosaic analysis were concatenated into timeseries files using the Concatenate macro v1.09 (Rabut and Ellenberg, 2004) and analysed with Imaris (Bitplane AG).

4.2.9 Cell tracking

All routines used for cell tracking and visualization were developed by Richard Adams, University of Cambridge (see also (Glickman et al., 2003)). Cell tracking was done with a modified version of NIH image. Each cell was traced over time by manually marking its approximate geometric center in three dimensions through each time frame, recording each division. The recordings of histoneH2B-mRFP were used for cell tracking, the fate was determined by GFP (and thus Rx3) expression recorded in the second channel. The data produced in this way was analyzed with routines

written in the analysis environment IDL (Research Systems Inc, CO). Final 3D representations were rendered by code generated for the ray-tracer POVray (POVray).

4.2.10 Immunostaining and *in situ* hybridization

Rx3-mYFP st16/17 embryos were genotyped by whole mount *in situ* hybridization for *Rx3* as described (Hauptmann and Gerster, 1994; Loosli et al., 1998) before performing immunostaining. A fluorescent signal was obtained by using Fast Red (Roche) as substrate for the alkaline phosphatase (Roche). YFP is also recognized by the anti-GFP antibody that was used in subsequent staining. Embryos were cryosectioned after whole mount *in situ* hybridization or directly after fixation with 4 % PFA in PBS/0.1 % Tween. For cryosections the embryos were washed three times in PBS/0.1 % Tween (PTW) and 3 times in PBS. After equilibration in 20 % sucrose/PBS overnight at 4°C the embryos were embedded in Tissue-Tek (Sakura) in plastic molds and frozen on dry ice. The blocks were sectioned on a Leica cryostat CM3050 and collected using SuperFrost Plus microscope slides, Menzel-Gläser. The sections were dried for at least two hours, washed three times in PTW for 5 minutes each and blocked for 30 minutes in PTW containing 5 % goat serum. Incubation with the primary antibody (rabbit anti-GFP, Molecular Probes, 1:200; mouse anti- α -tubulin, T9026, Sigma, 1:400) was done overnight at 4°C in PTW/5 % goat serum using wet chambers. Following 3 washes for 5 minutes and 3 washes for 20 minutes in PTW, the slides were incubated for 2 hours at room temperature with the secondary antibody diluted in 1 % goat serum/PTW. The following antibodies were used: TRITC-conjugated goat anti-rabbit (Jackson ImmunoResearch Lab, 1:400), Alexa Fluor 488-conjugated goat anti mouse (Molecular Probes, 1:500), Alexa Fluor 488-conjugated goat anti rabbit (Molecular Probes, 1:500), and Alexa Fluor 568-conjugated goat anti mouse (Molecular Probes, 1:500). After 3 washes in PTW and one in PBS to remove residual Tween for 5 minutes each, the sections were embedded in 80 % glycerol/18 % H₂O that contained 2 % (w/v) n-propyl-galate (Sigma) to prevent photo-bleaching and sealed with a cover slip.

4.2.11 Transplantation

Wild-type embryos of the Cab strain were injected with 120 ng/ μ l membrane-mRFP mRNA at the one-cell stage. These embryos were used as donors while embryos from an Rx3mYFP;el,B intercross were used as host. Both, host and donor embryos were dechorionated as described above and from thereon kept in BSS. At blastula stage (st10/11) (Iwamatsu, 1994) 30-50 cells of the host were transplanted to the animal pole of the donor embryo, using a dissection microscope (Leica, MZ FLIII) equipped with a micromanipulator. Transplantation needles GC120T-15 (Clark Electromedical Instruments) were used and an agarose coated 90 mm petri-dish with little molds to hold the embryos. The embryos were kept at 18°C until the next day and analysed by 4D imaging on a Zeiss LSM510 META workstation using routines developed by Gwen Rabut in the lab of Jan Ellenberg that allow imaging of multiple locations (Rabut and Ellenberg, 2004).

Abbreviations

3D	3-dimensional
4D	4-dimensional
A	anterior
ANB	anterior neural border
aPKC	atypical Protein kinase C
ATP	adenosine triphosphate
AVE	anterior visceral endoderm
bHLH	basic helix-loop-helix
Bmp	Bone morphogenetic protein
bp	base pairs
BrdU	Bromodeoxy uridine
BSS	Balanced salt solution
CE	convergent extension
CBD	catenin-binding domain
cM	centi Morgan
CNS	central nervous system
D	dorsal
DEL	deep layer
DMSO	dimethyl sulfoxide
DN	dominant-negative
DNA	deoxyribonucleic acid
ECM	extracellular matrix
EGF-CFC	epidermal growth factor-related Cripto-Frl-1-Cryptic family
EMT	epithelial-mesenchymal transition
ET cloning	RecE/RecT mediated recombination
EVL	enveloping layer
Fgf	fibroblast growth factor
Fgfr	fibroblast growth factor receptor
GFP	green fluorescent protein
GTP	guanosine triphosphate
H2B	histone 2B
HD	homeodomain
Hpf	hours postfertilization
INL	inner nuclear layer
IPL	inner plexiform layer
JMD	juxtamembrane domain
JNK	JUN-N-terminal kinase
MCS	multiple cloning site
MHB	mid-hindbrain boundary
mRFP	monomeric fluorescent protein
mYFP	membrane YFP
NR	neural retina
OLM	outer limiting membrane
<i>o</i> -NBA	<i>o</i> -nitrobenzyl acetate
ONL	outer nuclear layer

OPL	outer plexiform layer
OV	optic vesicle
P	posterior
PBS	phosphate-buffered saline
PCP	planar cell polarity
PCR	polymerase chain reaction
PDGF	Platelet derived growth factor
PEG	polyethylene glycol
PFA	paraformaldehyde
PGC	primordial germ cells
PI3K	Phosphoinositide-3 kinase
PIP ₂	phosphatidyl-inositol-4,5-biphosphate
PIP ₃	phosphatidyl-inositol-3,4,5-triphosphate
PKB	Protein kinase B
PTW	PBS with Tween20
RA	retinoic acid
RGC	retinal ganglion cell
RNA	ribonucleic acid
RPE	retinal pigmented epithelium
RTK	receptor tyrosine kinase
RXR	retinoic acid receptor
Sey	small eye
sFRP	secreted frizzled related protein
SS	somite stage
TGF β	transforming growth factor β
UV	ultraviolet
V	ventral
WT	wild-type
YFP	yellow fluorescent protein

5 REFERENCES

- Acampora, D., Avantaggiato, V., Tuorto, F., Briata, P., Corte, G. and Simeone, A.** (1998). Visceral endoderm-restricted translation of Otx1 mediates recovering of Otx2 requirements for specification of anterior neural plate and proper gastrulation. *Development* **125**, 5091-5104.
- Acampora, D., Mazan, S., Lallemand, Y., Avantaggiato, V., Maury, M., Simeone, A. and Brulet, P.** (1995). Forebrain and midbrain regions are deleted in Otx2-/- mutants due to a defective anterior neuroectoderm specification during gastrulation. *Development* **121**, 3279-3290.
- Adelmann, H. B.** (1936). The problem of cyclopia. Part II. *The Quarterly Review of Biology* **11**, 284-304.
- Adler, P. N.** (2002). Planar signaling and morphogenesis in Drosophila. *Dev Cell* **2**, 525-535.
- Anastasiadis, P. Z. and Reynolds, A. B.** (2000). The p120 catenin family: complex roles in adhesion, signaling and cancer. *J Cell Sci* **113 (Pt 8)**, 1319-34.
- Andreazzoli, M., Gestri, G., Angeloni, D., Menna, E. and Barsacchi, G.** (1999). Role of *Xrx1* in *Xenopus* eye and anterior brain development. *Development* **126**, 2451-2460.
- Andreazzoli, M., Gestri, G., Cremisi, F., Casarosa, S., Dawid, I. B. and Barsacchi, G.** (2003). *Xrx1* controls proliferation and neurogenesis in *Xenopus* anterior neural plate. *Development* **130**, 5143-54.
- Ang, S., Jin, O., Rhinn, M., Daigle, N., Stevenson, L. and Rossant, J.** (1996). A targeted mouse Otx2 mutation leads to severe defects in gastrulation and formation of axial mesoderm and to deletion of rostral brain. *Development* **122**, 243-252.
- Ara, T., Nakamura, Y., Egawa, T., Sugiyama, T., Abe, K., Kishimoto, T., Matsui, Y. and Nagasawa, T.** (2003). Impaired colonization of the gonads by primordial germ cells in mice lacking a chemokine, stromal cell-derived factor-1 (SDF-1). *Proc Natl Acad Sci U S A* **100**, 5319-23.
- Auman, H. J. and Yelon, D.** (2004). Vertebrate organogenesis: getting the heart into shape. *Curr Biol* **14**, R152-3.
- Austin, C. P., Feldman, D. E., Ida, J. A. and Cepko, C. L.** (1995). Vertebrate Retinal Ganglion Cells Are Selected From Competent Progenitors By the Action of Notch. *Development* **121**, 3637-3650.
- Bailey, T. J., El-Hodiri, H., Zhang, L., Shah, R., Mathers, P. H. and Jamrich, M.** (2004). Regulation of vertebrate eye development by Rx genes. *Int J Dev Biol* **48**, 761-770.
- Barbieri, A. M., Broccoli, V., Bovolenta, P., Alfano, G., Marchitello, A., Mocchetti, C., Crippa, L., Bulfone, A., Marigo, V., Ballabio, A. et al.** (2002). Vax2 inactivation in mouse determines alteration of the eye dorsal-ventral axis, misrouting of the optic fibres and eye coloboma. *Development* **129**, 805-13.
- Belliveau, M. J. and Cepko, C. L.** (1999). Extrinsic and intrinsic factors control the genesis of amacrine and cone cells in the rat retina. *Development - Supplement* **126**, 555-66.
- Belliveau, M. J., Young, T. L. and Cepko, C. L.** (2000). Late retinal progenitor cells show intrinsic limitations in the production of cell types and the kinetics of opsin synthesis. *J Neurosci* **20**, 2247-54.
- Bernier, G., Panitz, F., Zhou, X., Hollemann, T., Gruss, P. and Pieler, T.** (2000). Expanded retina territory by midbrain transformation upon overexpression of Six6 (Otx2) in *Xenopus* embryos. *Mechanisms of Development* **93**, 59-69.
- Bertet, C., Sulak, L. and Lecuit, T.** (2004). Myosin-dependent junction remodelling controls planar cell intercalation and axis elongation. *Nature (London)* **429**, 667-71.

- Bertrand, V., Hudson, C., Caillol, D., Popovici, C. and Lemaire, P.** (2003). Neural tissue in ascidian embryos is induced by FGF9/16/20, acting via a combination of maternal GATA and Ets transcription factors. *Cell* **115**, 615-627.
- Bertuzzi, S., Hindges, R., Mui, S. H., O'Leary, D. D. and Lemke, G.** (1999). The homeodomain protein *vax1* is required for axon guidance and major tract formation in the developing forebrain. *Genes & Development* **13**, 3092-3105.
- Bingham, S., Higashijima, S., Okamoto, H. and Chandrasekhar, A.** (2002). The Zebrafish trilobite gene is essential for tangential migration of branchiomotor neurons. *Dev Biol* **242**, 149-60.
- Bouwmeester, T., Kim, S., Sasai, Y., Lu, B. and De Robertis, E. M.** (1996). Cerberus is a head-inducing secreted factor expressed in the anterior endoderm of Spemann's organizer. *Nature (London)* **382**, 595-601.
- Bovolenta, P., Mallamaci, A., Puelles, L. and Boncinelli, E.** (1998). Expression pattern of *cSix3*, a member of the Six/sine oculis family of transcription factors. *Mechanisms of Development* **70**, 201-203.
- Braga, V.** (2000). The crossroads between cell-cell adhesion and motility. *Nat Cell Biol* **2**, E182-4.
- Braun, M. M., Etheridge, A., Bernard, A., Robertson, C. P. and Roelink, H.** (2003). Wnt signaling is required at distinct stages of development for the induction of the posterior forebrain. *Development* **130**, 5579-87.
- Bronner-Fraser, M.** (1994). Neural crest cell formation and migration in the developing embryo. *Faseb J* **8**, 699-706.
- Callaerts, P., Halder, G. and Gehring, W. J.** (1997). PAX-6 in development and evolution. *Annual Review of Neuroscience* **20**, 483-532.
- Campbell, R. E., Tour, O., Palmer, A. E., Steinbach, P. A., Baird, G. S., Zacharias, D. A. and Tsien, R. Y.** (2002). A monomeric red fluorescent protein. *Proc Natl Acad Sci U S A* **99**, 7877-7882.
- Carl, M., Loosli, F. and Wittbrodt, J.** (2002). Six3 inactivation reveals its essential role for the formation and patterning of the vertebrate eye. *Development* **129**, 4057-4063.
- Carl, M. and Wittbrodt, J.** (1999). Graded interference with FGF-signalling reveals its dorso-ventral asymmetry at the mid-hindbrain boundary. *Development* **126**, 5659-5667.
- Carmany-Rampey, A. and Schier, A. F.** (2001). Single-cell internalization during zebrafish gastrulation. *Curr Biol* **11**, 1261-5.
- Carreira-Barbosa, F., Concha, M. L., Takeuchi, M., Ueno, N., Wilson, S. W. and Tada, M.** (2003). Prickle 1 regulates cell movements during gastrulation and neuronal migration in zebrafish. *Development* **130**, 4037-46.
- Casarosa, S., Amato, M. A., Andreatzoli, M., Gestri, G., Barsacchi, G. and Cremisi, F.** (2003). Xrx1 controls proliferation and multipotency of retinal progenitors. *Mol Cell Neurosci* **22**, 25-36.
- Casarosa, S., Andreatzoli, M., Simeone, A. and Barsacchi, G.** (1997). Xrx1, a novel *Xenopus* homeobox gene expressed during eye and pineal gland development. *Mechanisms of Development* **61**, 187-98.
- Chen, J. N., Haffter, P., Odenthal, J., Vogelsang, E., Brand, M., van Eeden, F. J., Furutani-Seiki, M., Granato, M., Hammerschmidt, M., Heisenberg, C. P. et al.** (1996). Mutations affecting the cardiovascular system and other internal organs in zebrafish. *Development* **123**, 293-302.

- Chiang, C., Litingtung, Y., Lee, E., Young, K. E., Corden, J. L., Westphal, H. and Beachy, P. A.** (1996). Cyclopia and defective axial patterning in mice lacking Sonic Hedgehog gene function. *Nature (London)* **383**, 407-413.
- Choi, S. C. and Han, J. K.** (2002). *Xenopus* Cdc42 regulates convergent extension movements during gastrulation through Wnt/Ca²⁺ signaling pathway. *Dev Biol* **244**, 342-57.
- Chong, L. D., Park, E. K., Latimer, E., Friesel, R. and Daar, I. O.** (2000). Fibroblast growth factor receptor-mediated rescue of x-ephrin B1-induced cell dissociation in *Xenopus* embryos. *Mol Cell Biol* **20**, 724-34.
- Chow, R. L., Altmann, C. R., Lang, R. A. and Hemmati-Brivanlou, A.** (1999). Pax6 induces ectopic eyes in a vertebrate. *Development* **126**, 4213-4222.
- Chow, R. L. and Lang, R. A.** (2001). Early eye development in vertebrates. *Annual Review of Cell & Developmental Biology* **17**, 255-96.
- Christ, G. J., Spray, D. C., el-Sabban, M., Moore, L. K. and Brink, P. R.** (1996). Gap junctions in vascular tissues. Evaluating the role of intercellular communication in the modulation of vasomotor tone. *Circ Res* **79**, 631-46.
- Christiansen, J. H., Coles, E. G. and Wilkinson, D. G.** (2000). Molecular control of neural crest formation, migration and differentiation. *Curr Opin Cell Biol* **12**, 719-24.
- Chuang, J. C., Mathers, P. H. and Raymond, P. A.** (1999). Expression of three *Rx* homeobox genes in embryonic and adult zebrafish. *Mechanisms of Development* **84**, 195-198.
- Chuang, J. C. and Raymond, P. A.** (2001). Zebrafish genes *rx1* and *rx2* help define the region of forebrain that gives rise to retina. *Dev Biol* **231**, 13-30.
- Chuang, J. C. and Raymond, P. A.** (2002). Embryonic origin of the eyes in teleost fish. *Bioessays* **24**, 519-29.
- Ciesiolka, M., Delvaeye, M., Van Imschoot, G., Verschuere, V., McCrea, P., Van Roy, F. and Vleminckx, K.** (2004). p120 catenin is required for morphogenetic movements involved in the formation of the eyes and the craniofacial skeleton in *Xenopus*. *J. Cell Sci.* **117**, 4325-39.
- Concha, M. L. and Adams, R. J.** (1998). Oriented cell divisions and cellular morphogenesis in the zebrafish gastrula and neurula: a time-lapse analysis. *Development* **125**, 983-94.
- Cooke, J. E. and Moens, C. B.** (2002). Boundary formation in the hindbrain: Eph only it were simple. *Trends Neurosci* **25**, 260-7.
- Cope, J., Fluck, R., Nicklas, L., Plumhoff, L. A. and Sincock, S.** (1990). The stellate layer and rhythmic contractions of the *Oryzias latipes* embryo. *J Exp Zool* **254**, 270-5.
- Crossley, P. H. and Martin, G. R.** (1995). The mouse *Fgf8* gene encodes a family of polypeptides and is expressed in regions that direct outgrowth and patterning in the developing embryo. *Development* **121**, 439-51.
- Darken, R. S., Scola, A. M., Rakeman, A. S., Das, G., Mlodzik, M. and Wilson, P. A.** (2002). The planar polarity gene *strabismus* regulates convergent extension movements in *Xenopus*. *Embo J* **21**, 976-85.
- Davidson, B. P., Kinder, S. J., Steiner, K., Schoenwolf, G. C. and Tam, P. P.** (1999). Impact of node ablation on the morphogenesis of the body axis and the lateral asymmetry of the mouse embryo during early organogenesis. *Developmental Biology* **211**, 11-26.
- De Calisto, J., Araya, C., Marchant, L., Riaz, C. F. and Mayor, R.** (2005). Essential role of non-canonical Wnt signalling in neural crest migration. *Development* **132**, 2587-97.

- Del Bene, F., Tessmar-Raible, K. and Wittbrodt, J.** (2004). Direct interaction of geminin and Six3 in eye development. *Nature (London)* **427**, 745-9.
- Deschet, K., Bourrat, F., Ristoratore, F., Chourrout, D. and Joly, J.-S.** (1999). Expression of the medaka (*Oryzias latipes*) *Ol-Rx3* paired-like gene in two diencephalic derivatives, the eye and the hypothalamus. *Mechanisms of Development* **83**, 179-182.
- Diiorio, P. J., Runko, A., Farrell, C. A. and Roy, N.** (2005). Sid4: A secreted vertebrate immunoglobulin protein with roles in zebrafish embryogenesis. *Dev Biol* **282**, 55-69.
- Djiane, A., Riou, J., Umbhauer, M., Boucaut, J. and Shi, D.** (2000). Role of frizzled 7 in the regulation of convergent extension movements during gastrulation in *Xenopus laevis*. *Development* **127**, 3091-100.
- Doitsidou, M., Reichman-Fried, M., Stebler, J., Kopranner, M., Dorries, J., Meyer, D., Esguerra, C. V., Leung, T. and Raz, E.** (2002). Guidance of primordial germ cell migration by the chemokine SDF-1. *Cell* **111**, 647-59.
- Dorsky, R. I., Itoh, M., Moon, R. T. and Chitnis, A.** (2003). Two *tcf3* genes cooperate to pattern the zebrafish brain. *Development* **130**, 1937-1947.
- Dorsky, R. I., Sheldahl, L. C. and Moon, R. T.** (2002). A transgenic Lef1/ β -catenin-dependent reporter is expressed in spatially restricted domains throughout zebrafish development. *Dev Biol* **241**, 229-237.
- Driever, W.** (2000). Developmental biology. Bringing two hearts together. *Nature (London)* **406**, 141-2.
- Eggert, T., Hauck, B., Hildebrandt, N., Gehring, W. J. and Walldorf, U.** (1998). Isolation of a *Drosophila* homolog of the vertebrate homeobox gene *Rx* and its possible role in brain and eye development. *Proceedings of the National Academy of Sciences of the United States of America* **95**, 2343-2348.
- Ekker, S. C., Ungar, A. R., Greenstein, P., v. Kessler, D., Porter, J. A., Moon, R. T. and Beachy, P. A.** (1995). Patterning activities of vertebrate hedgehog proteins in the developing eye and brain. *Current Biology* **5**, 944-955.
- Elul, T. and Keller, R.** (2000). Monopolar protrusive activity: a new morphogenetic cell behaviour in the neural plate dependent on vertical interactions with the mesoderm in *Xenopus*. *Dev Biol* **224**, 3-19.
- Etienne-Manneville, S. and Hall, A.** (2002). Rho GTPases in cell biology. *Nature (London)* **420**, 629-35.
- Ezin, A. M., Skoglund, P. and Keller, R.** (2003). The midline (notochord and notoplate) patterns the cell motility underlying convergence and extension of the *Xenopus* neural plate. *Dev Biol* **256**, 100-113.
- Feldman, B., Gates, M. A., Egan, E. S., Dougan, S. T., Rennebeck, G., Sirotkin, H. I., Schier, A. F. and Talbot, W. S.** (1998). Zebrafish Organizer Development and Germ-Layer Formation Require Nodal-Related Signals. *Nature (London)* **395**, 181-185.
- Finley, K. R., Tennessen, J. and Shawlot, W.** (2003). The mouse secreted frizzled-related protein 5 gene is expressed in the anterior visceral endoderm and foregut endoderm during early post-implantation development. *Gene Expr. Patterns* **3**, 681-684.
- Fleig, R.** (1993). Embryogenesis in mouth-breeding cichlids (Osteichthyes, Teleostei): structure and fate of the enveloping layer. *Roux's Arch. Dev. Biol.* **203**, 124-130.

- Fluck, R., Gunning, R., Pellegrino, J., Barron, T. and Panitch, D.** (1983). Rhythmic contractions of the blastoderm of the medaka *Oryzias latipes*, a teleost. *Journal of Experimental Zoology* **226**, 245-253.
- Fluck, R. A., Killian, C. E., Miller, K., Dalpe, J. N. and Shih, T.-M.** (1984). Contraction of an embryonic epithelium, the enveloping layer of the medaka (*Oryzias latipes*), a teleost. *J. Exp. Zoology* **229**, 127-142.
- Fluck, R. A., Miller, A. L. and Jaffe, L. F.** (1991). Calcium waves accompany contraction waves in the *Oryzias latipes* (medaka) blastoderm. *Biol. Bull.* **181**, 352.
- Foley, A. C., Skromne, I. and Stern, C. D.** (2000). Reconciling different models of forebrain induction and patterning: a dual role for the hypoblast. *Development* **127**, 3839-54.
- Foley, A. C. and Stern, C. D.** (2001). Evolution of vertebrate forebrain development: how many different mechanisms? *J. Anat.* **199**, 35-52.
- Friedl, P., Hegerfeldt, Y. and Tusch, M.** (2004). Collective cell migration in morphogenesis and cancer. *Int J Dev Biol* **48**, 441-9.
- Fujiwara, M., Uchida, T., Osumi-Yamashita, N. and Eto, K.** (1994). Uchida rat (rSey): a new mutant rat with craniofacial abnormalities resembling those of the mouse Sey mutant. *Differentiation* **57**, 31-38.
- Furukawa, T., Kozak, C. A. and Cepko, C. L.** (1997). Rax, a Novel Paired-Type Homeobox Gene, Shows Expression in the Anterior Neural Fold and Developing Retina. *Proceedings of the National Academy of Sciences USA* **94**, 3088-3093.
- Furutani-Seiki, M. and Wittbrodt, J.** (2004). Medaka and zebrafish, an evolutionary twin study. *Mech Dev* **121**, 629-37.
- Gehring, W. J.** (2002). The genetic control of eye development and its implications for the evolution of the various eye-types. *Int J Dev Biol* **46**, 65-73.
- Gerlich, D., Beaudouin, J., Kalbfuss, B., Daigle, N., Eils, R. and Ellenberg, J.** (2003). Global chromosome positions are transmitted through mitosis in mammalian cells. *Cell* **112**, 751-64.
- Glaser, T., Walton, D. S. and Maas, R. L.** (1992). Genomic structure, evolutionary conservation and aniridia mutations in the human PAX6 gene. *Nat Genet* **2**, 232-239.
- Glickman, N. S., Kimmel, C. B., Jones, M. A. and Adams, R. J.** (2003). Shaping the zebrafish notochord. *Development* **130**, 873-887.
- Glinka, A., Wu, W., Delius, H., Monaghan, A. P., Blumenstock, C. and Niehrs, C.** (1998). Dickkopf-1 is a member of a new family of secreted proteins and functions in head induction. *Nature (London)* **391**, 357-362.
- Glinka, A., Wu, W., Onichtchouk, D., Blumenstock, C. and Niehrs, C.** (1997). Head induction by simultaneous repression of Bmp and Wnt signalling in *Xenopus*. *Nature (London)* **389**, 517-519.
- Gong, Y., Mo, C. and Fraser, S. E.** (2004). Planar cell polarity signalling controls cell division orientation during zebrafish gastrulation. *Nature (London)* **430**, 689-93.
- Goto, T. and Keller, R.** (2002). The planar cell polarity gene strabismus regulates convergence and extension and neural fold closure in *Xenopus*. *Dev Biol* **247**, 165-81.
- Grabher, C., Henrich, T., Sasado, T., Arenz, A., Furutani-Seiki, M. and Wittbrodt, J.** (2003). Transposon-mediated enhancer trapping in medaka. *Gene* **322**, 57-66.
- Grabher, C., Joly, J. S. and Wittbrodt, J.** (2004). Highly efficient zebrafish transgenesis mediated by the meganuclease I-SceI. *Methods Cell Biol* **77**, 381-401.
- Granadino, B., Gallardo, M. E., Lopez-Rios, J., Sanz, R., Ramos, C., Ayuso, C., Bovolenta, P. and Rodriguez de Cordoba, S.** (1999). Genomic cloning, structure,

- expression pattern, and chromosomal location of the human SIX3 gene. *Genomics* **55**, 100-105.
- Grindley, J. C., Davidson, D. R. and Hill, R. E.** (1995). The role of PAX6 in eye and nasal development. *Development* **121**, 1433-1442.
- Gritsman, K., Zhang, J. J., Cheng, S., Heckscher, E., Talbot, W. S. and Schier, A. F.** (1999). The EGF-CFC protein one-eyed pinhead is essential for nodal signaling. *Cell* **97**, 121-132.
- Grosshans, J. and Wieschaus, E.** (2000). A genetic link between morphogenesis and cell division during formation of the ventral furrow in *Drosophila*. *Cell* **101**, 523-31.
- Grunz, H. and Tacke, L.** (1989). Neural differentiation of *Xenopus laevis* ectoderm takes place after disaggregation and delayed reaggregation without inducer. *Cell Differentiation & Development* **28**, 211-217.
- Habas, R., Dawid, I. B. and He, X.** (2003). Coactivation of Rac and Rho by Wnt/Frizzled signaling is required for vertebrate gastrulation. *Genes Dev* **17**, 295-309.
- Habas, R., Kato, Y. and He, X.** (2001). Wnt/Frizzled activation of Rho regulates vertebrate gastrulation and requires a novel Formin homology protein Daam1. *Cell* **107**, 843-54.
- Halder, G., Callaerts, P. and Gehring, W. J.** (1995). Induction of ectopic eyes by targeted expression of the eyeless gene in *Drosophila*. *Science* **267**, 1788-1792.
- Hallonet, M., Hollemann, T., Pieler, T. and Gruss, P.** (1999). Vax1, a novel homeobox-containing gene, directs development of the basal forebrain and visual system. *Genes & Development* **13**, 3106-3114.
- Hansen, C. S., Marion, C. D., Steele, K., George, S. and Smith, W. C.** (1997). Direct neural induction and selective inhibition of mesoderm and epidermis inducers by Xnr3. *Development* **124**, 483-492.
- Hanson, I. M., Fletcher, J. M., Jordan, T., Brown, A., Taylor, D., Adams, R. J., Punnett, H. H. and van Heyningen, V.** (1994). Mutations at the PAX6 locus are found in heterogenous anterior segment malformations including Peter's anomaly. *Nat Genet* **6**, 168-173.
- Hardcastle, Z. and Papalopulu, N.** (2000). Distinct effects of XBF-1 in regulating the cell cycle inhibitor p27(XIC1) and imparting a neural fate. *Development* **127**, 1303-1314.
- Harris, W. A. and Hartenstein, V.** (1991). Neuronal determination without cell division in *Xenopus* embryos. *Neuron* **6**, 499-515.
- Hashimoto, H., Itoh, M., Yamanaka, Y., Yamashita, S., Shimizu, T., Solnica-Krezel, L., Hibi, M. and Hirano, T.** (2000). Zebrafish Dkk1 functions in forebrain specification and axial mesendoderm formation. *Dev Biol* **217**, 138-52.
- Hatta, K., Kimmel, C. B., Ho, R. K. and Walker, C.** (1991). The cyclops mutation blocks specification of the floor plate of the zebrafish central nervous system. *Nature (London)* **350**, 339-341.
- Hauptmann, G. and Gerster, T.** (1994). Two-color whole-mount in situ hybridization to vertebrate and *Drosophila* embryos. *Trends in Genetics* **10**, 266.
- Hawley, S. H., Wunnenber-Stapleton, K., Hashimoto, C., Laurent, M. N., Watabe, T., Blumberg, B. W. and Cho, K. W.** (1995). Disruption of BMP signals in embryonic *Xenopus* ectoderm leads to direct neural induction. *Genes Dev* **9**, 2923-35.
- Heisenberg, C. P., Houart, C., Take-uchi, M., Rauch, G. J., Young, N., Coutinho, P., Masai, I., Caneparo, L., Concha, M. L., Geisler, R. et al.** (2001). A mutation in the Gsk3-binding domain of zebrafish Masterblind/Axin1 leads to a fate transformation of telencephalon and eyes to diencephalon. *Genes & Development* **15**, 1427-1434.

- Heisenberg, C. P. and Nusslein-Volhard, C.** (1997). The function of *silberblick* in the positioning of the eye anlage in the zebrafish embryo. *Dev Biol* **184**, 85-94.
- Heisenberg, C. P., Tada, M., Rauch, G. J., Saude, L., Concha, M. L., Geisler, R., Stemple, D. L., Smith, J. C. and Wilson, S. W.** (2000). *Silberblick/Wnt11* mediates convergent extension movements during zebrafish gastrulation. *Nature (London)* **405**, 76-81.
- Hemmati-Brivanlou, A., Kelly, O. G. and Melton, D. A.** (1994). Follistatin, an antagonist of activin, is expressed in the Spemann organizer and displays direct neuralizing activity. *Cell* **77**, 283-95.
- Hemmati-Brivanlou, A. and Melton, D. A.** (1994). Inhibition of activin receptor signaling promotes neuralization in *Xenopus*. *Cell* **77**, 273-281.
- Herzog, W., Sonntag, C., Von Der Hardt, S., Roehl, H. H., Varga, Z. M. and Hammerschmidt, M.** (2004). *Fgf3* signaling from the ventral diencephalon is required for early specification and subsequent survival of the zebrafish adenohypophysis. *Development* **131**, 3681-92.
- Hill, R. E., Favor, J., Hogan, B. L. M., Ton, C. C. T., Saunders, G. F., Hanson, I. M., Prosser, J., Jordan, T., Hastie, N. D. and van Heyningen, V.** (1991). Mouse small eye results from mutations in a paired-like homeobox containing gene. *Nature (London)* **354**, 522-525.
- Hirose, Y., Varga, Z. M., Kondoh, H. and Furutani-Seiki, M.** (2004). Single cell lineage and regionalization of cell populations during Medaka neurulation. *Development* **131**, 2553-2563.
- Hirsch, N. and Harris, W. A.** (1997). *Xenopus Pax-6* and retinal development. *Journal of Neurobiology* **32**, 45-61.
- Hogan, B. L. M., Horsburgh, G., Cohen, J., Hetherington, C. M., Fisher, G. and Lyon, M. F.** (1986). Small eyes (*Sey*): a homozygous lethal mutation on chromosome 2 which affects the differentiation of both lens and nasal placodes in the mouse. *Journal of Embryology and Experimental Morphology* **97**, 95-110.
- Holder, N. and Klein, R.** (1999). Eph receptors and ephrins: effectors of morphogenesis. *Development* **126**, 2033-44.
- Holleman, T., Bellefroid, E. and Pieler, T.** (1998). The *Xenopus* homologue of the *Drosophila* gene *tailless* has a function in early eye development. *Development* **125**, 2425-2432.
- Holt, C. E., Bertsch, T. W., Ellis, H. M. and Harris, W. A.** (1988). Cellular determination in the *Xenopus* retina is independent of lineage and birth date. *Neuron* **1**, 15-26.
- Hongo, I., Kengaku, M. and Okamoto, H.** (1999). FGF signaling and the anterior neural induction in *Xenopus*. *Dev Biol* **216**, 561-581.
- Houart, C., Caneparo, L., Heisenberg, C., Barth, K., Take-Uchi, M. and Wilson, S.** (2002). Establishment of the telencephalon during gastrulation by local antagonism of Wnt signaling. *Neuron* **35**, 255-65.
- Houart, C., Westerfield, M. and Wilson, S. W.** (1998). A small population of anterior cells patterns for forebrain during zebrafish gastrulation. *Nature (London)* **391**, 788-792.
- Hudson, C., Darras, S., Caillol, D., Yasuo, H. and Lemaire, P.** (2003). A conserved role for the MEK signalling pathway in neural tissue specification and posteriorisation in the invertebrate chordate, the ascidian *Ciona intestinalis*. *Development* **130**, 147-159.

- Hyatt, G. A., Schmitt, E. A., Marsh-Armstrong, N., McCaffery, P., Drager, U. C. and Dowling, J. E.** (1996). Retinoic acid establishes ventral retinal characteristics. *Development* **122**, 195-204.
- Irvine, K. D. and Wieschaus, E.** (1994). Cell intercalation during *Drosophila* germband extension and its regulation by pair-rule segmentation genes. *Development* **120**, 827-41.
- Isaacs, H. V., Andreatzoli, M. and Slack, J. M.** (1999). Anteroposterior patterning by mutual repression of orthodenticle and caudal-type transcription factors. *Evol Dev* **1**, 143-152.
- Itoh, M., Kudoh, T., Dedekian, M., Kim, C. H. and Chitnis, A. B.** (2002). A role for *iro1* and *iro7* in the establishment of an anteroposterior compartment of the ectoderm adjacent to the midbrain-hindbrain boundary. *Development* **129**, 2317-2327.
- Iwamatsu, T.** (1994). Stages of normal development in the medaka *Oryzias latipes*. *Zoo. Sci.* **11**, 825-839.
- Jessen, J. R., Topczewski, J., Bingham, S., Sepich, D. S., Marlow, F., Chandrasekhar, A. and Solnica-Krezel, L.** (2002). Zebrafish trilobite identifies new roles for *Strabismus* in gastrulation and neuronal movements. *Nat Cell Biol* **4**, 610-5.
- Jordan, T., Hanson, I., Zaletayev, D., Hodgson, S., Prosser, J., Seawright, A., Hastie, N. and van Heyningen, V.** (1992). The human *PAX6* gene is mutated in two patients with aniridia. *Nat Genet* **1**, 328-32.
- Kastner, P., Grondona, J. M., Mark, M., Gansmuller, A., LeMeur, M., Decimo, D., Vonesch, J. L., Dolle, P. and Chambon, P.** (1994). Genetic analysis of RXR alpha developmental function: convergence of RXR and RAR signaling pathways in heart and eye morphogenesis. *Cell* **78**, 987-1003.
- Kawano, Y. and Kypta, R.** (2003). Secreted antagonists of the Wnt signalling pathway. *J. Cell Sci.* **116**, 2627-2634.
- Kazanskaya, O., Glinka, A. and Niehrs, C.** (2000). The role of *Xenopus dickkopf1* in prechordal plate specification and neural patterning. *Development* **127**, 4981-92.
- Keller, R.** (2002). Shaping the vertebrate body plan by polarized embryonic cell movements. *Science* **298**, 1950-1954.
- Keller, R., Davidson, L., Edlund, A., Elul, T., Ezin, M., Shook, D. and Skoglund, P.** (2000). Mechanisms of convergence and extension by cell intercalation. *Philos Trans R Soc Lond B Biol Sci* **355**, 897-922.
- Keller, R., Shih, J. and Sater, A.** (1992). The cellular basis of the convergence and extension of the *Xenopus* neural plate. *Dev Dyn* **193**, 199-217.
- Kennedy, B. N., Stearns, G. W., Smyth, V. A., Ramamurthy, V., van Eeden, F., Ankoudinova, I., Raible, D., Hurley, J. B. and Brockerhoff, S. E.** (2004). Zebrafish *rx3* and *mab2112* are required during eye morphogenesis. *Dev Biol* **270**, 336-349.
- Kenyon, K. L., Zaghloul, N. and Moody, S. A.** (2001). Transcription factors of the anterior neural plate alter cell movements of epidermal progenitors to specify a retinal fate. *Dev Biol* **240**, 77-91.
- Kiecker, C. and Niehrs, C.** (2001a). A morphogen gradient of Wnt/beta-catenin signalling regulates anteroposterior neural patterning in *Xenopus*. *Development* **128**, 4189-201.
- Kiecker, C. and Niehrs, C.** (2001b). The role of prechordal mesendoderm in neural patterning. *Curr Opin Neurobiol* **11**, 27-33.
- Kikuchi, Y., Segawa, H., Tokumoto, M., Tsubokawa, T., Hotta, Y., Uyemura, K. and Okamoto, H.** (1997). Ocular and cerebellar defects in zebrafish induced by

- overexpression of the LIM domains of the islet-3 LIM/homeodomain protein. *Neuron* **18**, 369-82.
- Kilian, B., Mansukoski, H., Barbosa, F. C., Ulrich, F., Tada, M. and Heisenberg, C. P.** (2003). The role of Ppt/Wnt5 in regulating cell shape and movement during zebrafish gastrulation. *Mech Dev* **120**, 467-476.
- Kim, C. H., Oda, T., Itoh, M., Jiang, D., Artinger, K. B., Chandrasekharappa, S. C., Driever, W. and Chitnis, A. B.** (2000). Repressor activity of Headless/Tcf3 is essential for vertebrate head formation. *Nature (London)* **407**, 913-6.
- Kimmel, C. B., Warga, R. M. and Schilling, T. F.** (1990). Origin and organization of the zebrafish fate map. *Development* **108**, 581-94.
- Kimura, C., Yoshinaga, K., Tian, E., Suzuki, M., Aizawa, S. and Matsuo, I.** (2000). Visceral endoderm mediates forebrain development by suppressing posteriorizing signals. *Dev Biol* **225**, 304-21.
- Klingensmith, J., Ang, S. L., Bachiller, D. and Rossant, J.** (1999). Neural induction and patterning in the mouse in the absence of the node and its derivatives. *Dev Biol* **216**, 535-549.
- Knaut, H., Werz, C., Geisler, R. and Nusslein-Volhard, C.** (2003). A zebrafish homologue of the chemokine receptor Cxcr4 is a germ-cell guidance receptor. *Nature (London)* **421**, 279-82.
- Kobayashi, D., Kobayashi, M., Matsumoto, K., Ogura, T., Nakafuku, M. and Shimamura, K.** (2002). Early subdivisions in the neural plate define distinct competence for inductive signals. *Development* **129**, 83-93.
- Kobayashi, M., Nishikawa, K., Suzuki, T. and Yamamoto, M.** (2001). The homeobox protein Six3 interacts with the Groucho corepressor and acts as a transcriptional repressor in eye and forebrain formation. *Dev Biol* **232**, 315-26.
- Kobayashi, M., Toyama, R., Takeda, H., Dawid, I. B. and Kawakami, K.** (1998). Overexpression of the forebrain-specific homeobox gene six3 induces rostral forebrain enlargement in zebrafish. *Development* **125**, 2973-2982.
- Koshiba-Takeuchi, K., Takeuchi, J. K., Matsumoto, K., Momose, T., Uno, K., Hoepker, V., Ogura, K., Takahashi, N., Nakamura, H., Yasuda, K. et al.** (2000). Tbx5 and the retinotectum projection. *Science* **287**, 134-137.
- Köster, R., Stick, R., Loosli, F. and Wittbrodt, J.** (1997). Medaka spalt acts as a target gene of hedgehog signaling. *Development* **124**, 3147-3156.
- Kurokawa, D., Kiyonari, H., Nakayama, R., Kimura-Yoshida, C., Matsuo, I. and Aizawa, S.** (2004). Regulation of Otx2 expression and its functions in mouse forebrain and midbrain. *Development* **131**, 3319-3331.
- Lagutin, O., Zhu, C. C., Furuta, Y., Rowitch, D. H., McMahon, A. P. and Oliver, G.** (2001). Six3 promotes the formation of ectopic optic vesicle-like structures in mouse embryos. *Dev Dyn* **221**, 342-349.
- Lagutin, O. V., Zhu, C. C., Kobayashi, D., Topczewski, J., Shimamura, K., Puelles, L., Russell, H. R. C., McKinnon, P. J., Solnica-Krezel, L. and Oliver, G.** (2003). Six3 repression of Wnt signaling in the anterior neuroectoderm is essential for vertebrate forebrain development. *Genes & Development* **17**, 368-379.
- Lamb, T. M., Knecht, A. K., Smith, W. C., Stachel, S. E., Economides, A. N., Stahl, N., Yancopolous, G. D. and Harland, R. M.** (1993). Neural induction by the secreted polypeptide noggin. *Science* **262**, 713-718.
- Lang, R. A.** (2004). Pathways regulating lens induction in the mouse. *Int J Dev Biol* **48**, 783-791.

- Launay, C., Fromentoux, V., Shi, D. L. and Boucaut, J. C.** (1996). A truncated FGF receptor blocks neural induction by endogenous *Xenopus* inducers. *Development* **122**, 869-880.
- Leise, W. F., 3rd and Mueller, P. R.** (2004). Inhibition of the cell cycle is required for convergent extension of the paraxial mesoderm during *Xenopus* neurulation. *Development* **131**, 1703-15.
- Leptin, M.** (1994). Morphogenesis. Control of epithelial cell shape changes. *Curr Biol* **4**, 709-12.
- Leptin, M.** (2005). Gastrulation movements: the logic and the nuts and bolts. *Dev Cell* **8**, 305-20.
- Li, H., Tierney, C., Wen, L., Wu, J. Y. and Rao, Y.** (1997). A single morphogenetic field gives rise to two retina primordia under the influence of the prechordal plate. *Development* **124**, 603-615.
- Li, X., Perissi, V., Liu, F., Rose, D. W. and Rosenfeld, M. G.** (2002). Tissue-specific regulation of retinal and pituitary precursor cell proliferation. *Science* **297**, 1180-3.
- Li, Z., Joseph, N. M. and Easter, S. S. J.** (2000). The morphogenesis of the zebrafish eye, including a fate map of the optic vesicle. *Developmental Dynamics* **218**, 175-188.
- Linker, C. and Stern, C. D.** (2004). Neural induction requires BMP inhibition only as a late step, and involves signals other than FGF and Wnt antagonists. *Development* **131**, 5671-5681.
- Lippincott-Schwartz, J. and Patterson, G. H.** (2003). Development and use of fluorescent protein markers in living cells. *Science* **300**, 87-91.
- Livesey, F. J. and Cepko, C. L.** (2001). Vertebrate neural cell-fate determination: lessons from the retina. *Nature Reviews Neuroscience* **2**, 109-18.
- Locascio, A. and Nieto, M. A.** (2001). Cell movements during vertebrate development: integrated tissue behaviour versus individual cell migration. *Curr Opin Genet Dev* **11**, 464-9.
- Londin, E. R., Niemiec, J. and Sirotkin, H. I.** (2005). Chordin, FGF signaling, and mesodermal factors cooperate in zebrafish neural induction. *Dev Biol* **279**, 1-19.
- Loosli, F., Koster, R. W., Carl, M., Krone, A. and Wittbrodt, J.** (1998). Six3, a medaka homologue of the *Drosophila* homeobox gene *sine oculis* is expressed in the anterior embryonic shield and the developing eye. *Mech Dev* **74**, 159-64.
- Loosli, F., Staub, W., Finger-Baier, K., Ober, E., Verkade, H., Wittbrodt, J. and Baier, H.** (2003). Loss of eyes in zebrafish caused by mutation of *chokh/rx3*. *EMBO Reports* **4**, 894-899.
- Loosli, F., Winkler, S., Burgtorf, C., Wurmbach, E., Ansorge, W., Henrich, T., Grabher, C., Arendt, D., Carl, M., Krone, A. et al.** (2001). Medaka *eyeless* is the key factor linking retinal dertermination and eye growth. *Development* **128**, 4035-4044.
- Loosli, F., Winkler, S. and Wittbrodt, J.** (1999). Six3 overexpression initiates the formation of ectopic retina. *Genes and Development* **13**, 649-654.
- Lopez-Rios, J., Tessmar, K., Loosli, F., Wittbrodt, J. and Bovolenta, P.** (2003). Six3 and Six6 activity is modulated by members of the groucho family. *Development* **130**, 185-195.
- Lupo, G., Liu, Y., Qiu, R., Chandraratna, R. A., Barsacchi, G., He, R. Q. and Harris, W. A.** (2005). Dorsoroventral patterning of the *Xenopus* eye: a collaboration of Retinoid, Hedgehog and FGF receptor signaling. *Development* **132**, 1737-48.

- Macdonald, R., Barth, K. A., Xu, Q., Holder, N., Mikkola, I. and Wilson, S. W.** (1995). Midline signalling is required for Pax gene regulation and patterning of the eyes. *Development* **121**, 3267-3278.
- Marlow, F., Topczewski, J., Sepich, D. and Solnica-Krezel, L.** (2002). Zebrafish Rho kinase 2 acts downstream of Wnt11 to mediate cell polarity and effective convergence and extension movements. *Curr Biol* **12**, 876-84.
- Marquardt, T. and Gruss, P.** (2002). Generating neuronal diversity in the retina: one for nearly all. *Trends Neurosci* **25**, 32-8.
- Martinez-Morales, J. R., Del Bene, F., Nica, G., Hammerschmidt, M., Bovolenta, P. and Wittbrodt, J.** (2005). Differentiation of the vertebrate retina is coordinated by an FGF signaling center. *Dev Cell* **8**, 565-74.
- Masai, I., Heisenberg, C.-P., Barth, K. A., Macdonald, R., Adamek, S. and Wilson, S. W.** (1997). *floating head* and *masterblind* regulate neuronal patterning in the roof of the forebrain. *Neuron* **18**, 43-57.
- Masai, I., Stemple, D. L., Okamoto, H. and Wilson, S. W.** (2000). Midline signals regulate retinal neurogenesis in zebrafish. *Neuron* **27**, 251-263.
- Mata, J., Curado, S., Ephrussi, A. and Rorth, P.** (2000). Tribbles coordinates mitosis and morphogenesis in Drosophila by regulating string/CDC25 proteolysis. *Cell* **101**, 511-22.
- Mathers, P. H., Grinberg, A., Mahon, K. A. and Jamrich, M.** (1997). The Rx homeobox gene is essential for vertebrate eye development. *Nature (London)* **387**, 603-607.
- Matsuda, M. and Keino, H.** (2001). Possible roles of beta-catenin in evagination of the optic primordium in rat embryos. *Dev Growth Differ* **43**, 391-400.
- Matsuo, I., Kuratani, S., Kimura, C., Takeda, N. and Aizawa, S.** (1995). Mouse Otx2 functions in the formation and patterning of rostral head. *Genes & Development* **9**, 2646-2658.
- Matsuo, T., Osumi-Yamashita, N., Noji, S., Ohuchi, H., Koyama, E., Myokai, F., Matsuo, N., Toniguchi, S., Dari, H., Jseki, S. et al.** (1993). A mutation at the *Pax-6* gene in rat small eye is associated with impaired migration of midbrain crest cells. *Nature Genetics* **3**, 299-304.
- Matz, M. V., Lukyanov, K. A. and Lukyanov, S. A.** (2002). Family of the green fluorescent protein: journey to the end of the rainbow. *Bioessays* **24**, 953-9.
- McFadden, D. G. and Olson, E. N.** (2002). Heart development: learning from mistakes. *Curr Opin Genet Dev* **12**, 328-35.
- Meda, P., Bruzzone, R., Knodel, S. and Orci, L.** (1986). Blockage of cell-to-cell communication within pancreatic acini is associated with increased basal release of amylase. *J Cell Biol* **103**, 475-83.
- Megason, S. G. and Fraser, S. E.** (2003). Digitizing life at the level of the cell: high-performance laser-scanning microscopy and image analysis for in toto imaging of development. *Mech Dev* **120**, 1407-20.
- Mlodzik, M.** (2002). Planar cell polarization: do the same mechanisms regulate Drosophila tissue polarity and vertebrate gastrulation? *Trends Genet* **18**, 564-571.
- Molyneaux, K. and Wylie, C.** (2004). Primordial germ cell migration. *Int J Dev Biol* **48**, 537-543.
- Molyneaux, K. A., Zinszner, H., Kunwar, P. S., Schaible, K., Stebler, J., Sunshine, M. J., O'Brien, W., Raz, E., Littman, D., Wylie, C. et al.** (2003). The chemokine SDF1/CXCL12 and its receptor CXCR4 regulate mouse germ cell migration and survival. *Development* **130**, 4279-86.

- Montero, J. A., Carvalho, L., Wilsch-Bräuninger, M., Kilian, B., Mustafa, C. and Heisenberg, C. P.** (2005). Shield formation at the onset of zebrafish gastrulation. *Development* **132**, 1187-1198.
- Montero, J. A. and Heisenberg, C. P.** (2004). Gastrulation dynamics: cells move into focus. *Trends Cell Biol* **14**, 620-627.
- Montero, J. A., Kilian, B., Chan, J., Bayliss, P. E. and Heisenberg, C. P.** (2003). Phosphoinositide 3-kinase is required for process outgrowth and cell polarization of gastrulating mesendodermal cells. *Curr Biol* **13**, 1279-89.
- Moon, R. T., Campbell, R. M., Christian, J. L., McGrew, L. L., Shih, J. and Fraser, S.** (1993). Xwnt-5A - A Maternal Wnt That Affects Morphogenetic Movements After Overexpression in Embryos of *Xenopus laevis*. *Development* **119**, 97-111.
- Moore, K. B., Mood, K., Daar, I. O. and Moody, S. A.** (2004). Morphogenetic movements underlying eye field formation require interactions between the FGF and ephrinB1 signaling pathways. *Dev Cell* **6**, 55-67.
- Morgan, R., Hooiveld, M. H., Pannese, M., Dati, G., Broders, F., Delarue, M., Thiery, J. P., Boncinelli, E. and Durston, A. J.** (1999). Calponin modulates the exclusion of Otx-expressing cells from convergence extension movements. *Nat Cell Biol* **1**, 404-8.
- Mui, S. H., Hindges, R., O'Leary, D. D., Lemke, G. and Bertuzzi, S.** (2002). The homeodomain protein Vax2 patterns the dorsoventral and nasotemporal axes of the eye. *Development* **129**, 797-804.
- Mui, S. H., Kim, J. W., Lemke, G. and Bertuzzi, S.** (2005). Vax genes ventralize the embryonic eye. *Genes Dev* **19**, 1249-59.
- Mukhopadhyay, M., Shtrom, S., Rodriguez-Esteban, C., Chen, L., Tsukui, T., Gomer, L., Dorward, D. W., Glinka, A., Grinberg, A., Huang, S. P. et al.** (2001). Dickkopf1 is required for embryonic head induction and limb morphogenesis in the mouse. *Dev Cell* **1**, 423-434.
- Muller, F., Albert, S., Blader, P., Fischer, N., Hallonet, M. and Strahle, U.** (2000). Direct action of the nodal-related signal cyclops in induction of sonic hedgehog in the ventral midline of the CNS. *Development* **127**, 3889-97.
- Munoz-Sanjuan, I. and Brivanlou, A. H.** (2002). Neural induction, the default model and embryonic stem cells. *Nat Rev Neurosci* **3**, 271-280.
- Myers, D. C., Sepich, D. S. and Solnica-Krezel, L.** (2002a). Bmp activity gradient regulates convergent extension during zebrafish gastrulation. *Dev Biol* **243**, 81-98.
- Myers, D. C., Sepich, D. S. and Solnica-Krezel, L.** (2002b). Convergence and extension in vertebrate gastrulae: cell movements according to or in search of identity? *Trends Genet* **18**, 447-55.
- Nagel, M., Tahinci, E., Symes, K. and Winklbauer, R.** (2004). Guidance of mesoderm cell migration in the *Xenopus* gastrula requires PDGF signaling. *Development* **131**, 2727-2736.
- Neumann, C. J.** (2001). Pattern formation in the zebrafish retina. *Semin Cell Dev Biol* **12**, 485-90.
- Neumann, C. J. and Nüsslein-Volhard, C.** (2000). Patterning of the zebrafish retina by a wave of sonic hedgehog activity. *Science* **289**, 2137-2139.
- Ninomiya, H., Elinson, R. P. and Winklbauer, R.** (2004). Antero-posterior tissue polarity links mesoderm convergent extension to axial patterning. *Nature (London)* **430**, 364-7.
- Nordstrom, U., Jessell, T. M. and Edlund, T.** (2002). Progressive induction of caudal neural character by graded Wnt signaling. *Nat Neurosci* **5**, 525-32.

- Ohuchi, H., Tomonari, S., Itoh, H., Mikawa, T. and Noji, S.** (1999). Identification of chick *rax/rx* genes with overlapping patterns of expression during early eye and brain development. *Mechanisms of Development* **85**, 193-195.
- Oliver, G., Mailhos, A., Wehr, R., Copeland, N. G., Jenkins, N. A. and Gruss, P.** (1995). Six3, a murine homologue of the sine oculis gene, demarcates the most anterior border of the developing neural plate and is expressed during eye development. *Development* **121**, 4045-4055.
- Pannese, M., Polo, C., Andreazzoli, M., Vignali, R., Kablar, B., Barsacchi, G. and Boncinelli, E.** (1995). The *Xenopus* homologue of *Otx2* is a maternal homeobox gene that demarcates and specifies anterior body regions. *Development* **121**, 707-20.
- Park, M. and Moon, R. T.** (2002). The planar cell-polarity gene *stbm* regulates cell behaviour and cell fate in vertebrate embryos. *Nat Cell Biol* **4**, 20-5.
- Pasquier, L., Dubourg, C., Blayau, M., Lazaro, L., Le Marec, B., David, V. and Odent, S.** (2000). A new mutation in the six-domain of *SIX3* gene causes holoprosencephaly. *Eur J Hum Genet* **8**, 797-800.
- Perea-Gomez, A., Lawson, K. A., Rhinn, M., Zakin, L., Brulet, P., Mazan, S. and Ang, S. L.** (2001a). *Otx2* is required for visceral endoderm movement and for the restriction of posterior signals in the epiblast of the mouse embryo. *Development* **128**, 753-65.
- Perea-Gomez, A., Rhinn, M. and Ang, S. L.** (2001b). Role of the anterior visceral endoderm in restricting posterior signals in the mouse embryo. *Int J Dev Biol* **45**, 311-20.
- Peters, M. A.** (2002). Patterning the neural retina. *Curr Opin Neurobiol* **12**, 43-8.
- Piccolo, S., Agius, E., Leyns, L., Bhattacharyya, S., Grunz, H., Bouwmeester, T. and De Robertis, E. M.** (1999). The head inducer *Cerberus* is a multifunctional antagonist of *Nodal*, *BMP* and *Wnt* signals. *Nature (London)* **397**, 707-10.
- Piccolo, S., Sasai, Y., Lu, B. and De Robertis, E. M.** (1996). Dorsoventral patterning in *Xenopus*: inhibition of ventral signals by direct binding of *chordin* to *BMP-4*. *Cell* **86**, 589-598.
- Pollard, T. D. and Borisy, G. G.** (2003). Cellular motility driven by assembly and disassembly of actin filaments. *Cell* **112**, 453-65.
- Pujic, Z. and Malicki, J.** (2004). Retinal patterning and the genetic basis of its formation in zebrafish. *Seminars in Cell & Developmental Biology* **15**, 105-114.
- Quiring, R., Walldorf, U., Kloter, U. and Gehring, W. J.** (1994). Homology of the eyeless gene of *Drosophila* to the small eye gene in mice and aniridia in humans. *Science* **265**, 785-789.
- Rabut, G. and Ellenberg, J.** (2004). Automatic real-time three-dimensional cell tracking by fluorescence microscopy. *J. Microsc.* **216**, 131-7.
- Raftopoulou, M. and Hall, A.** (2004). Cell migration: Rho GTPases lead the way. *Dev Biol* **265**, 23-32.
- Rauch, G. J., Hammerschmidt, M., Blader, P., Schauerte, H. E., Strahle, U., Ingham, P. W., McMahon, A. P. and Haffter, P.** (1997). *Wnt5* is required for tail formation in the zebrafish embryo. *Cold Spring Harb Symp Quant Biol* **62**, 227-234.
- Raz, E.** (2003). Primordial germ-cell development: the zebrafish perspective. *Nat Rev Genet* **4**, 690-700.
- Raz, E.** (2004). Guidance of primordial germ cell migration. *Current Opinion in Cell Biology* **16**, 169-173.
- Rebagliati, M. R., Toyama, R., Haffter, P. and Dawid, I. B.** (1998). *cyclops* encodes a nodal-related factor involved in midline signaling. *Proc Natl Acad Sci U S A* **95**, 9932-7.

- Rembold, M. and Wittbrodt, J.** (2004). In vivo time-lapse imaging in medaka--n-heptanol blocks contractile rhythmical movements. *Mech Dev* **121**, 965-70.
- Rhinn, M., Dierich, A., Le Meur, M. and Ang, S.** (1999). Cell autonomous and non-cell autonomous functions of Otx2 in patterning the rostral brain. *Development* **126**, 4295-304.
- Rhinn, M., Dierich, A., Shawlot, W., Behringer, R. R., Le Meur, M. and Ang, S. L.** (1998). Sequential roles for Otx2 in visceral endoderm and neuroectoderm for forebrain and midbrain induction and specification. *Development* **125**, 845-856.
- Rhinn, M., Lun, K., Amores, A., Yan, Y. L., Postlethwait, J. H. and Brand, M.** (2003). Cloning, expression and relationship of zebrafish gbx1 and gbx2 genes to Fgf signaling. *Mech Dev* **120**, 919-936.
- Rhinn, M., Lun, K., Luz, M., Werner, M. and Brand, M.** (2005). Positioning of the midbrain-hindbrain boundary organizer through global posteriorization of the neuroectoderm mediated by Wnt8 signaling. *Development* **132**, 1261-1272.
- Ridley, A. J., Schwartz, M. A., Burridge, K., Firtel, R. A., Ginsberg, M. H., Borisy, G., Parsons, J. T. and Horwitz, A. R.** (2003). Cell migration: integrating signals from front to back. *Science* **302**, 1704-9.
- Robertson, A.** (1979). Waves propagated during vertebrate development: observations and comments. *J Embryol Exp Morphol* **50**, 155-67.
- Rubenstein, J. L., Shimamura, K., Martinez, S. and Puelles, L.** (1998). Regionalization of the prosencephalic neural plate. *Annu Rev Neurosci* **21**, 445-477.
- Sambrook, J., Fritsch, E. F. and Maniatis, T.** (1989). *Molecular Cloning, A Laboratory Manual*: Cold Spring Harbor Laboratory Press.
- Sampath, K., Rubinstein, A. L., Cheng, A. M., Liang, J. O., Fekany, K., Solnica-Krezel, L., Korzh, V., Halpern, M. E. and Wright, C. V.** (1998). Induction of the zebrafish ventral brain and floorplate requires cyclops/nodal signalling. *Nature (London)* **395**, 185-189.
- Sasai, Y., Lu, B., Piccolo, S. and De Robertis, E. M.** (1996). Endoderm induction by the organizer-secreted factors chordin and noggin in *Xenopus* animal caps. *Embo J* **15**, 4547-4555.
- Sasai, Y., Lu, B., Steinbeisser, H. and De Robertis, E. M.** (1995). Regulation of neural induction by the Chd and Bmp-4 antagonistic patterning signals in *Xenopus*. *Nature (London)* **376**, 333-336.
- Schier, A. F. and Shen, M. M.** (2000). Nodal signalling in vertebrate development. *Nature (London)* **403**, 385-389.
- Schmitt, E. A. and Dowling, J. E.** (1994). Early eye morphogenesis in the zebrafish, *Brachydanio rerio*. *Journal of Comparative Neurology* **344**, 532-542.
- Schoenwolf, G. C. and Smith, J. L.** (1990). Mechanisms of neurulation: traditional viewpoint and recent advances. *Development* **109**, 243-70.
- Schulte, D., Furukawa, T., Peters, M. A., Kozak, C. A. and Cepko, C. L.** (1999). Misexpression of the Emx-related homeobox genes cVax and mVax2 ventralizes the retina and perturbs the retinotectal map. *Neuron* **24**, 541-53.
- Schwarz, M., Cecconi, F., Bernier, G., Andrejewski, N., Kammandel, B., Wagner, M. and Gruss, P.** (2000). Spatial specification of mammalian eye territories by reciprocal transcriptional repression of Pax2 and Pax6. *Development* **127**, 4325-4334.
- Seher, T. C. and Leptin, M.** (2000). Tribbles, a cell-cycle brake that coordinates proliferation and morphogenesis during *Drosophila* gastrulation. *Curr Biol* **10**, 623-9.

- Seo, H. C., Drivenes, O., Ellingsen, S. and Fjose, A.** (1998). Expression of two zebrafish homologues of the murine Six3 gene demarcates the initial eye primordia. *Mechanisms of Development* **73**, 45-57.
- Sguigna, C., Fluck, R. and Barber, B.** (1988). Calcium dependence of rhythmic contractions of the *Oryzias latipes* blastoderm. *Comp Biochem Physiol C* **89**, 369-74.
- Shanmugalingam, S., Houart, C., Picker, A., Reifers, F., Macdonald, R., Barth, A., Griffin, K., Brand, M. and Wilson, S. W.** (2000). Ace/Fgf8 is required for forebrain commissure formation and patterning of the telencephalon. *Development* **127**, 2549-61.
- Shih, J. and Fraser, S. E.** (1996). Characterizing the zebrafish organizer: microsurgical analysis at the early-shield stage. *Development* **122**, 1313-1322.
- Shih, J. and Keller, R.** (1992a). Cell motility driving mediolateral intercalation in explants of *Xenopus laevis*. *Development* **116**, 901-914.
- Shih, J. and Keller, R.** (1992b). Patterns of cell motility in the organizer and dorsal mesoderm of *Xenopus laevis*. *Development* **116**, 915-30.
- Shih, J. A. and Keller, R.** (1994). Gastrulation in *Xenopus laevis*: involution - a current view. *Semin Dev Biol* **5**, 85-90.
- Shirinsky, V. P., Biryukov, K. G., Hettasch, J. M. and Sellers, J. R.** (1992). Inhibition of the relative movement of actin and myosin by caldesmon and calponin. *J Biol Chem* **267**, 15886-92.
- Simeone, A., Acampora, D., Mallamaci, A., Stornaiuolo, A., Dapice, M. R., Nigro, V. and Boncinelli, E.** (1993). A Vertebrate Gene Related to orthodenticle Contains a Homeodomain of the bicoid Class and Demarcates Anterior Neuroectoderm in the Gastrulating Mouse Embryo. *The EMBO Journal* **12**, 2735-2747.
- Simon, J. Z. and Cooper, M. S.** (1995). Calcium oscillations and calcium waves coordinate rhythmic contractile activity within the stellate cell layer of medaka fish embryos. *J. Exp. Zoology* **273**, 118-129.
- Smith, W. C. and Harland, R. M.** (1992). Expression Cloning of noggin, a New Dorsalizing Factor Localized to the Spemann Organizer in *Xenopus* Embryos. *Cell* **70**, 829-840.
- Solnica-Krezel, L., Stemple, D. L., Mountcastle-Shah, E., Rangini, Z., Neuhaus, S. C., Malicki, J., Schier, A. F., Stainier, D. Y., Zwartkruis, F., Abdelilah, S. et al.** (1996). Mutations affecting cell fates and cellular rearrangements during gastrulation in zebrafish. *Development* **123**, 67-80.
- Spray, D. C., Nerbonne, J., Campos de Carvalho, A., Harris, A. L. and Bennett, M. V.** (1984). Substituted benzyl acetates: a new class of compounds that reduce gap junctional conductance by cytoplasmic acidification. *J Cell Biol* **99**, 174-9.
- Srinivas, S., Rodriguez, T., Clements, M., Smith, J. C. and Beddington, R. S. P.** (2004). Active cell migration drives the unilateral movements of the anterior visceral endoderm. *Development* **131**, 1157-1164.
- Stephens, L., Ellson, C. and Hawkins, P.** (2002). Roles of PI3Ks in leukocyte chemotaxis and phagocytosis. *Curr Opin Cell Biol* **14**, 203-13.
- Stern, C. D.** (2002). Induction and initial patterning of the nervous system - the chick embryo enters the scene. *Curr Opin Genet Dev* **12**, 447-51.
- Stoykova, A., Fritsch, R., Walther, C. and Gruss, P.** (1996). Forebrain patterning defects in Small eye mutant mice. *Development* **122**, 3453-65.
- Streit, A., Berliner, A. J., Papanayotou, C., Sirulnik, A. and Stern, C. D.** (2000). Initiation of neural induction by FGF signalling before gastrulation. *Nature (London)* **406**, 74-8.

- Streit, A., Lee, K. J., Woo, I., Roberts, C., Jessell, T. M. and Stern, C. D.** (1998). Chordin regulates primitive streak development and the stability of induced neural cells, but is not sufficient for neural induction in the chick embryo. *Development* **125**, 507-519.
- Sumanas, S. and Ekker, S. C.** (2001). Xenopus frizzled-7 morphant displays defects in dorsoventral patterning and convergent extension movements during gastrulation. *Genesis* **30**, 119-22.
- Sumanas, S., Kim, H. J., Hermanson, S. and Ekker, S. C.** (2001). Zebrafish frizzled-2 morphant displays defects in body axis elongation. *Genesis* **30**, 114-8.
- Svoboda, K. K. and O'Shea, K. S.** (1987). An analysis of cell shape and the neuroepithelial basal lamina during optic vesicle formation in the mouse embryo. *Development* **100**, 185-200.
- Tada, M. and Smith, J. C.** (2000). Xwnt11 is a target of Xenopus Brachyury: regulation of gastrulation movements via Dishevelled, but not through the canonical Wnt pathway. *Development* **127**, 2227-2238.
- Tada, S., Li, A., Maiorano, D., Mechali, M. and Blow, J. J.** (2001). Repression of origin assembly in metaphase depends on inhibition of RLF-B/Cdt1 by geminin. *Nature Cell Biology* **3**, 107-13.
- Take-uchi, M., Clarke, J. D. and Wilson, S. W.** (2003). Hedgehog signalling maintains the optic stalk-retinal interface through the regulation of Vax gene activity. *Development* **130**, 955-68.
- Thermes, V., Grabher, C., Ristoratore, F., Bourrat, F., Choulika, A., Wittbrodt, J. and Joly, J. S.** (2002). I-SceI meganuclease mediates highly efficient transgenesis in fish. *Mech Dev* **118**, 91-8.
- Thomas, P. Q., Brown, A. and Beddington, R. S. P.** (1998). Hex: a homeobox gene revealing peri-implantation asymmetry in the mouse embryo and an early transient marker of endothelial cell precursors. *Development* **125**, 85-94.
- Thoreson, M. A., Anastasiadis, P. Z., Daniel, J. M., Ireton, R. C., Wheelock, M. J., Johnson, K. R., Hummingbird, D. K. and Reynolds, A. B.** (2000). Selective uncoupling of p120(ctn) from E-cadherin disrupts strong adhesion. *J Cell Biol* **148**, 189-202.
- Ton, C. C., Hirvonen, H., Miwa, H., Weil, M. M., Monaghan, P., Jordan, T., van Heyningen, V., Hastie, N. D., Meijers-Heijboer, H., Drechsler, M. et al.** (1991). Positional cloning and characterization of a paired box- and homeobox-containing gene from the aniridia region. *Cell* **67**, 1059-74.
- Topczewski, J., Sepich, D. S., Myers, D. C., Walker, C., Amores, A., Lele, Z., Hammerschmidt, M., Postlethwait, J. and Solnica-Krezel, L.** (2001). The zebrafish glypican knypek controls cell polarity during gastrulation movements of convergent extension. *Dev Cell* **1**, 251-64.
- Torres, M., Gómez-Pardo, E. and Gruss, P.** (1996). Pax2 contributes to inner ear patterning and optic nerve trajectory. *Development* **122**, 3381-3391.
- Toy, J., Yang, J.-M., Leppert, G. and Sundin, O. H.** (1998). The Optx2 homeobox gene is expressed in early precursors of the eye and activates retina-specific genes. *Proceedings of the National Academy of Sciences USA* **95**, 10643-10648.
- Trinh, L. A. and Stainier, D. Y.** (2004). Fibronectin regulates epithelial organization during myocardial migration in zebrafish. *Dev Cell* **6**, 371-82.
- Tsien, R. Y.** (2005). Building and breeding molecules to spy on cells and tumors. *FEBS Letters* **579**, 927-932.
- Tucker, P., Laemle, L., Munson, A., Kanekar, S., Oliver, E. R., Brown, N., Schlecht, H., Vetter, M. and Glaser, T.** (2001). The *eyeless* mouse mutation (*ey1*)

- removes an alternative start codon from the *Rx/rax* homeobox gene. *Genesis* **31**, 43-53.
- Tuckett, F. and Morriss-Kay, G. M.** (1986). The distribution of fibronectin, laminin and entactin in the neurulating rat embryo studied by indirect immunofluorescence. *J Embryol Exp Morphol* **94**, 95-112.
- Turner, D. L., Snyder, E. Y. and Cepko, C. L.** (1990). Lineage-independent determination of cell type in the embryonic mouse retina. *Neuron* **4**, 833-45.
- Ulrich, F., Concha, M. L., Heid, P. J., Voss, E., Witzel, S., Roehl, H., Tada, M., Wilson, S. W., Adams, R. J., Soll, D. R. et al.** (2003). Slb/Wnt11 controls hypoblast cell migration and morphogenesis at the onset of zebrafish gastrulation. *Development* **130**, 5375-84.
- Uren, A., Reichsman, F., Anest, V., Taylor, W. G., Muraiso, K., Bottaro, D. P., Cumberledge, S. and Rubin, J. S.** (2000). Secreted frizzled-related protein-1 binds directly to Wingless and is a biphasic modulator of Wnt signaling. *J Biol Chem* **275**, 4374-82.
- van de Water, S., van de Wetering, M., Joore, J., Esseling, J., Bink, R., Clevers, H. and Zivkovic, D.** (2001). Ectopic Wnt signal determines the eyeless phenotype of zebrafish masterblind mutant. *Development* **128**, 3877-88.
- Varga, Z. M., Amores, A., Lewis, K. E., Yan, Y. L., Postlethwait, J. H., Eisen, J. S. and Westerfield, M.** (2001). Zebrafish smoothed functions in ventral neural tube specification and axon tract formation. *Development* **128**, 3497-509.
- Varga, Z. M., Wegner, J. and Westerfield, M.** (1999). Anterior movement of ventral diencephalic precursors separates the primordial eye field in the neural plate and requires cyclops. *Development* **126**, 5533-46.
- Vogel-Hopker, A., Momose, T., Rohrer, H., Yasuda, K., Ishihara, L. and Rapaport, D. H.** (2000). Multiple functions of fibroblast growth factor-8 (FGF-8) in chick eye development. *Mech Dev* **94**, 25-36.
- Voronina, V. A., Kozhemyakina, E. A., O'Kernick, C. M., Kahn, N. D., Wenger, S. L., Linberg, J. V., Schneider, A. S. and Mathers, P. H.** (2004). Mutations in the human *RAX* homeobox gene in a patient with anophthalmia and sclerocornea. *Human Molecular Genetics* **13**, 315-322.
- Wada, H., Iwasaki, M., Sato, T., Masai, I., Nishiwaki, Y., Tanaka, H., Sato, A., Nojima, Y. and Okamoto, H.** (2005). Dual roles of zygotic and maternal Scribble1 in neural migration and convergent extension movements in zebrafish embryos. *Development* **132**, 2273-85.
- Wallingford, J. B., Fraser, S. E. and Harland, R. M.** (2002). Convergent extension: the molecular control of polarized cell movement during embryonic development. *Dev Cell* **2**, 695-706.
- Wallingford, J. B. and Harland, R. M.** (2001). *Xenopus* Dishevelled signaling regulates both neural and mesodermal convergent extension: parallel forces elongating the body axis. *Development* **128**, 2581-2592.
- Wallingford, J. B. and Harland, R. M.** (2002). Neural tube closure requires Dishevelled-dependent convergent extension of the midline. *Development* **129**, 5815-5825.
- Wallingford, J. B., Rowning, B. A., Vogeli, K. M., Rothbacher, U., Fraser, S. E. and Harland, R. M.** (2000). Dishevelled controls cell polarity during *Xenopus* gastrulation. *Nature (London)* **405**, 81-5.
- Wallis, D. E., Roessler, E., Hehr, U., Nanni, L., Wiltshire, T., Richieri-Costa, A., Gillessen-Kaesbach, G., Zackai, E. H., Rommens, J. and Muenke, M.** (1999).

- Mutations in the homeodomain of the human SIX3 gene cause holoprosencephaly. *Nature Genetics*. **22**, 196-198.
- Walshe, J. and Mason, I.** (2003). Unique and combinatorial functions of Fgf3 and Fgf8 during zebrafish forebrain development. *Development* **130**, 4337-49.
- Walther, C. and Gruss, P.** (1991). Pax-6, a murine paired box gene, is expressed in the developing CNS. *Development* **113**, 1435-1449.
- Warga, R. M. and Kimmel, C. B.** (1990). Cell movements during epiboly and gastrulation in zebrafish. *Development* **108**, 569-80.
- Welch, M. D. and Mullins, R. D.** (2002). Cellular control of actin nucleation. *Annu Rev Cell Dev Biol* **18**, 247-88.
- Wetts, R. and Fraser, S. E.** (1988). Multipotent precursors can give rise to all major cell types of the frog retina. *Science* **239**, 1142-5.
- Wheelock, M. J. and Johnson, K. R.** (2003). Cadherins as modulators of cellular phenotype. *Annu Rev Cell Dev Biol* **19**, 207-35.
- Wilson, E. T., Cretekos, C. J. and Helde, K. A.** (1995). Cell mixing during early epiboly in the Zebrafish embryo. *Dev Genet* **17**, 6-15.
- Wilson, P. A. and Hemmati-Brivanlou, A.** (1995). Induction of epidermis and inhibition of neural fate by Bmp-4. *Nature (London)* **376**, 331-333.
- Wilson, R., Vogelsang, E. and Leptin, M.** (2005). FGF signalling and the mechanism of mesoderm spreading in Drosophila embryos. *Development* **132**, 491-501.
- Wilson, S. I. and Edlund, T.** (2001). Neural induction: toward a unifying mechanism. *Nat Neurosci* **4 Suppl**, 1161-8.
- Wilson, S. I., Graziano, E., Harland, R., Jessell, T. M. and Edlund, T.** (2000). An early requirement for FGF signalling in the acquisition of neural cell fate in the chick embryo. *Curr Biol* **10**, 421-9.
- Wilson, S. I., Rydström, A., Trimborn, T., Willert, K., Nusse, R., Jessell, T. M. and Edlund, T.** (2001). The status of Wnt signalling regulates neural and epidermal fates in the chick embryo. *Nature (London)* **411**, 325-330.
- Wilson, S. W. and Houart, C.** (2004). Early steps in the development of the forebrain. *Dev Cell* **6**, 167-81.
- Winklbauer, R., Medina, A., Swain, R. K. and Steinbeisser, H.** (2001). Frizzled-7 signalling controls tissue separation during Xenopus gastrulation. *Nature (London)* **413**, 856-60.
- Winklbauer, R., Nagel, M., Selchow, A. and Wacker, S.** (1996). Mesoderm migration in the Xenopus gastrula. *Int J Dev Biol* **40**, 305-311.
- Winklbauer, R., Selchow, A., Nagel, M. and Angres, B.** (1992). Cell interaction and its role in mesoderm cell migration during Xenopus gastrulation. *Dev Dyn* **195**, 290-302.
- Winkler, S., Loosli, F., Henrich, T., Wakamatsu, Y. and Wittbrodt, J.** (2000). The conditional medaka mutation eyeless uncouples patterning and morphogenesis of the eye. *Development* **127**, 1911-1919.
- Wittbrodt, J., Shima, A. and Schartl, M.** (2002). Medaka - A model organism from the Far East. *Nature Reviews Genetics* **3**, 53-64.
- Wohlschlegel, J. A., Dwyer, B. T., Dhar, S. K., Cvetic, C., Walter, J. C. and Dutta, A.** (2000). Inhibition of eukaryotic DNA replication by geminin binding to Cdt1. *Science* **290**, 2309-12.
- Woo, K. and Fraser, S.** (1995). Order and coherence in the fate map of the zebrafish nervous system. *Development* **121**, 2595-2609.

- Xu, Q., Alldus, G., Macdonald, R., Wilkinson, D. G. and Holder, N.** (1996). Function of the Eph-related kinase rtk1 in patterning of the zebrafish forebrain. *Nature (London)* **38**.
- Xu, R. H., Kim, J., Taira, M., Zhan, S., Sredni, D. and Kung, H. F.** (1995). A dominant negative bone morphogenetic protein 4 receptor causes neuralization in *Xenopus* ectoderm. *Biochem Biophys Res Commun* **212**, 212-219.
- Yamaguchi, T. P.** (2001). Heads or tails: Wnts and anterior-posterior patterning. *Curr Biol* **11**, R713-R724.
- Yamamoto, M., Saijoh, Y., Perea-Gomez, A., Shawlot, W., Behringer, R. R., Ang, S.-L., Hamada, H. and Meno, C.** (2004). Nodal antagonists regulate formation of the anteroposterior axis of the mouse embryo. *Nature (London)* **428**, 387-392.
- Yamamoto, T.** (1975). *Medaka (Killifish), Biology and Strains*. Tokyo: Keigaku Publishing Company.
- Yamanaka, H., Moriguchi, T., Masuyama, N., Kusakabe, M., Hanafusa, H., Takada, R., Takada, S. and Nishida, E.** (2002). JNK functions in the non-canonical Wnt pathway to regulate convergent extension movements in vertebrates. *EMBO Rep* **3**, 69-75.
- Yamashita, S., Miyagi, C., Fukada, T., Kagara, N., Che, Y. S. and Hirano, T.** (2004). Zinc transporter LIV1 controls epithelial-mesenchymal transition in zebrafish gastrula organizer. *Nature (London)* **429**, 298-302.
- Yang, X. J.** (2004). Roles of cell-extrinsic growth factors in vertebrate eye pattern formation and retinogenesis. *Semin Cell Dev Biol* **15**, 91-103.
- Yu, R. T., Chiang, M. Y., Tanabe, T., Kobayashi, M., Yasuda, K., Evans, R. M. and Umesono, K.** (2000). The orphan nuclear receptor Tlx regulates Pax2 and is essential for vision. *Proceedings of the National Academy of Sciences of the United States of America* **97**, 2621-2625.
- Zakin, L., Reversade, B., Virlon, B., Rusniok, C., Glaser, P., Elalouf, J. M. and Brulet, P.** (2000). Gene expression profiles in normal and *Otx2*^{-/-} early gastrulating mouse embryos. *Proc Natl Acad Sci U S A* **97**, 14388-93.
- Zhang, L., Mathers, P. H. and Jamrich, M.** (2000a). Function of Rx, but not Pax6, is essential for the formation of retinal progenitor cells in mice. *Genesis* **28**, 135-142.
- Zhang, X. M. and Yang, X. J.** (2001a). Regulation of retinal ganglion cell production by Sonic hedgehog. *Development* **128**, 943-57.
- Zhang, X. M. and Yang, X. J.** (2001b). Temporal and spatial effects of Sonic hedgehog signaling in chick eye morphogenesis. *Dev Biol* **233**, 271-90.
- Zhang, Y., Muyrers, J., Testa, G. and Stewart, A. F.** (2000b). DNA cloning by homologous recombination in *Escherichia coli*. *Nature Biotechnology* **18**, 1314-1317.
- Zhou, X., Hollemann, T., Pieler, T. and Gruss, P.** (2000). Cloning and expression of *xSix3*, the *Xenopus* homologue of murine *Six3*. *Mechanisms of Development* **91**, 327-330.
- Zimmerman, L. B., De Jesus-Escobar, J. M. and Harland, R. M.** (1996). The Spemann organizer signal noggin binds and inactivates bone morphogenetic protein 4. *Cell* **86**, 599-606.
- Zuber, M. E., Gestri, G., Viczian, A. S., Barsacchi, G. and Harris, W. A.** (2003). Specification of the vertebrate eye by a network of eye field transcription factors. *Development* **130**, 5155-67.
- Zuber, M. E., Perron, M., Philpott, A., Bang, A. and Harris, W. A.** (1999). Giant eyes in *Xenopus laevis* by overexpression of *XOpx2*. *Cell* **98**, 341-352.

Publications

Rembold, M. and Wittbrodt, J. (2004). In vivo time-lapse imaging in medaka – n-heptanol blocks contractile rhythmical movements. *Mech. Dev.* **121** (7-8):965-970

Loosli, F., Del Bene, F., Quiring, R., **Rembold, M.**, Martinez-Morales, J.R., Carl, M., Grabher, C., Iquel, C., Krone, A., Wittbrodt, B., Winkler, S., Sasado, T., Morinaga, C., Suwa, H., Niwa, K., Henrich, T., Deguchi, T., Hirose, Y., Iwanami, N., Kunimatsu, S., Osakada, M., Watanabe, T. Yasuoka, A., Yoda, H., Winkler, C., Elmasri, H., Kondoh, H., Furutani-Seiki, M., Wittbrodt, J. (2004). Mutations affecting retina development in Medaka. *Mech Dev.* **121** (7-8):703-714

Schafer, M., **Rembold, M.**, Wittbrodt, J., Scharl, M., Winkler, C. (2005) Medial floor plate formation in zebrafish consists of two phases and requires trunk-derived Midkine-a. *Genes Dev.* **19**:897-902

Acknowledgements

First of all I want to thank my supervisor Jochen Wittbrodt, who gave me the opportunity to work in his lab. He was always there for questions and discussions and to provide new directions for my work with his suggestions and ideas. With his enthusiasm he provides a great and stimulating working atmosphere that also shaped my scientific thinking.

I am grateful to Felix Loosli without whom this project had not been started and who was always there for help and discussions. A big ‘Thank you’ to him and Filippo Del Bene for critically reading this thesis.

A special thank goes to my Thesis Advisory Committee including Anne Ephrussi and Jan Ellenberg, who listened and gave important new ideas and suggestions for my work. I am also grateful to Prof. Elisabeth Pollerberg and Prof. Thomas Rausch that they agreed to be part of my committee and involved in the thesis defense.

I would also like to thank the members of the ALMF including Timo Zimmermann, Jens Rietdorf and Stefan Terjung who introduced me to all the microscopes (and I mean *all* of them) and imaging programmes at EMBL and helped in case of problems. A special thank to Timo for writing macros that allowed the first automated overnight time lapse recordings on the Leica SP2. Here I would also like to thank members of the group of Jan Ellenberg, especially Gwen Rabut and Daniel Gerlich, who provided and helped with macros developed to image several embryos simultaneously. This was a prerequisite for the mosaic analysis. I am very grateful to my collaborator Richard Adams from the University of Cambridge who spent a lot of time on modifying his routines for my needs.

I want to thank all the past and present members of the Wittbrodt group, Clemens, Matthias, Katherine, Hiroki, Staale, Claudia, Rebecca, Marcel, Caroline, Mirana, Thorsten, Annette, Beate, Aldona, Diana, Erika, Jan, Alexander and Prakash for providing a pleasant working atmosphere and for all the numerous occasions where they helped me or simply were there for a chat or a discussion. I really enjoyed working with all of you.

Filippo Del Bene - the best bench mate ever - became a friend and I want to thank him for numerous discussions about science, ideas and problems and all the other aspects of a PhD life at EMBL. Juan Ramon Martinez-Morales was always there to listen to problems and discuss and I would like to thank him for that.

Thank you to Lena, Alex, Anna, Esben and Daniel who became friends and without whom life in Heidelberg would not have been the same. Thank you, Frank for being at my side during all this time. I want to thank also my family who supported me throughout my scientific career and always gave me the freedom to choose whatever I wanted. Without all of you this would not have been possible!

I can't resist to say it: "So long, and thanks for all the fish!" (Douglas Adams, The Hitchhiker's Guide to the Galaxy)